主論文

Development of Catalytic Molecular Surface for Hydrogenation Reactions

（分子性の触媒表面の開発とその水素化反応への応用）

MIURA Takashi

三浦隆志

Department of Chemistry, Graduate School of Science
Nagoya University

2015

Preface

This thesis summarizes the author's study that has been carried out under the direction of University Professor Ryoji Noyori at the Graduate School of Science, Nagoya University, during the period of April 2010 to March 2015. This study is concerned with development of catalytic molecular surface for hydrogenation reactions.

The author wishes to express his sincerest gratitude to Professor Ryoji Noyori for his precise guidance, fruitful suggestions, and encouragement with warm enthusiasm. The author wishes to express his sincerest gratitude to Associate Professor Susumu Saito for his patient guidance, helpful discussion, and continuous encouragement through this work. The author is also deeply grateful to Dr. Hiroshi Naka for helpful guidance, technical assistance, and kind encouragement.

The author would like to express his appreciation to Professor Shigehiro Yamaguchi, Professor Kenichiro Itami, and Professor Masato Kitamura for their valuable suggestions and kind encouragement.

The author is grateful to Associate Professor Aiko Fukazawa, Associate Professor Yasutomo Segawa and Dr. Shohei Saito for their kind guidance for performing X-ray crystallography. The author is grateful to Ms. Yuriko Nakamura for her kind support. In addition, the author would like to thank Dr. Ken-ichi Oyama and Mr. Yutaka Maeda in shepherding the author through many compound characterizations. The author is thankful to Mr. Toshiaki Noda, Ms. Hideko Natsume, and Hisakazu Okamoto for their excellent craft of scientific glassware.

The author is grateful to Dr. Ingmar E. Held, Mr. Osamu Kose, Ms. Megumi Suzuki, Mr. Kazuki Iida, Mr. Masayuki Naruto, Mr. Yuki Takada, and Mr. Katsuaki Toda for their great assistance and collaborations. The author is grateful to Dr. Shunsuke Oishi, Dr. Foo Siong Wan, and Dr. Masakazu Nambo for their great assistance and fruitful discussions.

The author is deeply thankful to Ms. Aki Matsuoka for her kind encouragement and discussions during throughout the doctoral course. The author thanks the former and present members of the Noyori Laboratory for their kind considerations.

Dr. Santosh Agrawal
Dr. Zijun Liu
Dr. Du Ya
Dr. Yingsheng Zhao
Dr. Vasily Tsarev
Dr. Joaquim Caner
Dr. Sina Schwendemann
Dr. Adrian Schulte
Dr. Friederike Schröter
Mr. Junki Ando
Mr. Shun Oishi
Mr. Tadashi Tachinami
Mr. Kazuhiko Suzuki
Mr. Yusuke Yamazaki
Mr. Matthias Dahlkamp
Mr. Richiro Ushimaru
Ms. Erika Isshiki
Mr. Thomas Özgün
Mr. Shinsuke Iwata
Ms. Janine Fröhlich
Mr. Sota Nimura
Ms. Yuna Morioka
Mr. Takuho Nishimura
Mr. Takahiro Isogawa
Mr. Masaki Shibata
Mr. Yuya Akao
Mr. Kiyotaka Mori
Mr. Sunkook Lee
Mr. Taiki Shimomura
Mr. Toshiki Iwatsuki
Mr. Atsushi Nakamura
Mr. Takahiro Aoki
Mr. Alan K. Kimura
Mr. Byeong-Hyeon Jeong
Mr. Lyu Ming Wang
Mr. Lin Francis
Ms. Huang Hsiao Ching
Mr. Che-Sheng Hsu
Mr. Tatsuki Koyama
Mr. Guliano S. Goto

The author thanks all other members of Professor Yamaguchi's group, Professor Itami's group, and Professor Kitamura's group at Nagoya University for their kind support and encouragement.

The author thanks the Japan Society for the Promotion of Science (JSPS) for the Research Fellowships for Young Scientists (DC2). The author thanks the IGER program at Nagoya University for the fellowship and research funding.

Finally, the author wishes to express his sincerest gratitude to his family, Yasuo Miura, Naomi Miura, Isao Miura, Michiko Miura, Yuko Miura, and Eri Miura for their constant assistance and encouragement.

MIURA Takashi

Department of Chemistry
Graduate School of Science
Nagoya University
2015

Contents

Abbreviations

Ac	acetyl	Me	methyl
acac	acetylacetone	^{n}Bu	normal butyl
Ar	aryl	NMR	nuclear magnetic resonance
Bn	benzyl	^{n}Pr	normal propyl
Cp*	1,2,3,4,5-pentamethyl-cyclopentadienyl	ORTEP	Oak Ridge thermal ellipsoid
		p	para
Cy	cyclohexyl	P_{H2}	hydrogen pressure
δ	chemical shift, ppm	π	π-bond
DMF	*N,N*-dimethyl formamide	Ph	phenyl
Et	ethyl	R	alkyl group
equiv	equivalent	rt	room temperature
ESI	electrospray ionization	*t*	time
FAB	fast atom bombardment	*T*	temperature
Hz	hertz	^{t}Bu	tertiary butyl
HRMS	high-resolution mass spectra	Tf	trifluoromethanesulfonyl
I	intermediate	tmm	trimethylenemethane
^{i}Pr	isopropyl	triphos	bis(diphenylphosphinoethyl)-phenylphosphine
IR	infrared		
J	coupling constant	THF	tetrahydrofuran
M	metal	TS	transition state
M	molarity		

General Introduction

Hydrogenation is the addition reaction of molecular hydrogen (H_2 gas), obtained by steam reforming of fossil fuel[1] or photoreaction of water,[2] to unsaturated bonds. This powerful reduction technique is not merely limited to olefins; it is also effective towards carbonyls, imines, and other unsaturated bonds. Hydrogenation has received much attention in organic synthesis and catalysis because this approach is very useful and yet a green approach that does not produce harmful byproduct. In addition, it is highly atom-economic; the molecular hydrogen can be incorporated into a target product without loss of elements.[3] Over several decades, catalytic hydrogenation of aldehydes and ketones has been well studied and relevant technologies are successfully transferred to industrial applications.

In contrast, catalytic hydrogenation of inactive compounds available from nature and our surroundings such as biomass and synthetic materials is less explored (i.e. carboxylic acids, amides, esters, sugars, proteins, lignin, nylons, polyesters, etc.).[4] Biomass-related materials are highly oxidized or oxygenated/nitrogenated compounds (also containing many unsaturated bonds); Biomass is totally different from another natural resource — fossil fuel (a mixture of highly reduced alkyl chains). Thus, one of the effective chemical transformations of biomass-derived feedstock is hydrogenation or other reduction methods. Owing to their thermodynamic stability, catalytic hydrogenation of biomass-derived feedstock is so problematic. Transformations of these compounds hitherto are mainly based on the usage of extremely high thermal energy[5] or on powerful reducing agents such as $LiAlH_4$,[6] $NaBH_4$,[7] DIBAL,[8] RedAl,[9] borane (BH_3)[10] and silane (R_3SiH).[11] However, use of the latter reducing agents would decrease the atom efficiency, where a large amount of waste is co-generated along the reaction. Although several technologies for catalytic hydrogenation of biomass-derived feedstock using heterogeneous catalysis are available,[12] they also incur with several drawbacks, for instance, low chemoselectivity, harsh reaction conditions and a narrow substrate scope.

On the other hand, in the name of quality-life-style-improvement, human invented a number of new materials. However, most of them are undegradable and they most likely will stay in our environment for a long time (e.g. synthetic polymers, etc.). Hence, the efficient transformation approaches for these wastes to recover carbon sources are most

sought after. The author believes the catalytic hydrogenation should be the panacea of this problem because it allows us to reverse the synthetic polymers back into the useful carbon sources. This kind of approach is extremely essential for the creation of a sustainable and green environment for the future society.

In order to figure out a solution in the hydrogenation of biomass-derived feedstock and synthetic polymers, heterogeneous and homogeneous hydrogenation catalysts have been referred and studied. Generally, heterogeneous and homogeneous catalyst for hydrogenation can be divided into two main types; each of them has pros and cons.[12] Homogeneous catalysts can be designed flexibly but decomposed thermally and deactivated easily. On the contrary, heterogeneous catalysts are powerful and structurally robust but harsh conditions are frequently necessary; as a result, they often come with undesired side products. The author intended to design and synthesize a catalyst that combine the advantages of both heterogeneous and homogeneous catalyst and come out with a concept called ‘’catalytic molecular surface’’.

1. Background and research strategy in this thesis

1.1. Production of platform chemicals and other key compounds: existing method (oxidation) and future method (reduction)

Petroleum is an important carbon resource derived from organic remains of plant and animal deposited as sediments.[13] They are important energy source and chemical feedstock.[1b] In petroleum chemistry, oxidation of saturated hydrocarbons by steam reforming or pyrolysis produces useful unsaturated hydrocarbons such as carbon monoxide, olefin, acetylene, and so on.[1] The steam reforming of hydrocarbon has been a preferred method used industrially for the production of carbon monoxide and hydrogen. Generally, the steam reforming process involves two reactions: the splitting of hydrocarbons with steam and the water gas shift process (Figure 1a). On the other hand, unsaturated products such as ethylene, propylene and acetylene are formed by pyrolysis of saturated hydrocarbons during preheating at temperatures exceeding 873–973 K (Figure 1b). Nowadays, a wide range of useful compounds is derived from ethylene.

(**a**)

$$C_nH_m + nH_2O \longrightarrow nCO + (n + m/2)H_2$$

$$\text{for } n = 1: \Delta H^0_{298\ K} = +206.2\ \text{kJ/mol}$$

$$CO + H_2O \longrightarrow CO_2 + H_2$$

$$\Delta H^0_{298\ K} = -41.2\ \text{kJ/mol}$$

(**b**)

$$C_nH_mO_y \longrightarrow \text{tar} + H_2 + CO_2 + \text{ethylene} + \text{propylene} + \ldots$$

Figure 1. (**a**) Production of carbon monoxide and hydrogen by steam reforming of hydrocarbon; (**b**) Production of unsaturated hydrocarbons by pyrolysis of saturated hydrocarbon.

Those useful organic compounds derived from petroleum are widely used in so many anthropogenic activities, and after all, their combustion end up with carbon dioxide, the most oxidized form of carbon (Figure 2).

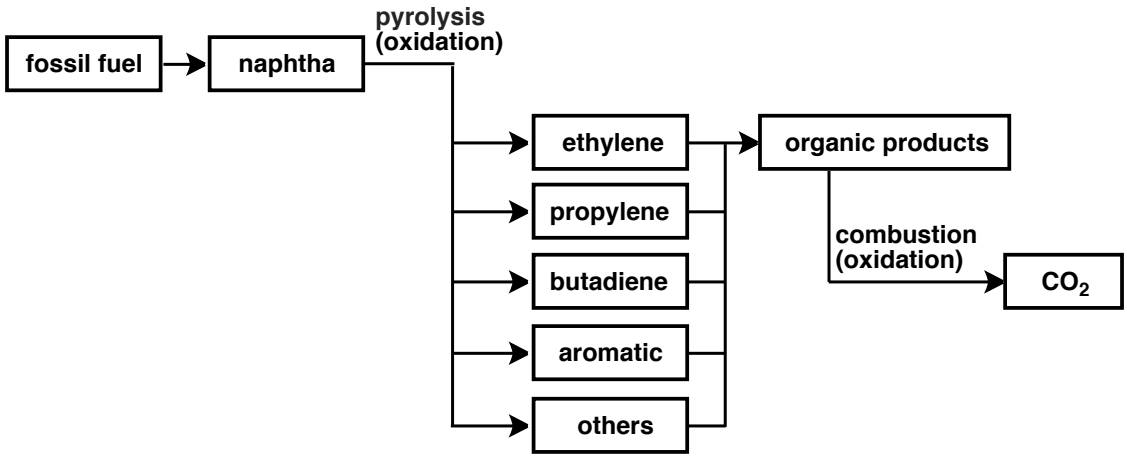

Figure 2. A rough flowchart of petrochemical process.

Carboxylic acid derivatives such as amide,[12,14] carboxylic acid[15] and ester[14] are classified as biomass-derived materials. Recently, the Department of Energy (DOE), US, selected more than twenty carboxylic acids, polyols, and their derivatives as "30 Top Value Added Chemicals from Biomass".[16] Effective transformation methods for these compounds are important. Moreover non-reusable polyamide- and polyester-type synthetic polymers should be considered as recycling material in the future. As we can see, developments of powerful reduction methods open up a possibility to use new carbon resources different from the petrochemical processes.

Biomass related compounds are at high oxidation states;[17] reduction is necessary to transform them into useful compounds. In view of sustainable society, biomass is a very attractive carbon source for the production of commodity chemicals (Figure 3).[4] However the number of reports on hydrogenation of carboxylic acid derivatives are quite few compared to that of ketone[18] and aldehyde; this might be owing to low electrophilicity of the carbonyl groups of carboxylic acid derivatives. The electrophilicity of carbonyl compounds can be arranged as follow:[19] amide < carboxylic acid < ester < anhydride < ketone ≈ aldehyde < acid chloride. The high resistance of carboxylic acid derivatives against their electrophilic chemical reactions is due to the resonance stabilization effects (Scheme 1). The lone pair electrons in the heteroatom (X) is donated to the carbonyl carbon p-orbital. Then, the electrophilicity of a carboxy carbon of amide and carboxylic acid is decreased and comparatively resistant to nucleophilic attack.

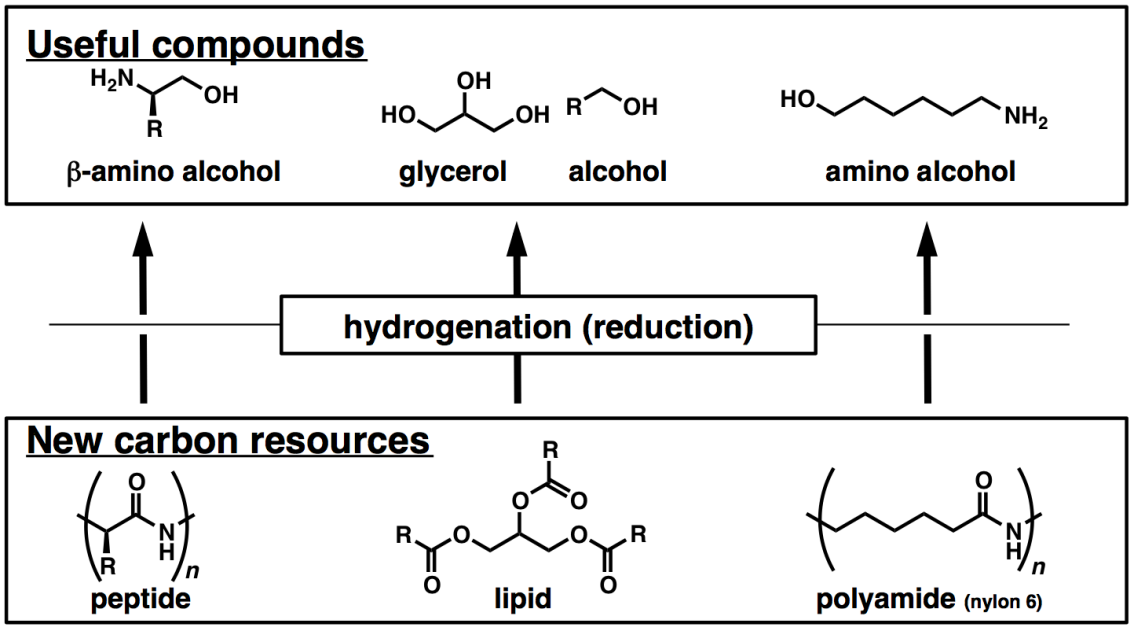

Figure 3. Potential application of carbon resource.

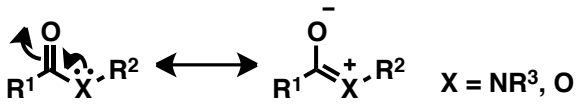

Scheme 1. Resonance stabilization effect of carboxylic acid derivatives.

New millennium carbon sources which are useful for organic synthesis and materials science should be obtained more favorably from bio-renewable resources in environmentally friendly ways. Transformation of such highly oxidized, carbon resource using catalytic hydrogenation and hydrogenolysis of the C–O bond of alcohols to obtain carbon sources is most suitable because it generates almost no waste; except the catalyst and water (Scheme 2).

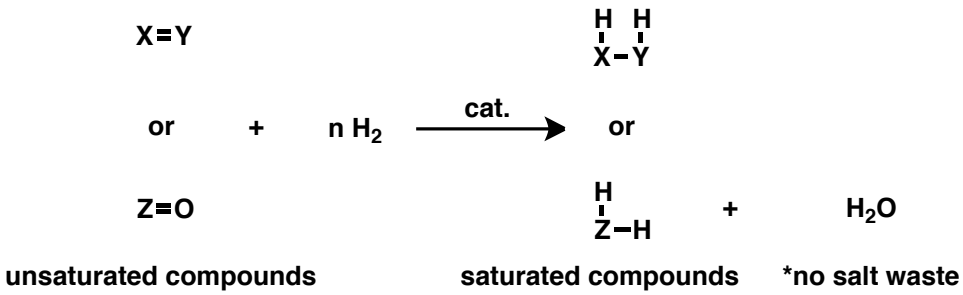

Scheme 2. Hydrogenation of unsaturated compounds.

1.2. Catalytic hydrogenation of amides

1.2.1. Heterogeneous hydrogenation of amides

Heterogeneous catalytic reaction is a type of catalysis, in which each substrate and catalyst occupies a different phase.[20] In a real sense, reaction systems typically consist of a solid phase catalyst and a gas or liquid phase substrate. Compared to homogeneous catalyst, ease of process operation is the biggest advantage of heterogeneous (solid) catalyst. Heterogeneous (solid) catalysts have main active sites on their robust surfaces. It can work under harsh reaction conditions without deactivation of catalyst. These simple facts are the reason why heterogeneous (solid) catalyst has been used extensively in many industrial processes. Heterogeneous catalysts can have two possible working mechanisms: Langmuir-Hinshelwood (L-H) mechanism and Eley-Rideal (E-R) mechanism (Figure 4).[21] In the L-H mechanism, both molecules A and B are adsorbed on the active site, and reaction takes place and generates product C. In the E-R mechanism, molecule A is adsorbed on the catalyst surface and react with molecule B, which is staying in a different phase.

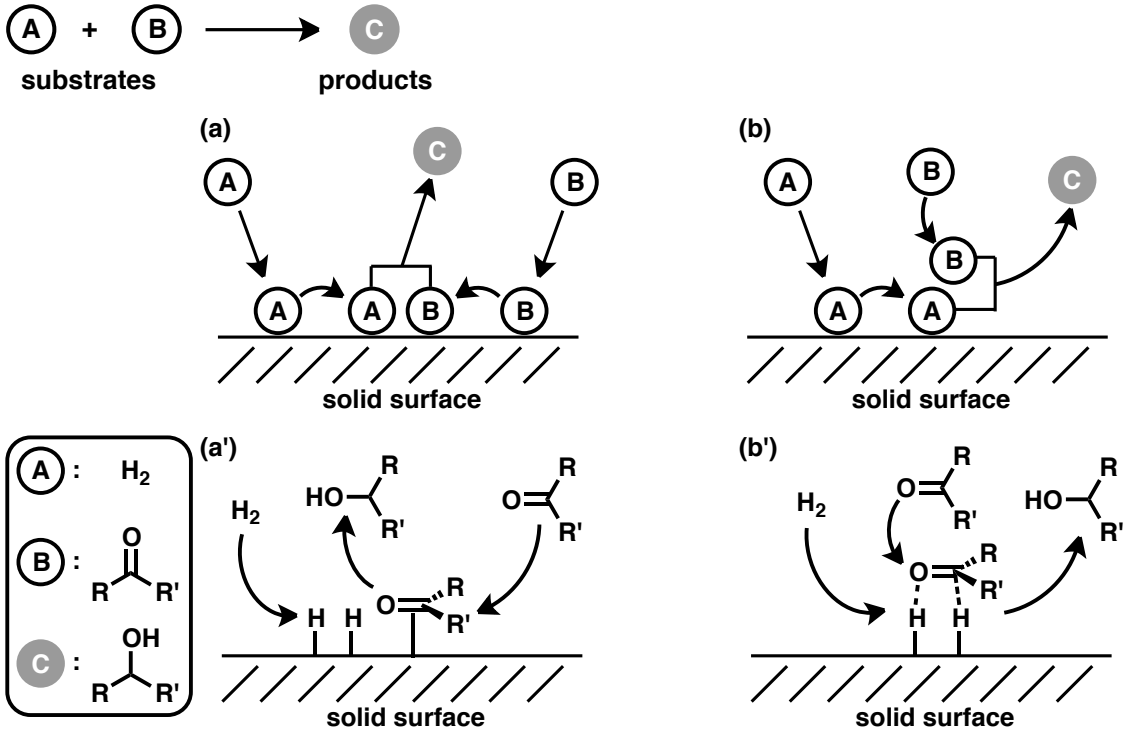

Figure 4. Catalytic reaction on solid surface: (**a**) Langmuir-Hinshelwood (L-H) mechanism; (**b**) Eley-Rideal (E-R) mechanism; (**a'**) Carbonyl hydrogenation via L-H mechanism; (**b'**) Carbonyl hydrogenation via E-R mechanism.

The L-H mechanism is advocated for hydrogen ("A" in Fig. 4) addition to ethylene[22] ("B" in Fig. 4) due to high adsorptive property of carbon–carbon double bond. On the other hand, hydrogenation of carbonyl compounds ("B" in Fig. 4) is supposed to be possible through both mechanisms. This is because sterically bulky carbonyl groups show poor ability to be adsorpted on the solid surface, whereas hydrogen is adsorbed more preferentially (Figures 4a' and 4b').

Maihle and coworkers reported the first hydrogenation of amide with heterogeneous catalyst in 1908 (Scheme 3).[23] They transformed vaporized amides such as acetamide and propionamide into a mixture of the corresponding primary (1°) and secondary (2°) amines by using a Ni catalyst. However conversion of substrates and yields of products were not determined accurately.

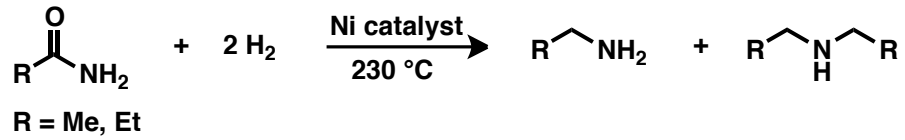

Scheme 3. The first hydrogenation of amide: Maihle, A. (1908).

Adkins and coworkers reported one of the most important researches in the initial-stage development of heterogeneous amide hydrogenation. With the aid of copper-chromium oxide, hydrogenation of 1°, 2° and tertiary (3°) amides were achieved in 1934 (Scheme 4).[24] However these reaction systems suffer from chemoselectivity. Hydrogenation of 1° amides under the optimized reaction conditions (hydrogen pressure (P_{H2}) = 20–30 MPa, reaction temperature (T) = 250 °C) led to the formation of the 2° amine as major product, for example, *n*-heptylamide was transformed to *n*-heptylamine (39%) and di(*n*-heptyl)amine (58%).

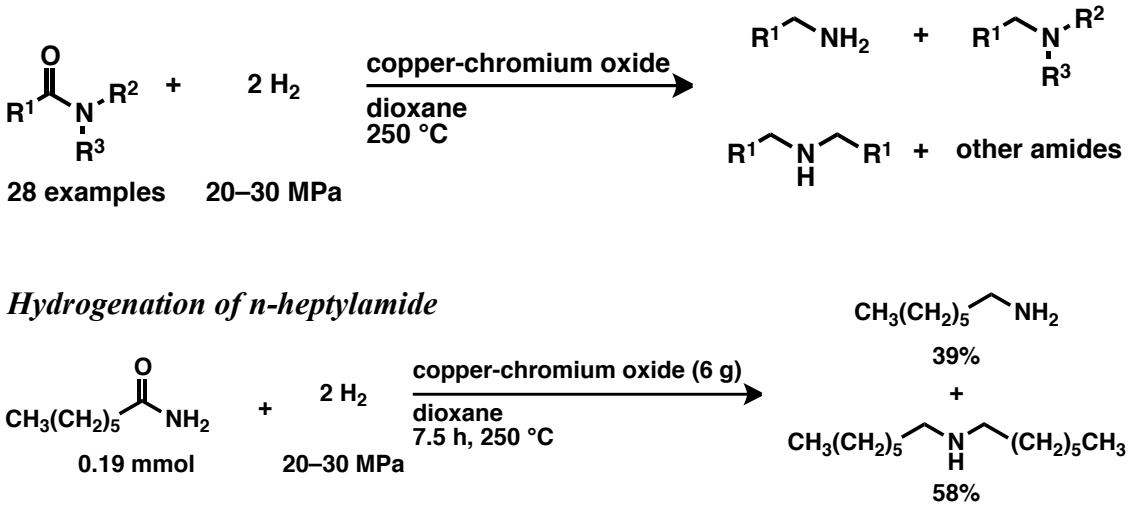

Scheme 4. Important researches in the initial-stage of amide hydrogenation: Adkins, H. (1934).

After Adkins's report, bimetallic or multimetallic catalysts have been studied extensively in the field of amide hydrogenation. Fuchikami and coworkers reported an important results in 1996 (Scheme 5a).[25a] They prepared a variety of heterogeneous catalysts by combining transition metals from groups 8–10 with groups 6 and 7. Use of different metal–carbonyl complexes showed different catalytic activities, and a combination of $Rh_6(CO)_{16}$ and $Re_2(CO)_{10}$ provided as one of the most active catalysts. However these catalyst systems are also facing low chemoselectivity, for example, benzene ring reduction of aromatic amides. When the Rh^0/Re^0 catalyst system was used under P_{H2} = 10 MPa with T = 180 °C and t = 16 h, *N*-(cyclohexylmethyl)ethanamine was obtained in 88% yield from *N*-benzylacetamide. In 2010, Whyman and coworkers reported hydrogenation of amides with $Ru_3(CO)_{12}$ and $Mo(CO)_6$ (Scheme 5b).[25b] They demonstrated recyclability of catalyst. The residue of the reaction mixture was separated by centrifugation, and the supernatant liquid containing products was removed from the mixture. After several washing of the solid residue with 1,2-dichloroethane, the resulting catalyst residue was dried and reused. However, this catalyst system also incurred with low chemoselectivity as in the case of Fuchikami's results.

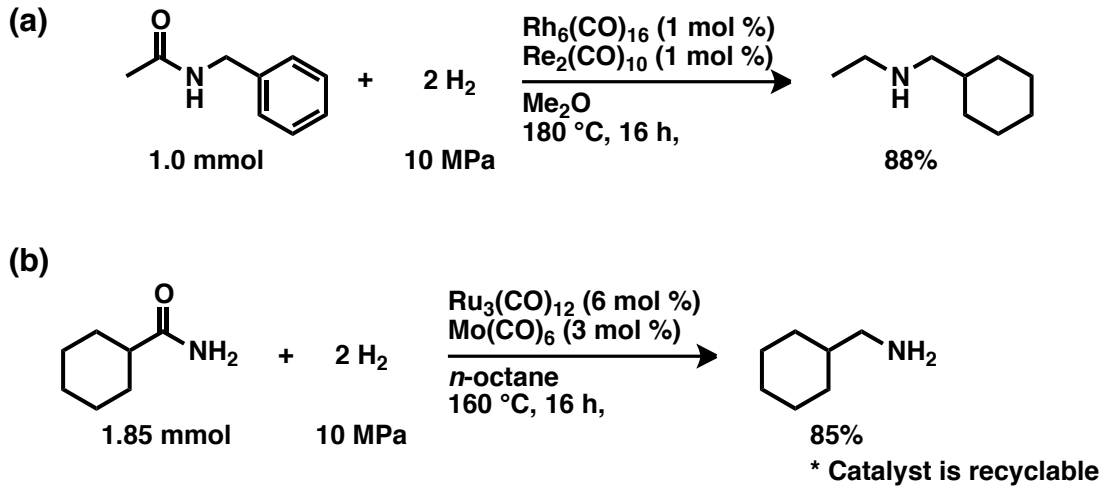

Scheme 5. Hydrogenation of amides with bimetallic catalyst: (**a**) Fuchikami, T. (1996); (**b**) Whyman, R. (2010).

In 2013, Breit reported a catalytic hydrogenation of rather activated amides such as anilides under milder conditions with Pd/Re/graphite (Pd 2%, Re 10%; P_{H2} = 3 MPa, T = 160 °C) (Scheme 6).[26] This heterogeneous catalyst was synthesized by loading Pd and Re on a graphite support. Prior to their report, at least P_{H2} = 10 MPa was necessary for the hydrogenation of amides using heterogeneous catalysts. 2° and 3° amides were hydrogenated and higher amines were obtained selectively as products with C=O bond cleavage. When the reaction temperature was increased and the reaction time was prolonged, high yields can be achieved even with relatively deactivated and bulky amides such as *N-tert*-butyl-isobutyramide. The catalyst can be removed from the reaction mixture by filtration and it is reusable. However, benzene rings do not withstand the active hydrogenation catalyst and is readily converted into the corresponding cyclohexyl groups. Hydrogenation of 1 ° amides generates 2° amines in preference to 1° amines.

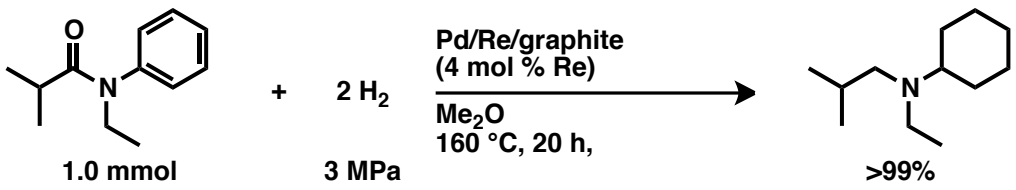

Scheme 6. Pd/Re/graphite (Pd 2%, Re 10%) catalyzed amide hydrogenation: Breit, B. (2013).

As summarized in this section, heterogeneous systems provide competent catalysts that have high activity and endurance. Nevertheless, these catalysts also have some drawbacks such as chemoselectivity, needs of harsh reaction conditions, and so on. On the other hand, it is difficult to gain an molecular insight into the nature of heterogeneous catalyst systems, because the reaction proceeds on solid surface, which has diverse natures owing to the existence of different islands (different active sites) that have different reactivity. Therefore, molecularly well designed heterogeneous catalyst is barely possible.

1.2.2. Homogeneous hydrogenation of amides

During the course of homogeneous catalysis, catalyst is in the phase identical to that of substrates and products — most often in liquid phase.[20b] Thus, detailed information of the active species is possible to be acquired. The reaction mechanism can be elucidated through detection and/or isolation of the possible intermediate species or in situ spectroscopic analysis by characterization methods including NMR, electron spray ionization-mass spectroscopy (ESI-MS) and IR. Electronic nature and reactivity of homogeneous catalysts can suitably be tuned by changing ancillary ligands. Many homogeneous catalysts offer potential advantages of high selectivity and are suited for controlled synthesis of high-value-added fine chemicals.

Kilner and coworkers issued a patent of the homogeneous catalytic hydrogenation of amide in 2003 (Scheme 7a).[27a] Their catalyst was prepared from $Ru(acac)_3$ and triphos. The 1° amide **1** was hydrogenated under P_{H2} = 6.8 MPa, with T = 164 °C and t = 14 h. A mixture of 2° amine **2**, 1° alcohol **3**, ester **4** and 2° amide **5** were obtained; however, yields of products were not determined quantitatively. In 2007, Cole-Hamilton and coworkers tried to improve the chemoselectivity in the same catalytic system by adding water. However, the chemoselectivity was still not satisfying: *ca.* a 1:1 mixture of 2° amine **7** (48%) and 3° amine **8** (51%) was obtained by the hydrogenation of 1° amide **6** under P_{H2} = 4 MPa, with T = 164 °C and t = 14 h (Scheme 7b).[27b] In 2013, Cole-Hamilton, Leitner and coworkers found that a catalytic amount of methanesulfonic acid (MSA) with $Ru(acac)_3$ and triphos can improve significantly the chemoselectivity in Ru/triphos catalyst systems (Scheme 7c).[27c] Hydrogenation of 2° and 3° amides were succeeded under P_{H2} =1 MPa, and the desired amines were obtained in up to 94% yield, albeit with high T (200–220 °C). Other side reactions, such as aromatic ring reduction,

barely proceeded. However the substrate scope is limited to activated amides, which have *N*-aryl substituents. In 2014, Leitner and coworkers reported hydrogenation of amides with Ru(triphos)(tmm) as catalyst precursor (Scheme 7d).[15] The catalyst precursor was transformed to a dihydride complex via oxidative addition of H_2. These Ru/triphos systems can catalyze amide hydrogenation in C=O bond cleavage fashion.

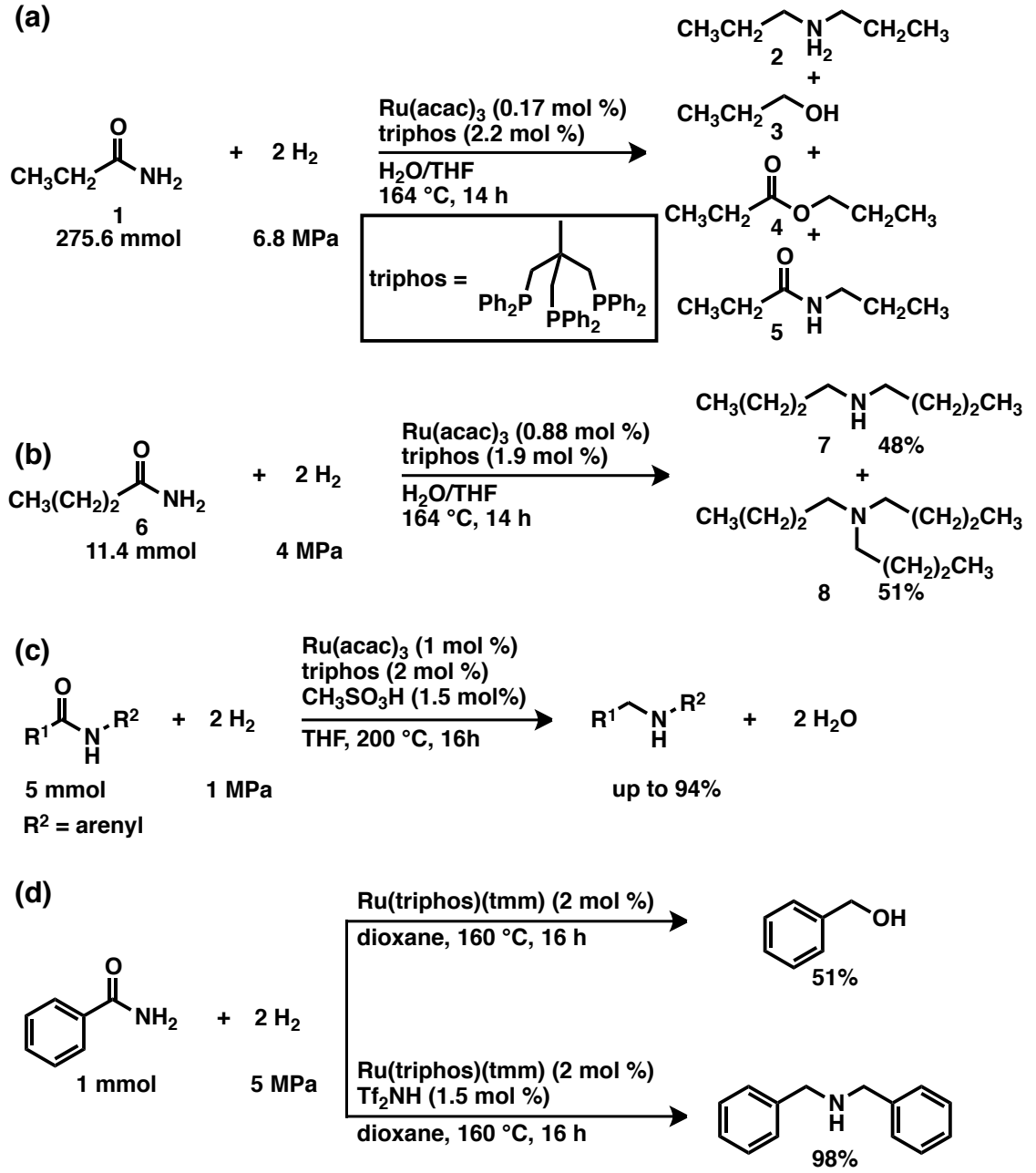

Scheme 7. Hydrogenation of amides with the aid of $Ru(acac)_3$ and triphos: (**a**) Kliner, M. (2003); (**b**) Cole-Hamilton, D. J. (2007); (**c**) Cole-Hamilton, D. J. and Leitner, W. (2013) ; (**d**) Leitner, W. (2014).

In 2007, Ikariya and coworkers reported selective C–N bond cleavage in imide hydrogenation, which should be following a pathway involving a bifunctional mechanism (Scheme 8a).[28a] A protic amine ligand (bearing NH groups) is playing an important role in this reaction. They synthesized a wide variety of Cp*Ru(PN) complexes from various kinds of PN-type bidentate ligands. This catalyst system shows high chemoselectivity and reaction conditions are mild (P_{H2} = 1–3 MPa, T = 80 °C, t = 2–24 h). Thenceforth, they have reported a set of nice pieces of work, related to hydrogenation of different carboxylic acid derivatives. In 2009, hydrogenation of *N*-acylcarbamates and *N*-acylsulfonamides was achieved with the same catalyst precursor (Scheme 8b).[28b] In 2010, hydrogenation of bicyclic imides was reported. The reaction conditions are relatively mild (P_{H2} = 3 MPa, T = 80 °C), and accommodate high chemoselectivity (Scheme 8c).[28c] In 2011, they reported new catalyst precursors [Cp*Ru(NN)] that contain NN type bidentate ligands (Scheme 8d).[28d] The catalysis is also designed to fit with the bifunctional mechanism. Similar to their previous works, this reaction system shows high selectivity, and is effective for hydrogenation of several reactive amides. These results indicate a catalyst designed based on the bifunctional mechanism is effective for hydrogenation of "difficult" substrates such as amides. However, there is much room for improvement of these systems in terms of catalytic activity, because the reported catalysts only hydrogenate a range of strongly or moderately activated amides. In contrast, a non-activated substrate, *N*-benzylpyrrolidinone, was reluctant to the hydrogenation under similar conditions.

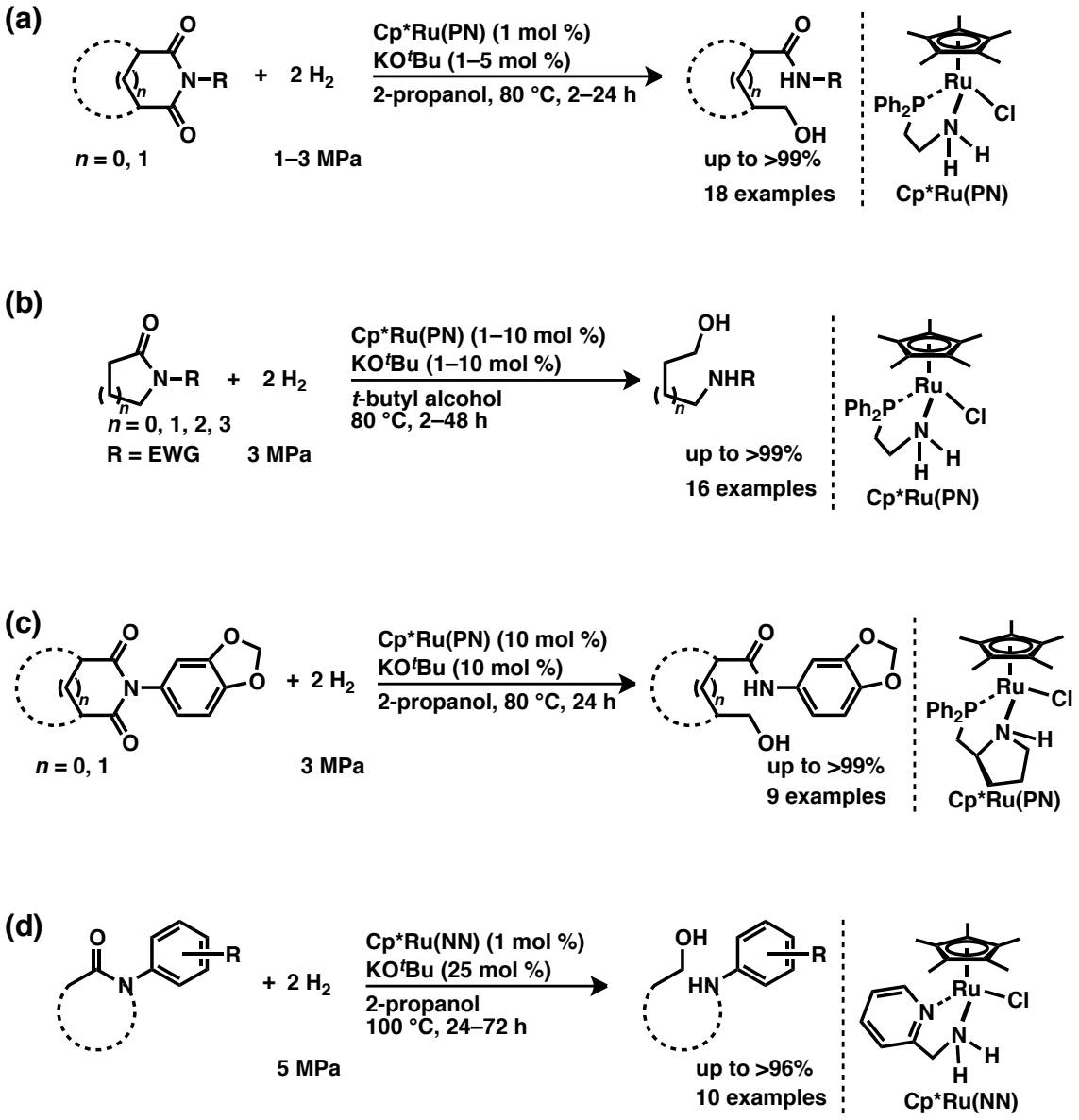

Scheme 8. Bifunctional catalysts for amide hydrogenation reported by Ikariya et al. (2007–2011).

In 2011, Bergens and coworkers reported a catalytic hydrogenation of amides with the aid of a Ru complex bearing a PN-type ligand (Scheme 9).[29] The catalyst precursor ($[Ru(\eta^3\text{-}C_3H_5)(Ph_2P(CH_2)_2NH_2)_2]BF_4$) was prepared with two molar equivalents of $Ph_2P(CH_2)_2NH_2$ and one molar equivalent of *cis*-$[Ru(CH_3CN)_2(\eta^3\text{-}C_3H_5)(cod)]BF_4$. These reactions were carried out with the Ru complex (0.1 mol %) and $KN[Si(CH_3)_3]_2$ (4–5 mol %) under P_{H2} = 5 MPa with T = 100 °C and t = 24 hours. The resulting Ru catalyst should bear protic amine ligands, so that the authors proposed that this catalyst should also be subjected to the bifunctional mechanism. They found that the activity of Noyori catalyst [Ru((*R*)-binap)$(H)_2$((*R*,*R*)-dpen)][30] towards activated amides, for instance, *N*-methylsulfonylpyrrolidin-2-one and *N*-acetyl- pyrrolidin-2-one was low to moderate. They reasoned that [Ru((*R*)-binap)$(H)_2$((*R*,*R*)-dpen)] is intrinsically active towards amide hydrogenation, but it decomposes at a higher temperature (>100 °C).

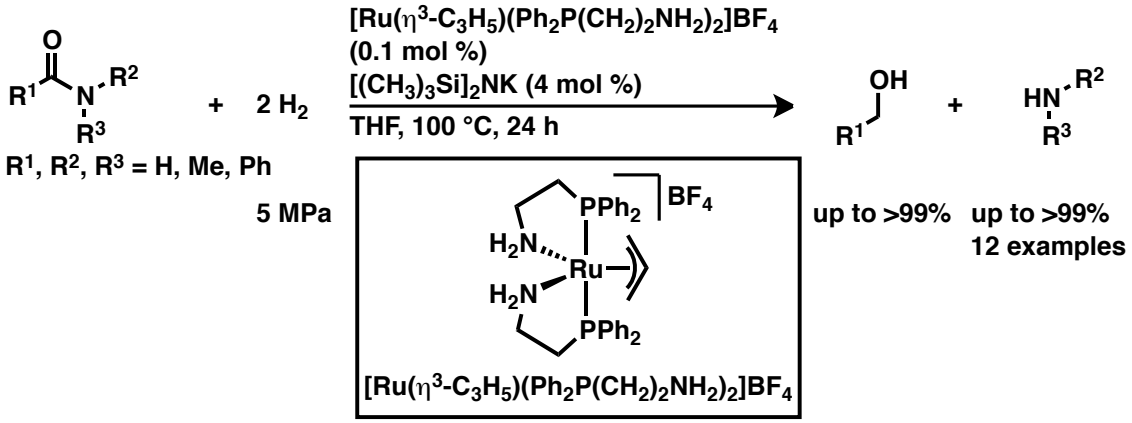

Scheme 9. Bifunctional catalyst for amide hydrogenation: Bergens, H. (2011).

In 2010, Milstein and coworkers reported hydrogenation of 2° and 3° amides with selective cleavage of C–N bonds (Scheme 10).[31] Their catalyst is a pincer type Ru complex, which was synthesized from 6-di-*tert*-butylphosphinomethyl-2,2'-bipyridine (PNN-type ligand). This catalyst system is comptent under comparatively mild reaction conditions (P_{H2} = 1 MPa, T = 110 °C, t = 48 h). Many rather activated amides, especially those containing an ether group at the α-position of the carbonyl group, can be hydrogenated effectively. They proposed a different mechanism from the bifunctional mechanism, where they advocate the catalytic cycle involving a direct interaction of Ru center and amide (see section 1.3.1., page 23).

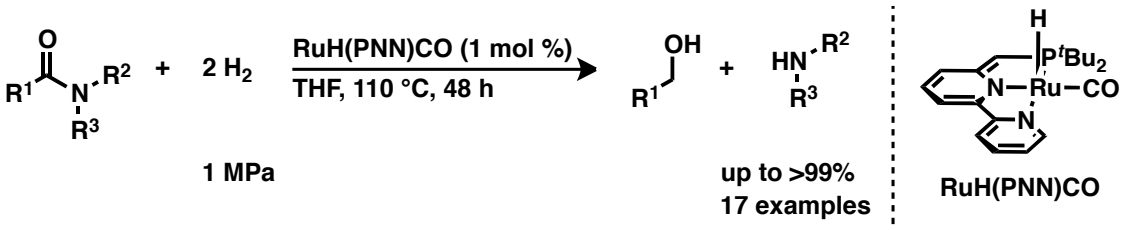

Scheme 10. Hydrogenation of amide with Ru(II)/bipyridyl-based pincer precatalyst: Milstein, D. (2010).

1.3. Mechanistic aspects of homogeneous hydrogenation/dehydrogenation

Homogeneous hydrogenation catalysis can be divided into two main categories, that involves inner-sphere mechanism and outer-sphere mechanism, in term of the addition pattern of hydrogen to the catalyst and reaction mode of substrate. In an inner-sphere mechanism, catalytic reaction proceeds via a direct interaction of a metal center with substrate such as carbonyl compounds (Figure 5a). On the other hand, an outer-sphere mechanism involves non-interaction of the metal center with substrate (Figure 5b).

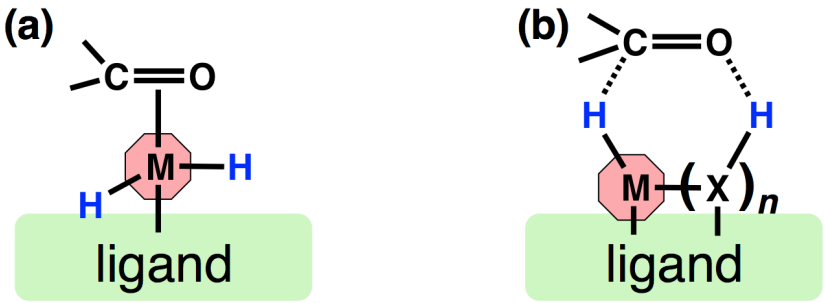

Figure 5. (a) Inner-sphere mechanism and (b) Outer-sphere mechanism (transition state) in hydrogenation.

1.3.1. Inner-sphere mechanism

The Wilkinson complex [$RhCl(PPh_3)_3$] (**9**) is one of the most widely used homogeneous catalysts, and the catalyst hydrogenate substrates through an inner-sphere mechanism.[32] It can be synthesized by reacting $RhCl_3 \cdot H_2O$ and an excess amount of PPh_3 in hot ethanol. This complex works excellently in hydrogenation of unsaturated hydrocarbons at ambient temperatures and pressures. Under hydrogenation conditions, coordinatively unsaturated species [$RhCl(PPh_3)_2$] (**10**) would be formed from Wilkinson complex [$RhCl(PPh_3)_3$] (**9**) by elimination of one phosphine ligand (PPh_3), and **10** works as catalyst.[32b] The sequence of the catalytic cycle involves, step 1: oxidative addition of H_2 (**10** + H_2 → **11**); step 2: forming a six-coordinate complex by addition of alkene (**11** + $R_2C{=}CR_2$ → **12**); step 3: alkene insertion into a rhodium-hydrogen bond to form an alkyl complex (**12** → **13**); step 4: reductive elimination of products and regeneration of catalyst (**13** → **10** + $R_2HC{-}CHR_2$) (Scheme 11). Kinetic studies concluded that hydride insertion into alkenes (step 3) is the rate-determining (turnover-limiting) step.

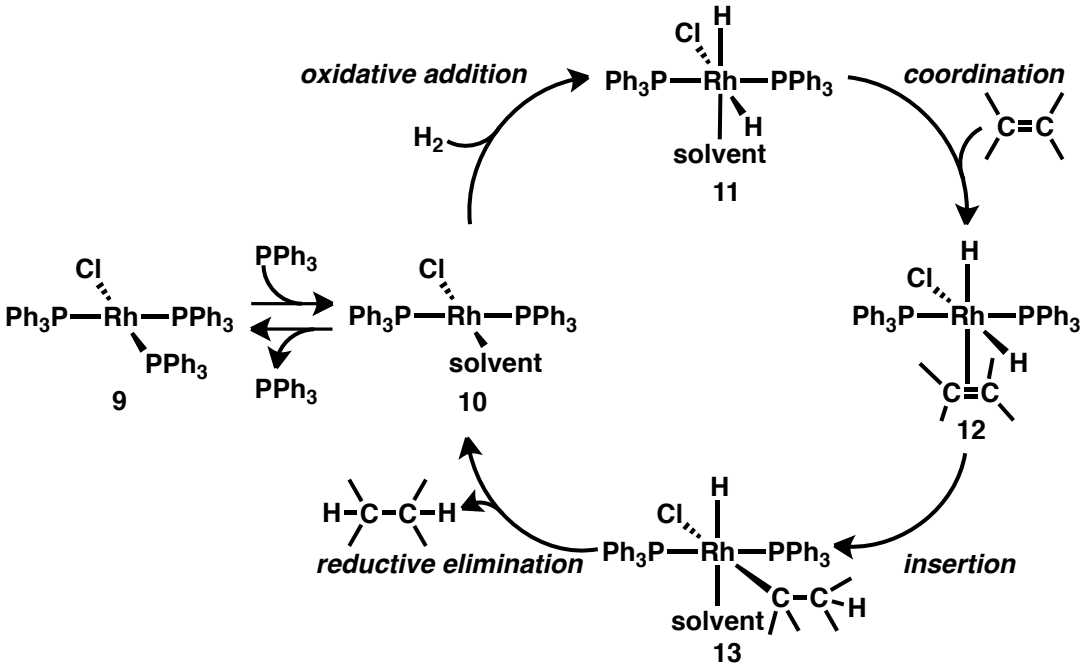

Scheme 11. Catalytic cycle of alkene hydrogenation with Wilkinson complex.

As described in section 1.2.2, Milstein and coworkers reported the catalytic hydrogenation of amides (Scheme 10), and they propose an inner-sphere mechanism (Scheme 12).[31] Initially, dihydrogen addition to complex **14** results in aromatization, to form the coordinatively saturated, trans dihydride complex **15**. Decoordination of a pyridyl "arm" provides a site for amide coordination, to give the complex **16**. Subsequent hydride transfer to the carbonyl group of the amide ligand leads to the complex **17**. Deprotonation of the benzylic arm by the adjacent NH group leads to the amine product and a complex **18**, bearing a coordinated aldehyde. H_2 addition to complex **18** forms the aromatic dihydride complex **19**, followed by hydride transfer to the aldehyde to generate the alkoxy complex **20**. Deprotonation of the benzylic arm by the alkoxy ligand generates the product alcohol and regenerates complex **14**. The overall process does not involve a change in the metal oxidation state (Ru^{II}).

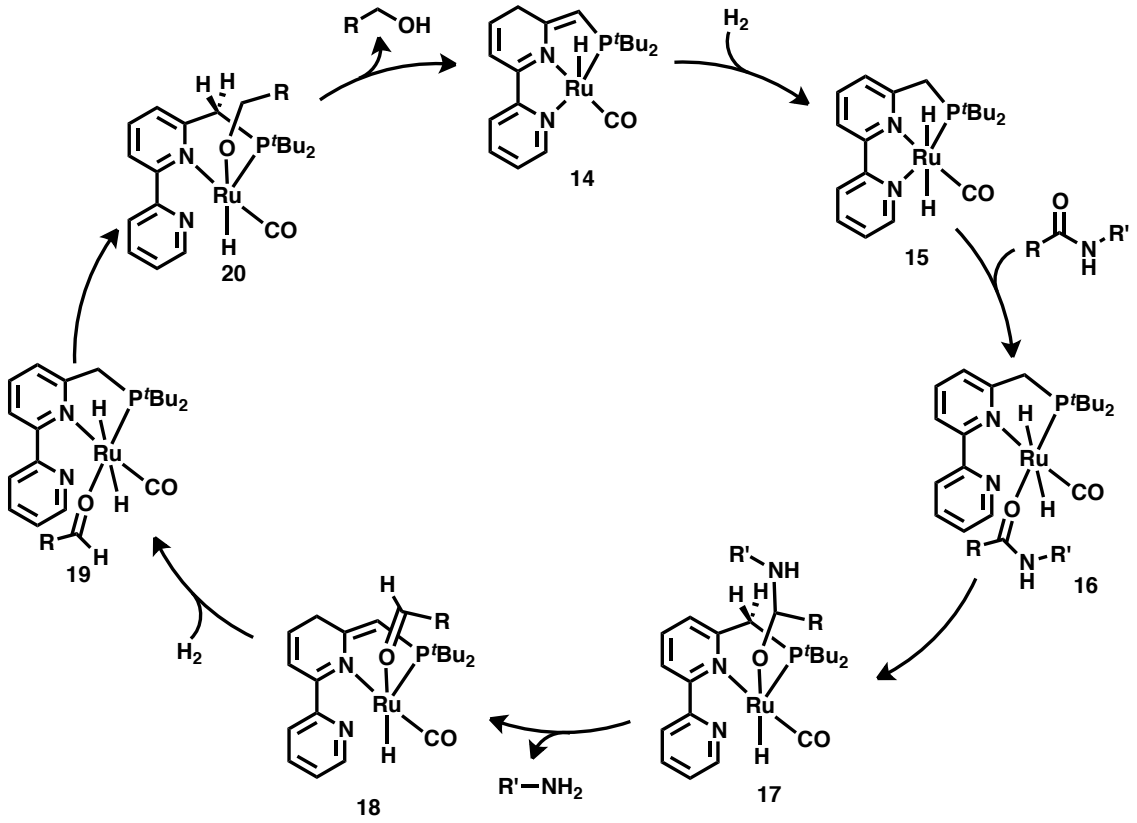

Scheme 12. Catalytic cycle of amide hydrogenation with Milstein's complex.

1.3.2. Outer-sphere mechanism

Many types of metal-ligand bifunctional catalysts, which catalyze the reaction through an outer-sphere mechanism, have been reported to date.[33] One of the first examples may be the Shvo's complex, which was reported in 1984.[34a] This catalyst is applicable for various hydrogen transfer reactions, including hydrogenation,[34b,c] transfer hydrogenation[34d] and Oppenauer-type oxidation.[34e,f] The precatalyst, a binuclear metal complex, is activated by heating, by which the binuclear complex dissociates into two active monoruthenium complexes, 18 electron complex **21** and 16 electron complex **22** (Scheme 13a).[34g] The complex **21** works as hydrogenation catalyst and **22** works as dehydrogenation catalyst. Based on the mechanistic studies done by Casey and coworkers,[34g] a bifunctional mechanism was proposed (Scheme 13b). The hydride from the metal center and the proton from the hydroxycyclopentadienyl ligand were transferred to the carbonyl group, without a direct interaction of substrate with the metal center.

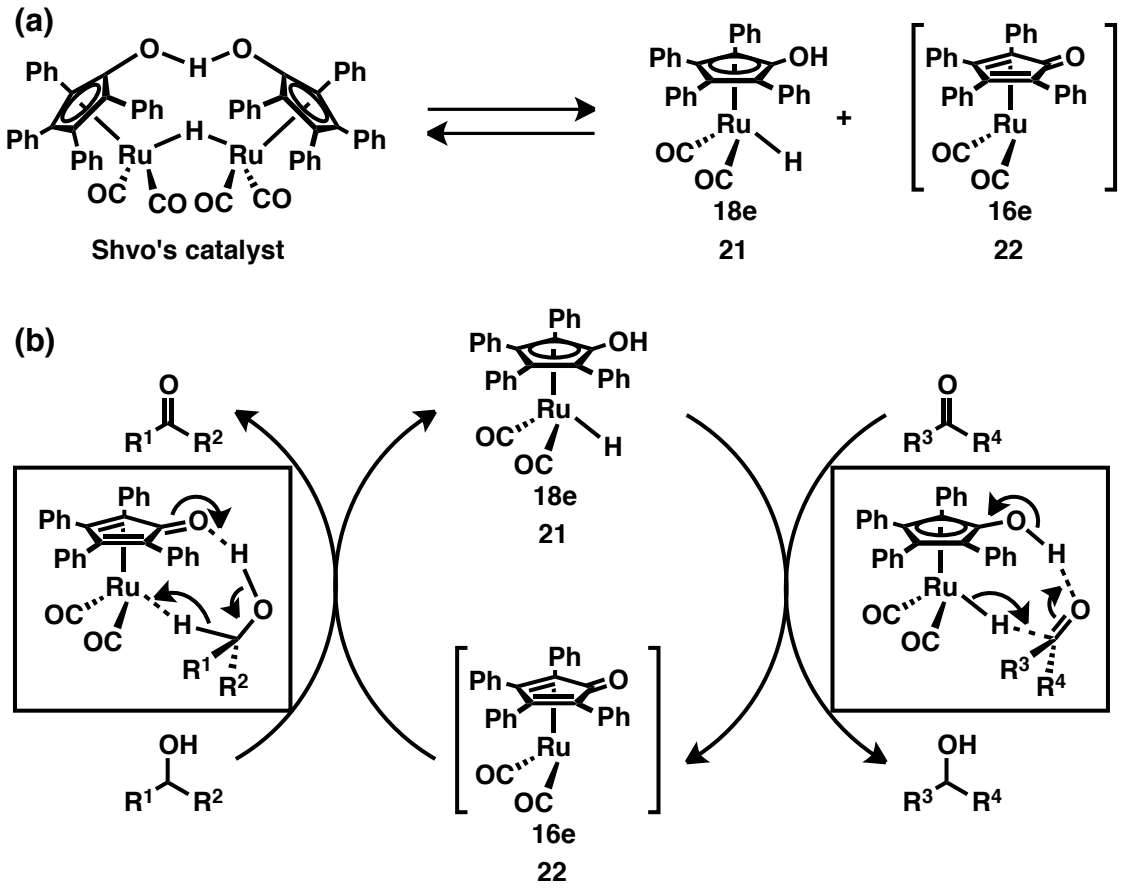

Scheme 13. Reaction mechanism of Shvo's catalyst.

Noyori and coworkers reported an asymmetric hydrogenation of ketones with Ru complexes. The reaction mechanism of this catalytst system was studied thoroughly (Scheme 14).[30] With assistance of a chiral diphosphine and a diamine ligand, a chiral 2° alcohol is obtained in high chemical yield with high enantiomeric ratio (*er*). This catalyst system involves an acid–base cooperative mechanism (Scheme 15). In the catalytic cycle, the 18e precatalyst **23** dissociates the BH_4^- to generate the cationic complex **24**, which upon deprotonation forms the 16e Ru amide complex **25**. All these steps are reversible, in principle. The cationic 16e complex reacts **24** with H_2 reversibly to form the 18e complex **26**, which undergoes deprotonation from the η^2-H_2 ligand to generate the Ru dihydride **27**. Reaction of **27** and ketone gives the 16e amido Ru species **25** and the alcoholic product. Protonation of the nitrogen atom of **25** by alcoholic solvent regenerates **24**. The coordinatively saturated metal complex **27** reacts with the organic substrate directly through a metal-ligand bifunctional mechanism. Thus, reduction of ketones with **27** proceeds via the six-membered pericyclic transition state, in which the C=O function does not interact with the Ru center. Delivery of a hydride from the Ru–H part and of a proton from the NH_2 ligand takes place simultaneously, giving alcohols without forming ruthenium alkoxide intermediates.

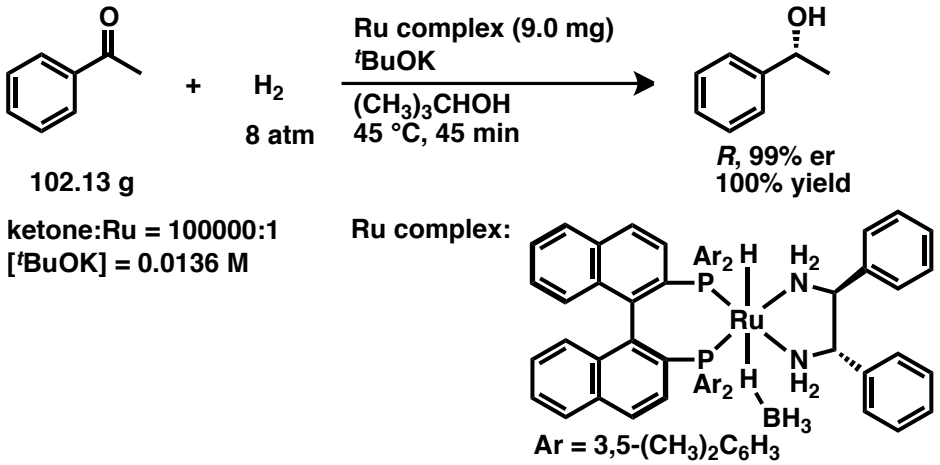

Scheme 14. Asymmetric hydrogenation of ketone with $RuCl_2$(diphosphine)(1,2-diamine) complexes reported by Noyori et al.

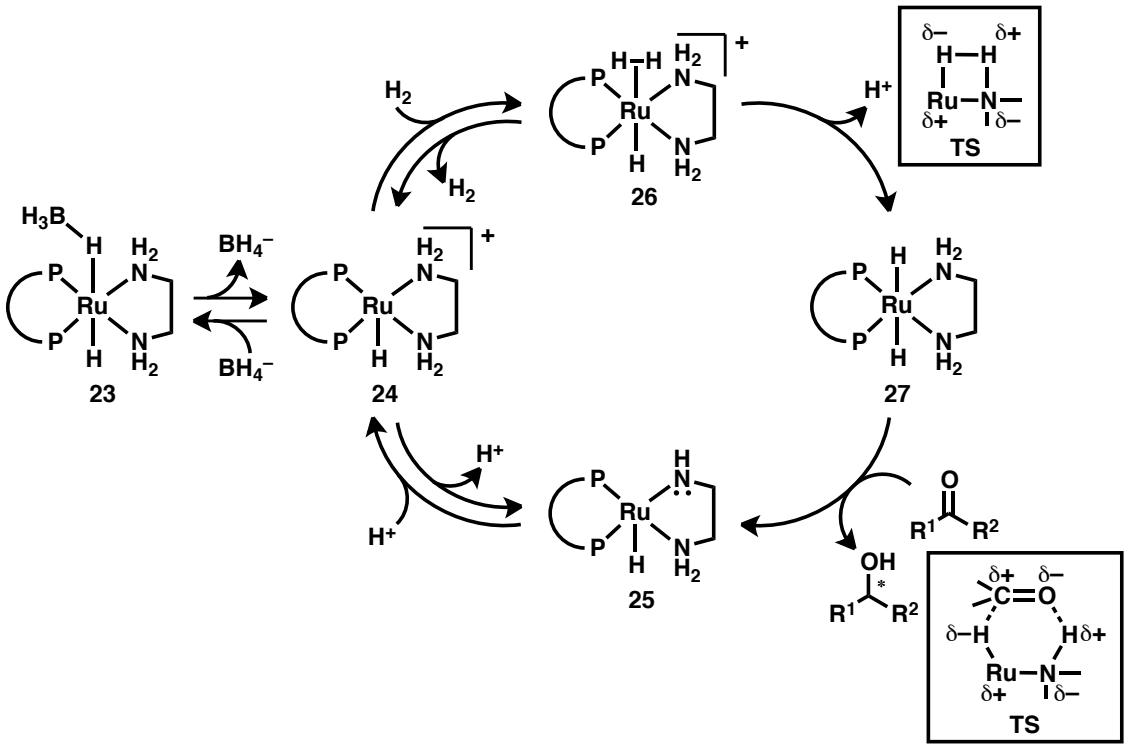

Scheme 15. Reaction mechanism of ketone hydrogenation: Six-membered ring transition state.

Fujita and coworkers reported an acceptorless alcohol dehydrogenation using Cp*Ir(bpyO) (bpyO = α,α'-bipyridonate) (Scheme 16).[35] This precatalyst works well under mild conditions, even in the dehydrogenation of aliphatic alcohols. The iridium center and the ligand bpyO work cooperatively via an aromatization/dearomatization of the pyridine rings. Catalytic cycle proceeds via alcohol dehydrogenation and elimination of molecular hydrogen from the iridium complex. The theoretical calculation indicate that an outer-sphere reaction is more favorable than an inner-sphere mechanism.[35c]

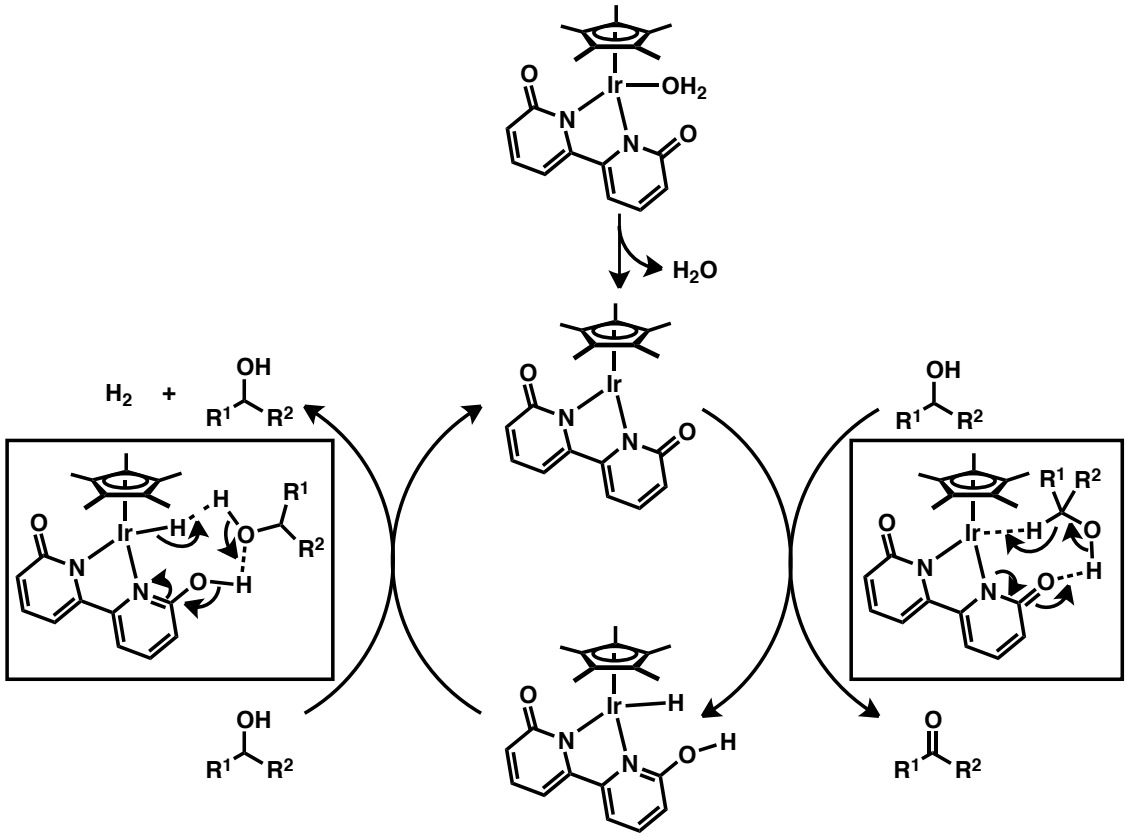

Scheme 16. Reaction mechanism of Fujita's catalyst.

As is clear from these investigations (Schemes 13–16), considering a bifunctional mechanism is a promising approach in new catalyst design for hydrogenation. However, in many cases, catalyst decomposition during the reaction is a significant problem to be addressed. A new concept, catalytic molecular surface (robust catalyst), would be more effective to retain the structure of the catalyst, which is one of the most important topics should be discussed in this thesis.

1.4. Concept of catalytic molecular surface

As discussed in previous sections, homogeneous and heterogeneous catalysts are working in hydrogenation of some special classes of amides, but each of them incurs different kinds of drawbacks.[12] Thus, the author comes out with a new concept called "catalytic molecular surface" (Figure 6). To solve the issues, the author planned not only to synthesize flexibly, but also to finely tune a homogeneous catalyst so that structural robustness of heterogeneous catalysts could be put into the homogeneous catalyst.

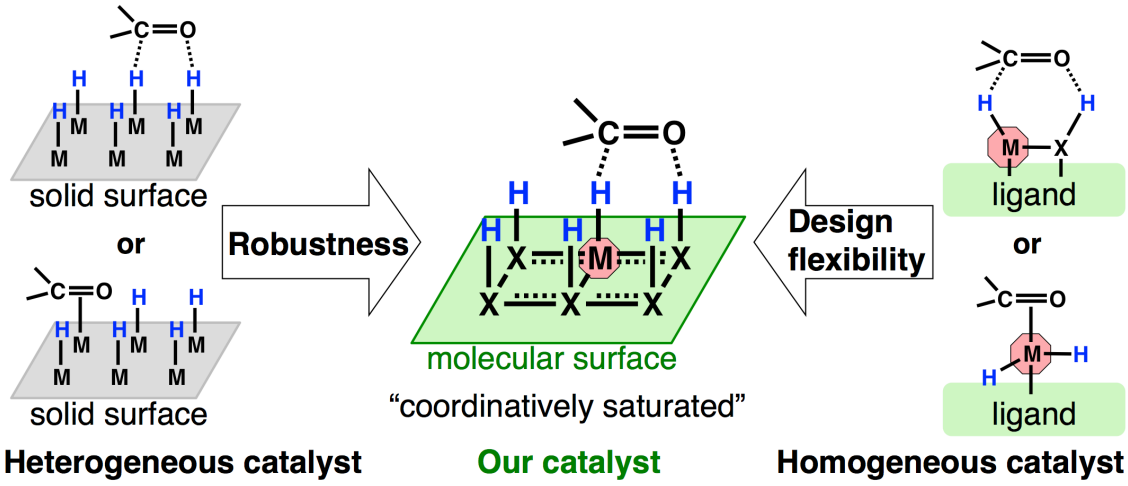

Figure 6. Concept of catalytic molecular surface.

Structural robustness of catalyst is important because it can increase ability to withstand harsh reaction conditions. The newly designed molecular surface consists of a Ru and ligands that make a coordinatively saturated Ru center. In addition, the catalyst is tailor-made by taking into account the concept of bifunctional mechanism.[33] This kind of arrangement would preclude a substrate to have a direct interaction (coordination) with a Ru center. By doing so, a chance of substrate- or product-inhibition of catalyst would also be reduced to a minimum extent. Additionally, hydrogen transfer to amide carbonyls would be kinetically accelerated through a stabilized transition state, in which substrate could directly interact with two hydrogen atoms on a catalytic molecular surface.

Another essence inherent to and also the most intriguing aspect of "catalytic molecular surface" is structural and reactivity diversity of active catalyst, which can be derived by diverse activation of the same precatalyst "molecular surface" (Figure 7). By controlling catalyst preactivation conditions, the number of hydrogen atoms adsorbed on the catalytic molecular surface can be varied. In other words, different adsorption modes of hydrogen atoms on the catalytic molecular surface cause different reactivity among catalysts, and thus different substrate–catalyst interactions. Thus, the author foresee a wide range of potential application of the catalytic molecular surface in the diverse research fields of hydrogenation. In preceding attempts, a precatalyst is designed specifically to work for one target reaction: for one functional group conversion or one C–X (X = H, C, N, O, etc.) bond formation or cleavage reaction, namely, different catalysts are developed on one-by-one basis. This approach finally leads to chemoselectivity if the catalyst would be highly competent for transforming one out of different functional groups. However, an endeavor to synthesize and use one precatalyst leading to a single catalyst only applicable to one target reaction is cost- and time consuming. Given a metal complex precatalyst, which can be activated differently for achieving different catalytic reactions, such a versatile precatalyst would finally be more cost-efficient for many different applications and highly attractive for organic synthesis.

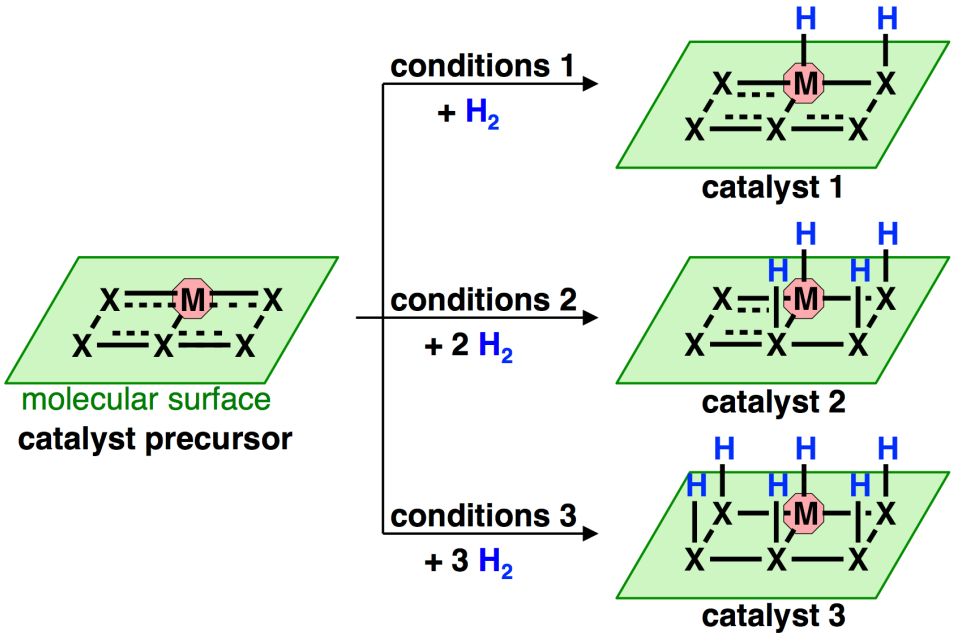

Figure 7. Generation of diverse catalysts from one catalyst precursor.

Although nobody has ever propose the concept of catalytic molecular surface, this concept is partially hidden behind some of the well-known catalysts — Milstein's catalysts. These catalysts comprise of pincer ligands containing a bipyridine frameworks. A molecular surface is made of a bipyridyl–CH_2–L unit and Ru center (Figure 8 and Schemes 10 and 12). They proposed the mechanism based on aromatization–dearomatization of the pyridyl methylene unit (see section 1.3.1., page 23).[31,36] Deprotonation of a pyridinylmethylenic hydrogen of pincer complexes **20** can lead to dearomatization. Then, the dearomatized complex **14** regains aromatization via splitting of one molecular hydrogen into two hydrogen atoms. Additionally, the outcome of DFT calculation demonstrates that the interaction of substrate not only limited to the activated hydrogen of N–H, but also potentially possible with the C–H on the dearomatized pyridine ring in the pincer ligand.[36] Therefore, many tautomers in an equilibrium could be assumed, and one or more of C–H hydrogen atoms of tautomers may also have a chance to involve in hydrogen transfer processes (Figure 8).

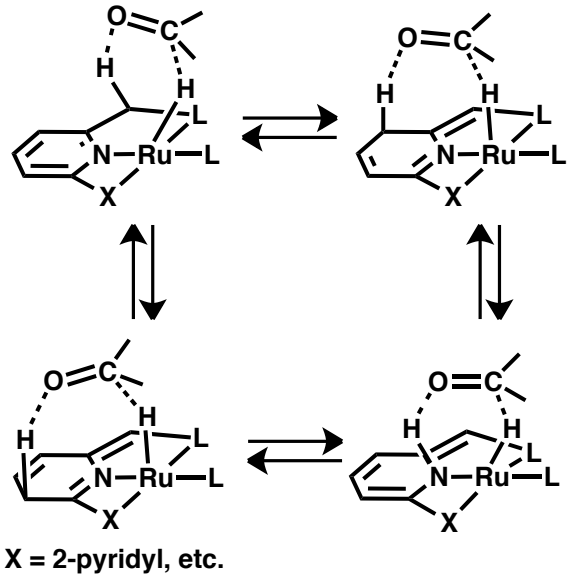

Figure 8. Plausible equilibrium of a catalytic molecular surface by tautomerization.

2. Survey of this thesis

In this thesis, the author has developed a novel concept called catalytic molecular surface. Since previous ruthenium complexes, which have been widely used in hydrogenation catalysis, seem not to be suitable for hydrogenation of unactivated amides, new ruthenium complexes introduced by us are used in this study as precatalysts. Hydrogen atoms on the molecular surface (Ru–H and N–H or C–H) are foreseen to enhance concerted hydrogen transfer. Ru–H is used for hydride transfer and both N–H and C–H would have chance to involve in proton transfer. In this way, the energy barrier for overall hydrogen transfer becomes lower and the reaction proceeds smoothly via bifunctional mechanism.

In Chapter 1, a general method for catalytic hydrogenation of unactivated amides was achieved under rather harsh reaction conditions (P_{H2} = 2–8 MPa, T = 120–160 °C) using RUPCY as a first generation precatalyst (Scheme 17). During the induction period of catalyst, the interior unsaturated bonds of the pyridines ligand in RUPCY were fully hydrogenated. On the other hand, a large amount of hydrogenated ligands liberated from the Ru center was detected. In other words, only a small amount of catalyst is working. Nevertheless, the reaction mechanism is expected to be subjected to a bifunctional mechanism. Even if one of the two ligands would be fallen apart, the Ru catalyst having a H–Ru–N–H functionality can still be retained. Then, the hydrogenation should proceed with the outer, rather than the inner, sphere of the Ru catalyst.

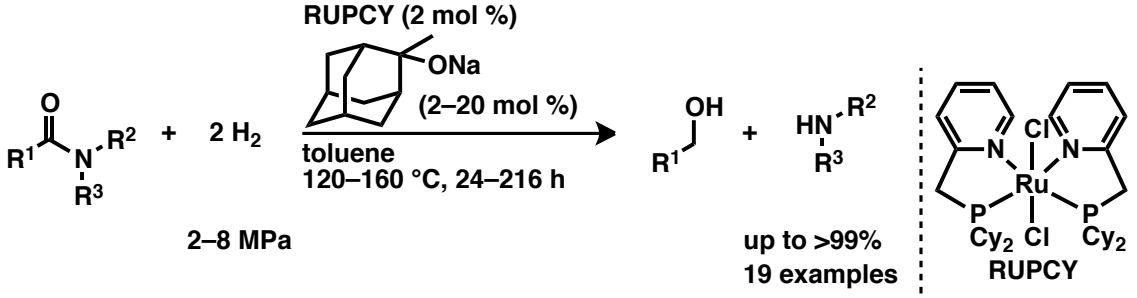

Scheme 17. Hydrogenation of unactivated amides using RUPCY.

In Chapter 2, structural modifications of RUPCY are carried out to improve a poor robustness of RUPCY which is reported in Chapter 1. The new precatalysts are RUPIP2 and RUPCY2. They provide as much more robust "molecular surface" and the Ru–ligand platform framework can survive even under harsh reaction conditions because the ligand has a higher coordination ability than the bidentate ligand of RUPCY (Figure 9). Through diverse activation of a "molecular surface" (a group of 15 planar atoms) incorporated into RUPCY2 and RUPIP2, catalytic hydrogenation of a variety of amides (formamides through polyamides) is achieved under a wide range of reaction conditions (Scheme 18). That is, versatile "catalytic molecular surfaces" (catalyst diversity) is induced by diverse activation of a single molecular surface within the precatalyst when the conditions are varied. According to the electrospray ionization mass spectroscopy (ESI-MS), different "catalytic molecular surface" have different numbers of adsorbed hydrogen atoms and resting state structures. Nevertheless, the common active site in the different structures should be the "H–Ru–N–H" group, but the involvement of "H–Ru–N=C–C–H" group for hydrogen transfer to the carbonyl group of amides could not be fully ruled out.

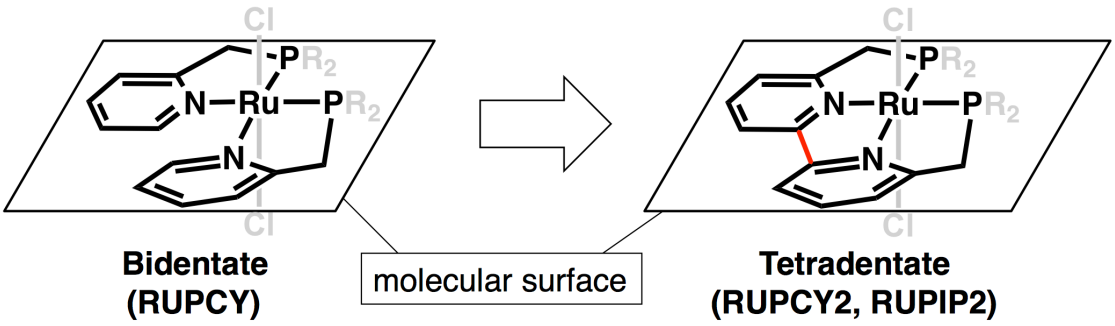

Figure 9. Improvement of the catalyst precursor by small modification.

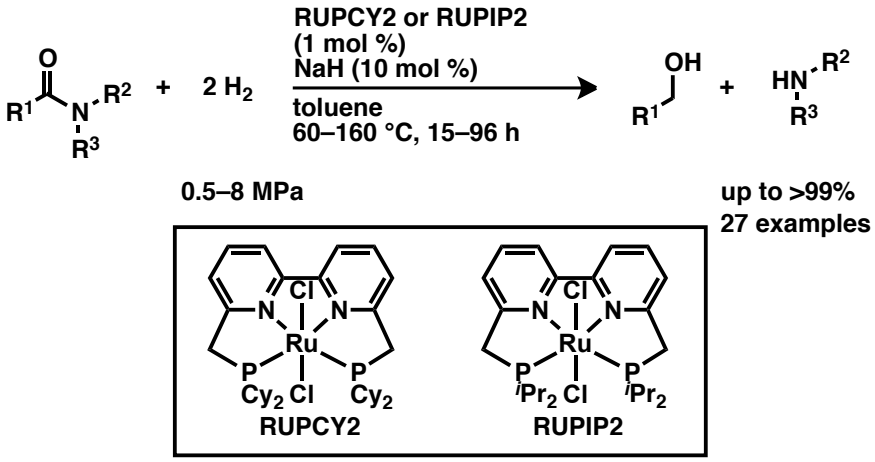

Scheme 18. Hydrogenation of amides with improved catalyst precursor (RUPIP2 or RUPCY2).

In Chapter 3, substrate scope of RUPCY-, RUPCY2-, and RUPIP2-promoted hydrogenation is thoroughly investigated. Since a diverse set of "catalytic molecular surface" can be generated from an identical precatalyst via different activation methods, the reactivity and selectivity of substrates other than amides under different hydrogenation conditions were examined in the studies. As a result, hydrogenation of a range of unsaturated compounds was succeeded (Scheme 19). The concept and versatility of "catalytic molecular surface" is fully demonstrated and supported herein.

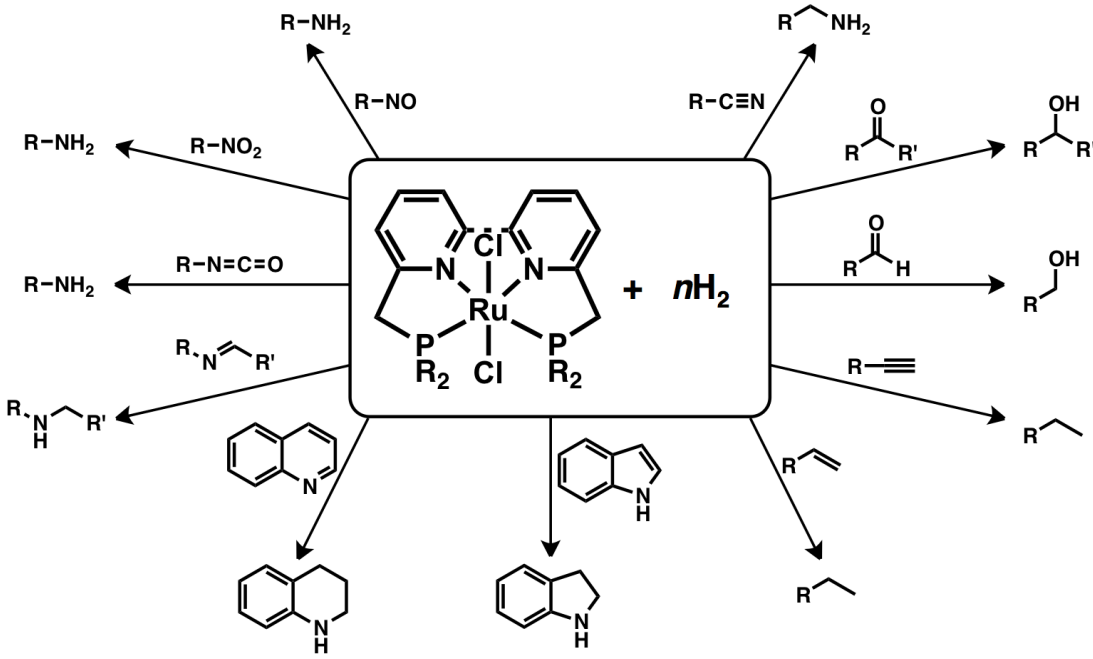

Scheme 19. Hydrogenation of unsaturated compounds with single precatalyst.

3. Reference

(1) (a) *Industrielle Organische Chemie*; Weissermel, K.; Arpe, H.-J., Eds.; VCH Verlagsgesellschaft mbH: Weinheim, 1994. (b) Navarro Yerga, R. M.; Fierro, J. L. G. *Chem. Rev.* **2007**, *107*, 3952–3991.

(2) (a) Kudo, A.; Miseki, Y. *Chem. Soc. Rev.* **2009**, *38*, 253–278. (b) Navarro Yerga, R. M.; Galván, M. C. Á; del Valle, F.; de la Mano, J. A. V.; Fierro, J. L. G. *ChemSusChem* **2009**, *2*, 471–485.

(3) Anastas, P. T.; Kirchhoff, M. M. *Acc. Chem. Res.* **2002,** *35*, 686-694.

(4) (a) Huber, G. W.; Iborra, S.; Corma, A. *Chem. Rev.* **2006,** *106*, 4044−4098. (b) Corma, A.; Iborra, S.; Velty, A. *Chem. Rev.* **2007,** *107*, 2411−2502. (c) Alonso, A. M.; Bond, J. Q.; Dumesic, J. A. *Green Chem.* **2010**, *12*, 1493–1513. (d) Chheda, J. N.; Huber,G. W.; Dumesic, J. A. *Angew. Chem. Int. Ed.* **2007**, *46*, 7164 – 7183.

(5) (a) Baxter, L. *Biomass and Bioenergy* **1993**, 4, 85–102. (b) Sjöström, K.; Chen, G.; Yu, Q.; Brage, C.; Rosén, C. *Fuel* **2005**, 84, 1295–1302. (c) Baxter, L. *Fuel* **2005**, 84, 1295–1302.

(6) (a) Morrison, A. L.; Long, R. F.; Konigstein, M. *J. Chem. Soc.* **1951**, 952–955. (b) Micovic, V. M.; Mihailovic, M. L. *J. Org. Chem.* **1953**, *18*, 1190–1200. (c) Hinman, R. L. *J. Am. Chem. Soc.* **1956**, *78*, 2463–2467.

(7) (a) Ellzey, S. E.; Mack, C. H.; Connick, W. J. *J. Org. Chem.* **1967**, *32*, 846–847. (b) Kikugawa, Y.; Ikegami, S.; Yamada, S. *Chem. Pharm. Bull.* **1969**, *17*, 98–104.

(8) (a) Yanagita, Y.; Nakamura, H.; Shirokane, K.; Kurosaki, Y.; Sato, T.; Chida, N. *Chem. Eur. J.* **2013**, *19*, 678–684. (b) Nahm, K. *Bull. Korean. Chem. Soc.* **2014**, *35*, 546–550.

(9) Affani, R.; Dugat, D. *Synthetic Communications* **2007**, *37*, 3729–3740.

(10) (a) Brown, H. C.; Heim, P. *J. Org. Chem.* **1973**, *38*, 912–916. (b) Alcantara, A. F. D.; dos Santos Barroso, H.; Pilo-Veloso, D. *Quim. Nova* **2002**, *25*, 300–311.

(11) Sunada, Y.; Kawakami, H.; Imaoka, T.; Motoyama, Y.; Nagashima, H. *Angew. Chem. Int. Ed.* **2009**, *48*, 9511–9514.

(12) Smith, A. M.; Whyman, R. *Chem. Rev.* **2014**, *114*, 5477−5510.

(13) Martin, R. L.; Winters, J. C.; Williams, J. A. *Nature* **1963**, *199*, 110–113.

(14) Werkmeister, S.; Junge, K.; Beller, M. *Org. Process Res. Dev.* **2014**, *18*, 289−302.

(15) vom Stein, T.; Meuresch, M.; Limper, D.; Schmitz, M.; Hölscher, M.; Coetzee, J.; Cole-Hamilton, D. L.; Klankermayer, J.; Leitner, W. *J. Am. Chem. Soc.* **2014**, *136*, 13217−13225.

(16) Werpy, T.; Petersen, G.; Aden, A.; Bozell, J.; Holladay, J.; White, J.; Manheim, A.; Gerber, M.; Ibsen, K.; Lumberg, L.; Kelley, S. *Top Value Added Chemicals from Biomass, Volume II: Results of Screening for Potential Candidates from Sugars and Synthesis Gas;* Pacific Northwest National Laboratory: Richland, WA, 2007.

(17) Shiramizu, M.; Toste, F. D. *Angew. Chem. Int. Ed.* **2012**, *51*, 8082 –8086.

(18) (a) Noyori, R.; Hashiguchi, S. *Acc. Chem. Res.* **1997,** *30*, 97-102. (b) Klingler, F. D. *Acc. Chem. Res.* **2007,** *40,* 1367–1376.

(19) McAlees, A. J.; McCrindle, R. *J. Chem. Soc. C* **1969**, 2425–2435.

(20) (a) *Handbook of Heterogeneous Catalytic Hydrogenation for Organic Synthesis*; Nishimura, S., Ed.; Wiley-VCH: Weinheim, 1999. (b) *Inorganic and Bio-Inorganic Chemistry-Volume 2*; Bertiniaytexasphl, I., Ed.: Encyclopedia of Life Support Systems: 2009.

(21) Pöschl, U.;Rudich, Y.; Ammann, M. *Atmos. Chem. Phys*. **2007**, *7*, 5989–6023.

(22) (a) *Catalytic Chemistry*; Misono, M., Saito, Y., Eds.; Maruzen: Tokyo, 2009. (b) Laidler, K. J.; Townshend, R. E. *Trans. Faraday Soc.* **1961**, 57, 1590-1602.

(23) Maihle, A. *Chem. Ztg.* **1908**, *31*, 1146–1147.

(24) (a) Wojcik, B.; Adkins, H. *J. Am. Chem. Soc.* **1934**, *56*, 247– 2419. (b) Adkins, H. U.S. Patent 2143751, 1939.

(25) (a) Hirosawa, C.; Wakasa, N.; Fuchikami, T. *Tetrahedron Lett.* **1996**, *37*, 6749–6752. (b) Beamson, G.; Papworth, A. J.; Philipps, C.; Smith, A. M.; Whyman, R. *Adv. Synth. Catal.* **2010**, *352*, 869–883.

(26) Stein, M.; Breit, B. *Angew. Chem., Int. Ed.* **2013**, *52*, 2231–2234.

(27) (a) Kliner, M.; Tyers, D. V.; Crabtree, S. P.; Wood, M. A.; World Patent WO03/093208A1, 2003. (b) Magro, A. A. N.; Eastham, G. R.; Cole-Hamilton, D. *J. Chem. Commun.* **2007**, *43*, 3154–3156. (c) Coetzee, J.; Dodds, D. L.; Klankermeyer, J.; Brosinski, S.; Leitner, W.; Slawin, A. M. Z.; Cole-Hamilton, D. J. *Chem. Eur. J.* **2013**, *19*, 11039–11050.

(28) (a) Ito, M.; Sakaguchi, A.; Kobayashi, C.; Ikariya, T. *J. Am. Chem. Soc.* **2007**, *129*, 290–291. (b) Ito, M.; Koo, L. W.; Himizu, A.; Kobayashi, C.; Sakaguchi, A.;

Ikariya, T. *Angew. Chem., Int. Ed.* **2009**, *48*, 1324–1327. (c) Ito, M.; Kobayashi, C.; Himizu, A.; Ikariya, T. *J. Am. Chem. Soc.* **2010**, *132*, 11414–11415. (d) Ito, M.; Ootsuka, T.; Watari, R.; Shiibashi, A.; Himazu, A.; Ikariya, T. *J. Am. Chem. Soc.* **2011**, *133*, 4240–4242.

(29) John, J. M.; Bergens, S. H. *Angew. Chem., Int. Ed.* **2011**, *50*, 10377–10380.

(30) (a) Noyori, R.; Ohkuma, T. *Angew. Chem. Int. Ed.* **2001**, *40*, 40–73. (b) Ohkuma, T.; Koizumi, M.; Muñiz, K.; Hilt, G.; Kabuto, C.; Noyori, R. *J. Am. Chem. Soc.* **2002**, *124*, 6508–6509. (c) Sandoval, C. A.; Ohkuma, T.; Muñiz, K.; Noyori, R. *J. Am. Chem. Soc.* **2003**, *125*, 13490–13503.

(31) Balaraman, E.; Gnanaprakasam, B.; Shimon, L. J. W.; Milstein, D. *J. Am. Chem. Soc.* **2010**, *132*, 16756–16758.

(32) (a) Osborn, J. A.; Jardine, F. H.; Yung, J. F.; Wilkinson, G. *J. Chem. Soc. A*, **1966**, 1711–1732. (b) Halpern, J. *Inorg. Chim. Acta.* **1981**, *50*, 11–19.

(33) *Topics in Organometallic Chemistry 37 "Bifunctional Molecular Catalysis"*; Ikariya, T.; Shibasaki, M., Eds.; Springer: Heidelberg, 2011.

(34) (a) Blum, Y.; Shvo, Y. *Isr. J. Chem.* **1984**, 24, 144–148. (b) Shvo, Y.; Czarkie, D.; Rahamim, Y. *J. Am. Chem. Soc.* **1986**, *108*, 7400–7402. (c) Menashe, N.; Shvo, Y. *Organometallics* **1991**, *10*, 3885–3891. (d) Samec, J. S. M.; Bäckvall, J.-E. *Chem. Eur. J.* **2002**, *8*, 2955–2961. (e) Csjernyik, G.; Éll, A. H.; Fadini, L.; Pugin, B; Bäckvall, J.-E. *J. Org. Chem.* **2002,** *67*, 1657–1662. (f) Éll, A. H.; Samec, J. S. M.; Brasse, C.; Bäckvall, J.-E. *Chem. Commun.* **2002**, 1144–1145. (g) Casey,C. P.; Singer, S. W.; Powell, D. R.; Hayashi, R. K.; Kavana, M. *J. Am. Chem. Soc.* **2001,** *123*, 1090–1100.

(35) (a) Kawahara, R.; Fujita, K.; Yamaguchi, R. *Angew. Chem. Int. Ed.* **2012**, *51*, 12790–12794. (b) Fujita, K.; Tanaka, Y.; Kobayashi, M.; Yamaguchi, R. *J. Am. Chem. Soc.* **2014**, *136*, 4829–4832. (c) Zeng, G.; Sakaki, S.; Fujita, K.; Sano, H.; Yamaguchi, R. *ACS Catal.* **2014**, *4*, 1010–1020.

(36) Li, H.; Wang, X.; Huang, F.; Lu, G.; Jiang, J.; Wang, Z.-X. *Organometallics* **2011**, *30*, 5233–5247.

Chapter 1.

Catalytic Hydrogenation of Unactivated Amides Enabled by Hydrogenation of Catalyst Precursor

Abstract: The author developed a general method for catalytic hydrogenation of unactivated amides. During the catalyst induction period, a novel structural change was observed involving full hydrogenation of the interior unsaturated bonds of the pyridines of the Ru-containing catalyst precursor (RUPCY). Based on this observation, the mechanism of amide hydrogenation may involve a two-step pathway, wherein the Ru catalyst having an H–Ru–N–H functionality is generated in the first step, followed by the amide carbonyl group interacting with the outer, rather than the inner, sphere of the Ru catalyst.

1.1. Introduction

Amides[1a] are abundant functional groups which can be found, for example, in the repeating units of polypeptide macromolecules and artificial polymeric materials (e.g., polyacrylamide), nylons, Kevlar, and their respective monomers (e.g., α,β-unsaturated carboxamides, caprolactams), which can be produced on an enormous scale via existing industrial processes. They also exist as potent pharmacophores,[1d,e,g–i] which are useful building blocks accessible via many synthetic methods.[1b,c,f,j,k] Were it possible to develop catalytic transformations of amide resources without the salt-containing wastes formed in stoichiometric amounts with respect to the amide, such chemical processes would provide a shortcut or alternative route to presently known and/or unknown materials or chemicals. However, the salt-free transformation of amides[2] is a significant challenge, as there is a lack of basic knowledge concerning the catalytic activation. Such activation is frequently hampered by high thermodynamic stability[3] and kinetic inertness due to the low electrophilicity of the amide carbonyl carbon among carbon(x)yl functionalities.[1a] In particular, the catalytic hydrogenation of unactivated amides has rarely been accomplished using existing homogeneous catalysis methods. Recently, Cole-Hamilton,[4] Ikariya,[5] Milstein[6a] and Bergens[7] reported the use of different ruthenium (Ru) complexes which hydrogenate a range of strongly or moderately activated amides, including *N*-aryl-, *N*-acyl-, and α-alkoxy[8] amides and morpholino ketones, as well as relatively small amides. Heterobimetallic clusters are able to hydrogenate larger, more inert amides, whereby dehydrative cleavage of the C=O bonds affords higher amines, albeit with accompanying dearomatic hydrogenation.[9] The author reports a more general and selective method for the hydrogenation of unactivated amides, affording selective C–N or C=O bond cleavage using a new Ru complex (RUPCY) **1a**. (Scheme 1)

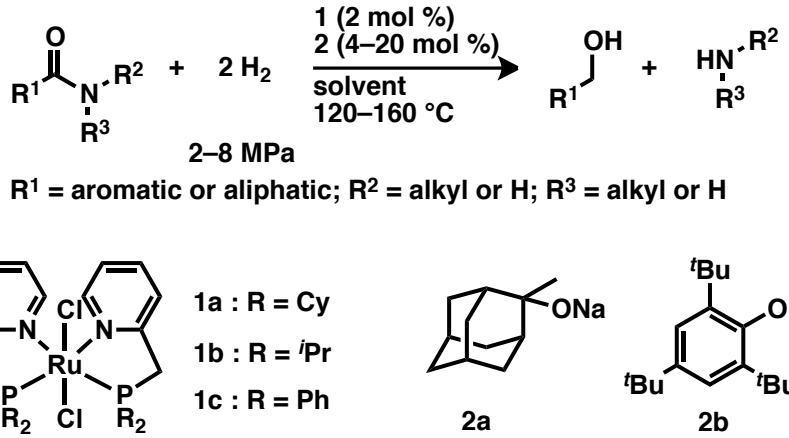

Scheme 1. Hydrogenation of unactivated amides using new Ru complex.

1.2. Results and discussion

1.2.1. Strategy and design of ruthenium catalyst.

Since the need for harsh reaction conditions was anticipated for this otherwise difficult unactivated amide hydrogenation, the 'structural robustness' of the catalyst precursor was the foremost consideration in the initial molecular design of a Ru complex catalyst. Such robustness may obviate the facile detachment of the ligands from the Ru center during the induction period of the catalyst. Accordingly, the emphasis was placed on imposing a 'coordinatively saturated Ru center' on a catalyst precursor with sterically demanding and strongly coordinative ligand(s), with the additional expectation that only an H_2 molecule could make easy access to the narrow space (though large enough to accept an H_2) around the metal center of an intermediate active species that subsequently forms a metal hydride. Indeed, the derivation of a metal hydride species from H_2 is frequently rate-determining.[10] To satisfy such primary criteria for catalyst design, a bidentate (*P,N*)-ligand[11,12] as in **1a** was chosen first (Scheme 1).[13] Additional Ru complexes **1b** and **1c** were also prepared for control experiments. Since *N*-benzylbenzamide (**3a**) was hydrogenated previously in moderate yield [**4a**: 57%; ruthenium complex (1 mol %), H_2 pressure (P_{H2}) = 1 MPa, 110 °C, 48 h],[6a] examination of **3a** is thought to be a good starting point for analysis.

1.2.2. Relationship between structure and catalytic activity of Ru complex 1a.

Treatment of a toluene solution of **3a** and **1a** (2 mol %) with sterically bulky base **2a** (20 mol %) under P_{H2} = 8 MPa at 160 °C for 24 h gave both **4a** and **5a** in 92% yield (Table 1, entry 1). The steric bulkiness of the base was more important than its basicity under similar conditions ([**1a**]$_0$ = 6.7 mM; P_{H2} = 6 MPa, 160 °C, 24 h): use of phenoxide **2b** in place of **2a** gave **4a** with similar effectiveness (entries 2, 3), while either NaO^{t}Bu, KO^{t}Bu, NaOMe, or NaOH was less satisfactory (**4a**: 43%, 27%, ~2%, and 31%, respectively; **5a**: 44%, 26%, ~1%, and 26%, respectively). Although toluene was the best solvent of those tested in terms of enabling smooth conversion of **3a**, a sterically more demanding alcohol solvent was better than a smaller one [**4a**: <1% (MeOH); 4% (EtOH); 45% (^{i}PrOH); 61% (^{t}BuOH). [**1a**]$_0$ = 6.7 mM; P_{H2} = 8 MPa, 160 °C, 24 h]. Ru complex **1b** showed a similar effectiveness but with formation of a byproduct (entry 4), while the reaction using **1c**[14] led to the formation of a fine, black powder precipitate, and almost full recovery of **3a** (entry 5). Obviously, the combined use of **1a** and a base additive such as **2a** or **2b**, both being sterically demanding, is crucial for selective hydrogenation. The preference for formation of Ru–OR with alkoxides of 1° alcohols [or partial formation of the Ru–O bond as in Ru$^+$(HOR)] was recently explained as being due to their higher acidity and lower steric congestion,[15] and this preference may be detrimental to the initiation of a catalytically active RuH species in the present system. In contrast, 4 mol % instead of 20 mol % of **2a** was satisfactory to obtain a high conversion of **3a** by prolonging the reaction time to 36h (**4a**: 88%; **5a**: 88%) under regular conditions.

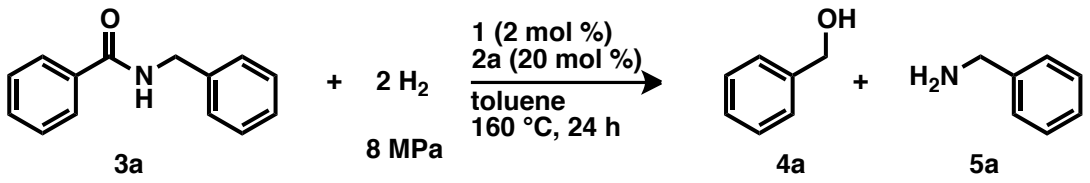

entry	Ru complex	result[a] (%)		
		conv.	4a	5a
1	1a (R = Cy)	92	92	92
2[b]	1a (R = Cy)	75	74	75
3[b,c]	1a (R = Cy)	94	94	86
4[d]	1b (R = ^{i}Pr)	98	84	92
5	1c (R = Ph)	<5	0	0

[a] Determined by ^{1}H NMR. [b] 2b instead of 2a; P_{H2} = 6 MPa.
[c] 48 h. [d] $PhCH_2NH(CH_2)Ph$ (6%) was obtained.

Table 1. Different Ru complexes **1a–c** for hydrogenation of **3a**.

1.2.3. Substrate scope.

This hydrogenation method was more selective (i.e., negligible dearomatization) and showed a wider substrate scope with respect to unactivated amides (Table 2) than the established methods. Selective C–N bond cleavage of linear amides was uniformly observed.[5–7] The active species maintained its catalytic integrity even after a lengthy reaction time (entries 3, 4, 17, 18). The hydrogenation of ε-caprolactam (**3l**), a cyclic amide, which serves as the monomer of nylon-6, showed a similar pattern of bond cleavage (entry 14). Hydrogenation was rather sluggish with **3m** derived by *N*-methylation of **3l** (entry 15). Products **4l** and **4m** could be a synthetic precursor of *N,N*-dimethyl-6-amino-1-hexanol, a polymerization initiator.[16] In contrast, C=O bond cleavage predominated with five- and six-membered lactams **3n**,**o** (entries 16, 17). This apparent C=O bond scission can be explained by a multi step reaction sequence consisting of hydrogenative C–N bond cleavage of the amides giving $NH_2(CH_2)_nOH$, followed by oxidation of the $HOCH_2$_ group giving $NH_2(CH_2)_{n-1}CHO$, then intramolecular imine formation, and finally, imine hydrogenation. In fact, when **4n** was used as the starting material in the absence of H_2 or with P_{H2} = 8 MPa under otherwise identical conditions (160 °C, 24 h), amide **3n** and piperidine (**5n**) were obtained in 53% and 25%, and 28% and 48% yields, respectively. Primary and tertiary amides **3c** and **3b**,

and simple aliphatic amides **3i** and **3j**, were also applicable substrates, but marginal hydrogenation took place with more bulky **3k** (entry 13). Hydrogenation of urea[6c] **3p** (entry 18) is important with respect to the methanol economy,[6b,17] since ureas are excellent chemical reservoirs and carriers of CO_2. However, a larger amount of base (20 mol %) only ensured a reasonable reaction rate for the more inert aliphatic amides. In addition, hydrogenation was sluggish and required harsh reaction conditions (entries 3, 4, 17, 18), so additional optimized conditions for generating catalytic species were evaluated.

Table 2. Hydrogenation of amide **3** using **1a** and **2a**.

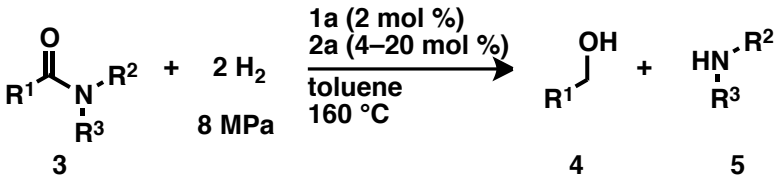

3 4 5

entry	3	conditions[a]	result[b] (%)		
			conv.	4	5
1	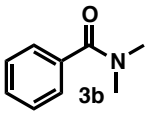 3b	A	84	83	—
2	3b	B	92	85	—
3	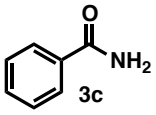 3c	A[c]	87	74	—
4	3c	B[d]	96	71	—
5	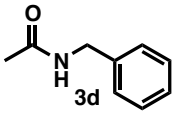 3d	A	95	—	95
6	3d	B	99	—	87
7	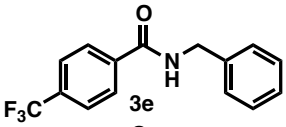 3e	A[e]	99	99	99
8	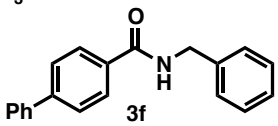 3f	A[e]	83	83	76

[a] conditons A: 1a:2a:3 = 2:20:100, 24 h; conditions B: 1a:2a:3 = 2:4:100, 36h.

[b] Determined by ^{1}H NMR. [c] 216 h. [d] 168 h. [e] P_{H2} = 6 MPa.

entry	3	conditions[a]	result[b] (%)		
			conv.	4	5
9	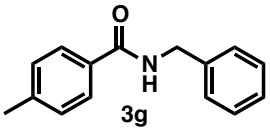 3g	A[e]	74	73	70
10	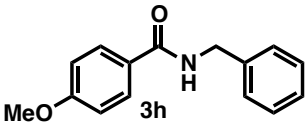 3h	A	67	62	67
11	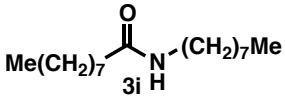 3i	A[f]	94	88	94
12	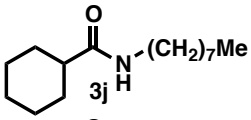 3j	A[f]	66	66	59
13	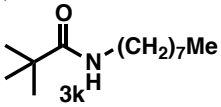 3k	A	9	9	6
14	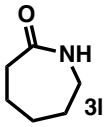 3l	A[e]	94	92[g]	—
15	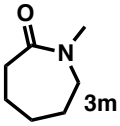 3m	A	64	64[h]	—
16	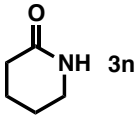 3n	A[f]	88	4[i]	78[j]
17	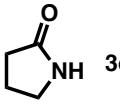 3o	A[c]	73	5[k]	62[l]
18[m]	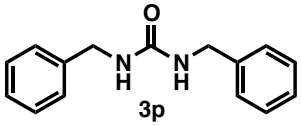 3p	B	97	—	74
19	3p	B[d]	99	—	97

[a] conditons A: 1a:2a:3 = 2:20:100, 24 h; conditions B: 1a:2a:3 = 2:4:100, 36h.

[b] Determined by ^{1}H NMR. [c] 216 h. [d] 168 h. [e] P_{H2} = 6 MPa. [f] 48 h. [g] $HO(CH_2)_6NH_2$. [h] $HO(CH_2)_6NHMe$.

[i] $HO(CH_2)_5NH_2$. [j]  [k] $HO(CH_2)_4NH_2$. [l]  [m] (CHO)NHCH$_2$Ph (13%) was obtained.

1.2.4. Reaction mechanism.

Catalytic species could be generated following a deprotonation pathway similar to those disclosed by Milstein (Figure 1),[6,18] in which a base deprotonates the methylene group vicinal to the phosphorus atom ($PyCH_2P$) of **1a**. However, the primary (**3c**) and secondary (**3a**, **3d–l**, and **3n,o**) amides used here have acidic hydrogens in excess quantity relative to **1a**. Thus, deprotonation of the NH hydrogen of those **3** would prevail over that of **1a**. Due to the less basic nature of the deprotonated form (the conjugate base) of **3**, deprotonation of **1a** might be sluggish, and thus, a high temperature and a high P_{H2} may be required either to produce a catalytic species from **1a**, or for the hydrogenation of **3**.

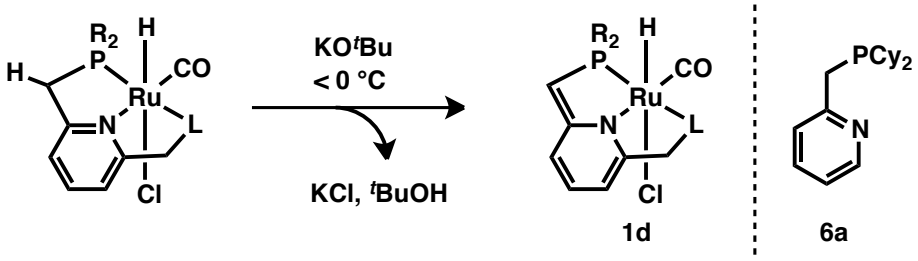

Figure 1. Milstein's mechanism for pyridine dearomatization (L = Et_2N or $^{i}Pr_2P$) and the ligand used here, **6a**.

To probe this speculation, **2a** (4 mol %) was exposed to a toluene solution of **1a** (2 mol %) in the absence of amide **3** (160 °C, 5 h, P_{H2} = 8 MPa) for preactivation of the catalyst, and the resulting matured catalyst was used for the hydrogenation of **3a** under milder conditions with a shortened reaction time (140 °C, P_{H2} = 4 MPa, 12 h). Indeed, **4a** and **5a** were produced in 89% and 89% yields, respectively. Another important aspect is that both **2a** and H_2 are critical to inducing the catalyst. When preactivation was carried out in the absence of H_2 (toluene, 160 °C, 5 h), **1a** was recovered almost unchanged. This feature, namely the structural robustness of **1a** toward bulky base **2a**, is in contrast to previous observation, in which the $PyCH_2P$ moiety was deprotonated below 0 °C without H_2, giving, for example, **1d**.[18]

The mercury test[19] was also employed, in which Hg(0) was added during the hydrogenation step to probe the possibility of catalysis by a Ru nanoparticle. The catalytic activity was not perturbed during the course of the reaction (**4a**: 94%; **5a**:

92%). This preactivation procedure using 4 mol % of **2a** also improved the yields of **4h** and **4i** obtained previously using 20 mol % of **2a** (Table 2, entries 10, 11, 62% and 88%, respectively) to 80% (160 °C, 19 h) and 92% (160 °C, 30 h), respectively, with shorter reaction times (P_{H2} = 8 MPa). When even milder conditions were used for the hydrogenation of **3a** (120 °C, P_{H2} = 2 MPa), a high yield of **4a** (93%) and **5a** (92%) was still obtained by prolonging the reaction time to 60 h. Preactivation of **1a** over a shorter time (1 h, 160 °C, P_{H2} = 8 MPa) or keeping the induction period at 5 h but at a lower temperature and P_{H2} (140 °C, 4 MPa) was found to be less promising (**4a**: ~55% with hydrogenation conditions: 140 °C, P_{H2} = 4 MPa, 12 h).

The $^{31}P\{^{1}H\}$ NMR (toluene-d_8, ppm) spectrum (Figure 2) of the reaction mixture obtained after the optimal induction period of the catalyst showed a medium intensity singlet at δ –15.2 corresponding to **7** (Figure 5), with an additional set of small signals (δ 45.8, 71.0, 73.3, 88.1), which are all different from that of **1a** (δ 66.2) and the free ligand **6a** (δ 4.3) (Figure 2). A ^{1}H NMR of the same sample lacks signals in the 6–9 ppm region which would correspond to the protons of the original Py of **1a** or of partially decomposed products.

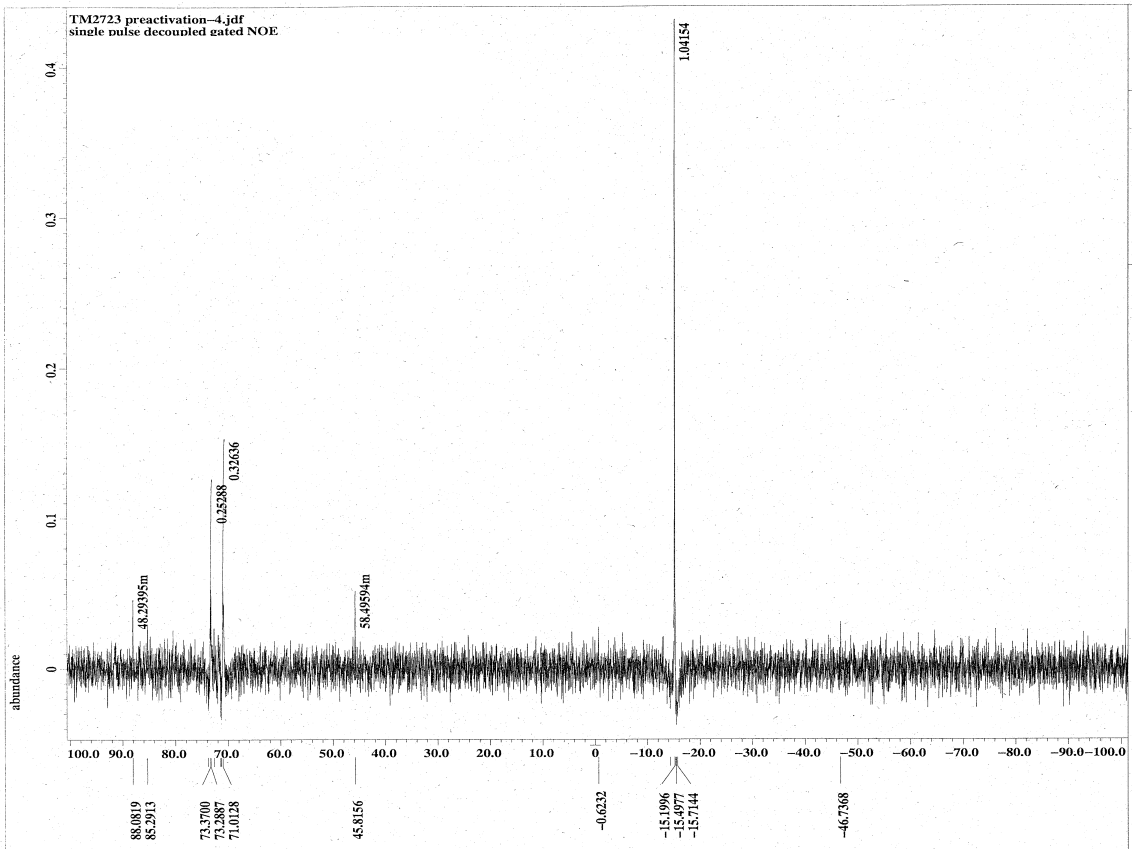

Figure 2. $^{31}P\{^{1}H\}$ NMR (toluene-d_8) spectrum of preactivated Ru catalyst.

In order to further confirm the identity of the catalytic species involving **7**, the reaction mixture was quenched with excess BH_3 · THF (25 °C, 12 h) and was analyzed via electrospray ionization mass spectroscopy (ESI-MS) (Figure 3). The base peak obtained matched fully hydrogenated **7** complexed with BH_3 (Found: *m/z* = 310.2837; Calcd for **7** · BH_3+H^+: 310.2829).[20] The mixture obtained following a shorter induction period (1 h) showed a negligible ESI-MS signal for **7** · BH_3 and an intense signal consistent with unreacted **1a** (Found: *m/z* = 750.2335; Calcd for $\mathbf{1a}^+$: 750.2334) (Figure 4). These results, with the Hg test, suggest that $\mathbf{cat_A}$ or $\mathbf{cat_B}$ is likely to be responsible for the hydrogenation of amides.[21] Based on the fact that at least 2 equiv of **2a** relative to **1a** was required to ensure a high reaction rate,[22] **1a** is first converted into $\mathbf{I_A}$ (16e complex) upon η^2-coordination of H_2. The olefins of the two partially decomposed Pys of $\mathbf{I_A}$ are in turn hydrogenated (intramolecularly), and finally, the structure is fully saturated, giving piperidines as in $\mathbf{cat_A}$, $\mathbf{cat_B}$ and **7** during the induction period of catalyst (Figure 5).

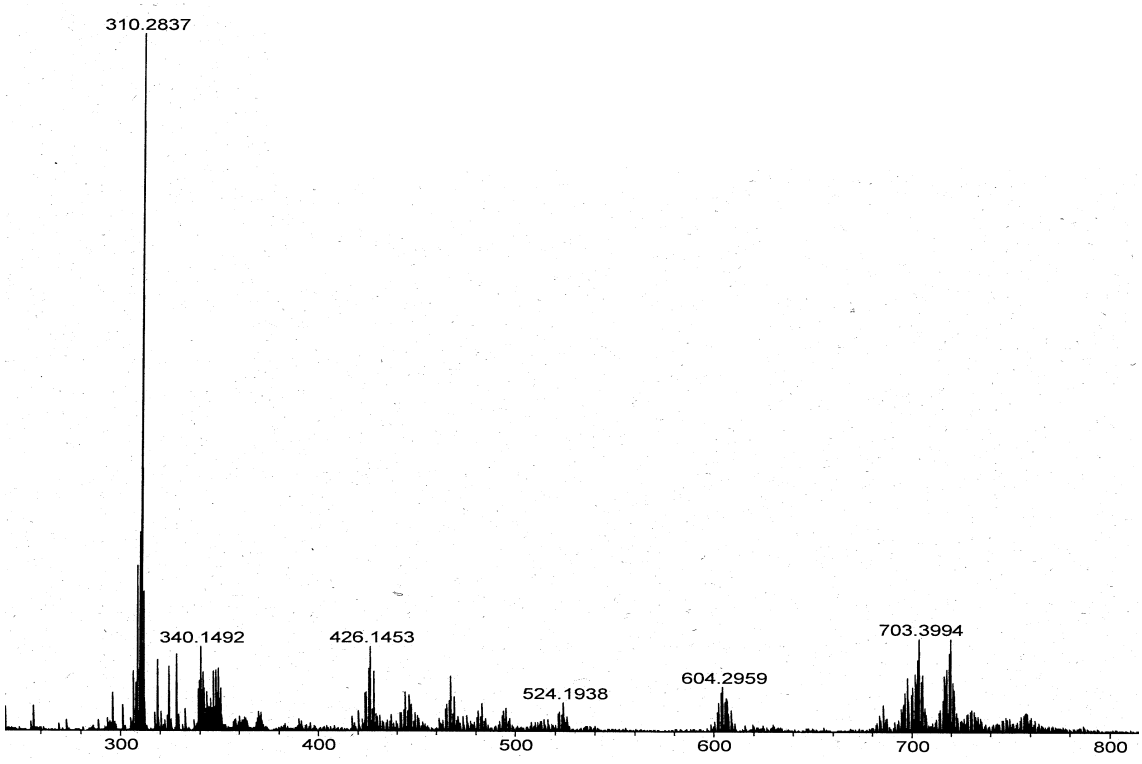

Figure 3. ESI-MS spectrum of [(preactivated Ru catalyst) + BH_3].

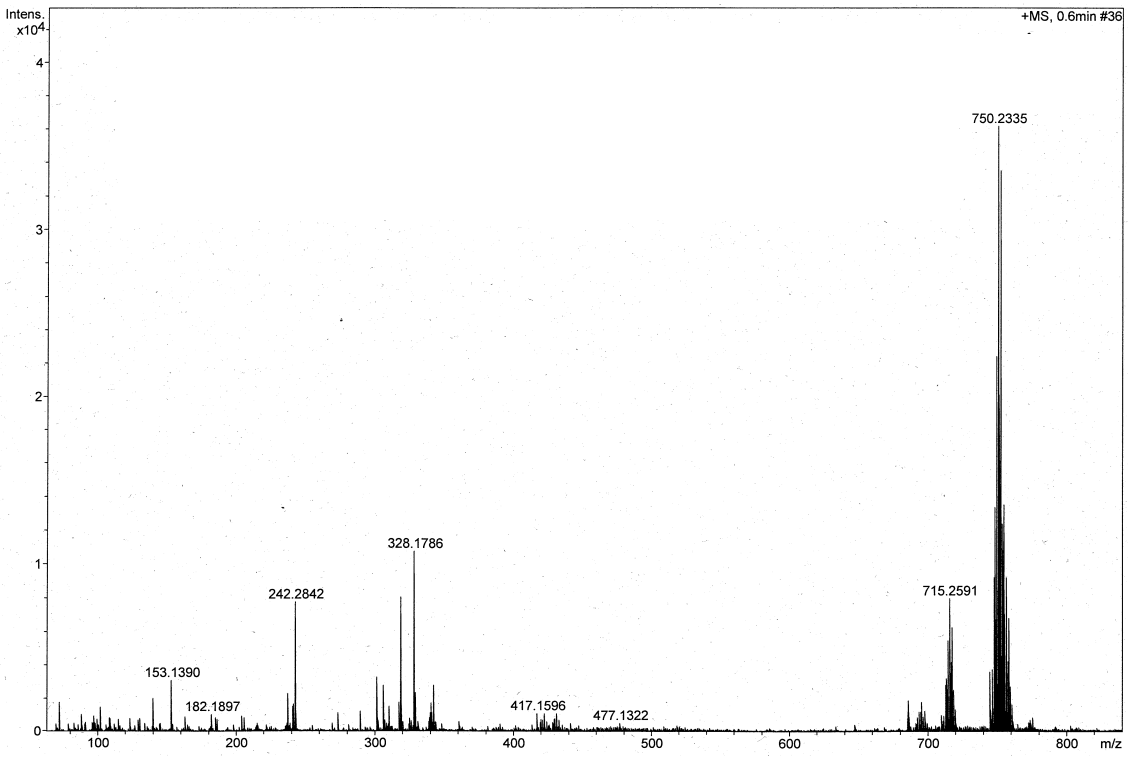

Figure 4. ESI-MS spectrum: After 1 h preactivation (160 °C, P_{H2} = 8 MPa) followed by treatment with BH_3.

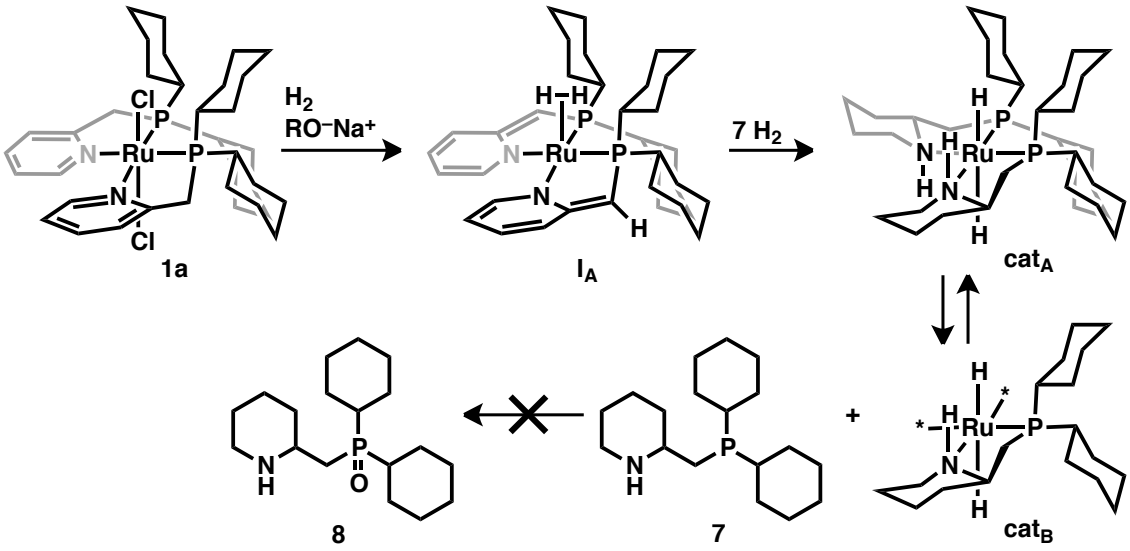

Figure 5. Plausible pathway giving prospective catalytic species $\mathbf{cat_A}$/$\mathbf{cat_B}$ via formation of $\mathbf{I_A}$. Hydrogen atoms may occupy * positions afterward.

1.3. Conclusion

In summary, a sterically congested and coordinatively saturated Ru complex **1a** (catalyst precursor), combined with a bulky base, has been demonstrated to be effective for the hydrogenation of a range of unactivated amides. A novel structural change involving multiple hydrogenation of the interior Py of **1a** during the catalyst induction period was also clarified. Such insight into a catalytic species reinforces the promise of further improvement of molecular catalysts for the hydrogenation of even more kinetically inert and thermodynamically stable unsaturated chemical bonds.

1.4. Experimental section

1.4.1. General

All experiments were performed under an Ar atmosphere unless otherwise noted. ^{1}H NMR spectra were measured on JEOL ECA–600 (600 MHz), JEOL ECA–500 (500 MHz) at ambient temperature. Data were recorded as follows: chemical shift in ppm from internal tetramethylsilane on the δ scale, multiplicity (br = broad, s = singlet, d = doublet, t = triplet, m = multiplet), coupling constant (Hz), integration, and assignment. ^{13}C NMR spectra were measured on JEOL ECA–600 (150 MHz), JEOL ECA–500 (126 MHz) at ambient temperature. Chemical shifts were recorded in ppm from the solvent resonance employed as the internal standard (chloroform-*d* at 77.06 ppm). ^{31}P NMR spectra were measured on JEOL ECA–600 (243 MHz), JEOL ECA–500 (202 MHz) at ambient temperature. Chemical shifts were recorded in ppm from the solvent resonance employed as the external standard (phosphoric acid (85 wt% in H_2O) at 0.0 ppm). ^{11}B NMR spectra were measured on JEOL ECA-600 (125 MHz) with quartz NMR tubes at ambient temperature. Chemical shifts were recorded in ppm from the solvent resonance employed as the external standard ($BF_3 \cdot OEt_2$ at 0.0 ppm). High–resolution mass spectra (HRMS) were obtained from JEOL JMS700 (FAB), PE Biosystems QSTAR (ESI). IR spectra were obtained from JASCO FT/IR6100. For thin–layer chromatography (TLC) analysis through this work, Merck precoated TLC plates (silica gel 60 GF254 0.25 mm) were used. The products were purified by preparative column chlomatography on silica gel 60 (230–400 mesh; Merk).

1.4.2. Materials

NaH (60% oil dispersion), octylamine, *N,N*-dimethylbenzamide, δ-valerolactam, ε-caprolactam, were purchased from Aldrich. NaO^{t}Bu, NaOMe, $RuCl_2(PPh_3)_3$, chlorodicyclohexylphosphine, chlorodiisopropylphosphine, acetanilide, *N*-benzyl acetamide, 2-pyrrolidinone, EtOAc, hexane, were purchased from Wako Pure Chemical industries, Ltd. 2-picoline, MeOH (anhydrous), EtOH (anhydrous), ^{i}PrOH (anhydrous), ^{t}BuOH (anhydrous), THF (anhydrous), dichloromethane, hexane (anhydrous), toluene (anhydrous), Et_2NH, ^{n}BuLi (1.65 M in hexane), nonanoyl chloride were purchased from Kanto Chemicals, Ltd. 1,1,2,2-tetrachloroethane, BH_3–THF complex (0.9 M in hexane), 2-methyl-2-adamantanol, benzamide, cyclohexanecarbonyl chloride,

biphenyl-4-carboxylic acid, *N*-methyl-ε-caprolactam and 5-amino-1pentanol were purchased from TCI, Ltd. *N*-benzylbenzamide was purchased from Across Organics, Ltd. Hydrogen gas was purchased from Alphasystem. These chemicals were used without further purification. *N*-benzyl-4-methoxybenzamide (**3h**),[23] *N*-benzyl-4-methylbenzamide (**3g**),[24] *N*-benzyl 4-(trifluoromethyl)benzamide (**3e**),[25] *N*-octylnonanamide (**3i**),[26] 2-[(diphenylphosphino)methyl]pyridine,[27] and *N,N'*--dibenzylurea (**3p**)[28] are all known compounds and synthesized according to the literature.

1.4.3. Experimental procedure.

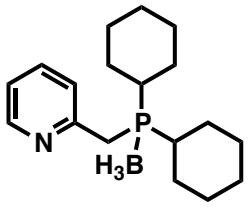

2-((dicyclohexylphosphino)methyl)pyridine−borane complex: To an anhydrous THF (150 mL) solution of 2-picoline (6.7 mL, 67.5 mmol) was added a 1.65 M hexane solution of Bu^{n}Li (42.4 mL, 70 mmol) at –78 °C (MeOH-dry ice) under Ar, and the mixture was stirred at –78 °C for 3 h. To the reddish suspension was added chlorodicyclohexylphosphine–borane complex {prepared by mixing chlorodicyclohexylphosphine (9.9 mL, 45 mmol) and BH_3–THF complex (1 M in THF, 45 mL, 45 mmol) in THF (75 mL), followed by being stirred for 30 min at room temperature under Ar} dropwise at the same temperature. The reaction mixture was allowed to warm to room temperature and stirred for 5 h. The mixture was quenched by adding a small portion of water (*ca.* <5 mL), and the organic phase was removed *in vacuo* (*ca.* 50 mmHg, 40 °C). The residue was dissolved into CH_2Cl_2 (100 mL), washed with H_2O (100 mL), and extracted with CH_2Cl_2 (100 mL×2). The organic layer was dried over Na_2SO_4 and filtrated. The evaporation of the filtrate gave an yellow crude oil, which was purified by column chromatography on silica gel (EtOAc/hexane = 1/4) to give solids, which were recrystallized from CH_2Cl_2/hexane to afford the target compound (10.05 g, 74%) as colorless solid. IR (neat): 2927, 2850, 2365, 2355, 2254, 1589, 1438, 1305, 1067, 831, 797, 753, 618 cm^{-1}. ^{1}H NMR ($CDCl_3$, 500 MHz): δ 0.04–0.70 (m, 3H), 1.15–2.05 (m, 22H), 3.23 (d, J = 11.5 Hz, 2H), 7.16 (t, J = 4.6 Hz, 1H), 7.36 (d, J = 6.9 Hz, 1H), 7.61 (t, J = 5.7 Hz, 1H), 8.49 (d, J = 4.6 Hz, 1H). ^{13}C NMR ($CDCl_3$, 126 MHz): δ 26.4, 27.0, 27.1, 27.3, 27.4, 31.0 (d, $^1J_{PC}$ = *35*.1 Hz), 32.1 (d, $^1J_{PC}$ = 41.4 Hz), 122.3, 125.5, 136.6, 149.5, 155.4. ^{31}P{^{1}H} NMR ($CDCl_3$, 202 MHz): δ 28.6. HRMS (FAB, M – H$^+$) calcd for $C_{18}H_{30}BNP^+$: 302.2203. Found *m*/*z* = 302.2220.

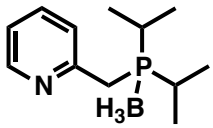

2-((diisopropylphosphino)methyl)pyridine–borane complex: To an anhydrous THF (50 mL) solution of 2-picoline (2.96 mL, 30.0 mmol) was added a 1.65 M hexane solution of Bu^{n}Li (20 mL, 33.0 mmol) at –78 °C (MeOH-dry ice) under Ar and the mixture was stirred at –78 °C for 3 h. To the reddish suspension was added chlorodiisopropylphosphine–borane complex {prepared by mixing chlorodiisopropylphosphine (3.18 mL, 20.0 mmol) and BH_3–THF complex (1 M in THF, 20 mL, 20 mmol) in THF (20 mL), followed by being stirred for 30 min at room temperature under Ar} dropwise at the same temperature. The reaction mixture was allowed to warm to room temperature and stirred for 5 h. The mixture was quenched by adding a small portion of water (*ca.* <1 mL), and the organic phase was removed *in vacuo* (*ca.* 50 mmHg, 40 °C). The residue was dissolved into CH_2Cl_2 (40 mL), washed with H_2O (40 mL), and extracted with CH_2Cl_2 (40 mL×2). The organic layer was dried over Na_2SO_4 and filtrated. The evaporation of the filtrate gave a yellow crude oil, which was purified by column chromatography on silica gel (EtOAc/hexane = 1/8) to afford the target compound (3.46 g, 78%) as yellow oil. IR (neat): 2964, 2934, 2875, 2368, 1591, 1471, 1434, 1253, 1153, 1066, 886, 801, 747, 679 cm^{-1}. ^{1}H NMR ($CDCl_3$, 500 MHz): δ 0.07–0.82 (m, 3H), 1.10–1.28 (m, 12H), 2.05–2.19 (m, 2H), 3.24 (d, J = 11.7 Hz, 2H), 7.15 (t, J = 7.6 Hz, 1H), 7.37 (d, J = 7.6 Hz, 1H), 7.61 (t, J = 7.6 Hz, 1H), 8.48 (d, J = 4.1 Hz, 1H). ^{13}C NMR ($CDCl_3$, 126 MHz): δ 17.0, 22.0 (d, $^1J_{PC}$ = 41.4 Hz), 30.7 (d, $^1J_{PC}$ = 35.0 Hz), 122.0, 125.1, 136.4, 149.2, 154.9. ^{31}P{^{1}H} NMR ($CDCl_3$, 202 MHz): δ 36.4. HRMS (FAB, M – H$^+$) calcd for $C_{12}H_{22}BNP^+$: 222.1577. Found m/z = 222.1552.

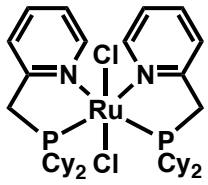

Dichlorobis(dicyclohexylphosphinomethylpyridine)–ruthenium (II), RUPCY (1a): An anhydrous Et_2NH (10 mL) solution of dicyclohexylphosphinomethylpyridine–borane complex (280 mg, 0.923 mmol) was heated at 65 °C for 48 h under Ar. The solution was cooled to room temperature and Et_2NH was removed *in vacuo* (*ca.* 10 mmHg, room temperature). To the residue was added sequentially dichlorotris(triphenylphosphino)ruthenium (II) (442.5 mg, 0.46 mmol) and an anhydrous toluene (10 mL). The resulting mixture was heated at 110 °C for 5 h under Ar, and was cooled to room temperature. Then to the mixture was added an anhydrous hexane (20 mL) to afford the yellow suspension. The mixture of the suspension was

stirred at room temperature for 12 h and filtered through a filtration paper. The obtained yellowish orange solid was dried *in vacuo* (*ca.* 0.1 mmHg, room temperature) and dissolved in CH_2Cl_2. This solution was purified by column chromatography on silica gel (EtOAc/hexane =1/4) to afford RUPCY (**1a**) as orange powder (237 mg, 68%). ^{1}H NMR ($CDCl_3$, 500 MHz): δ 1.06–1.85 (m, 44H), 2.21 (br, 4H), 7.11 (t, J = 5.8 Hz, 2H), 7.44 (d, J = 7.5 Hz, 2H), 7.63 (t, J = 7.5 Hz, 2H), 8.48 (d, J = 5.2 Hz, 2H). ^{13}C NMR ($CDCl_3$, 126 MHz): δ 26.1, 27.4, 27.5, 29.3, 37.2, 37.9, 121.4, 121.9, 135.7, 154.9, 165.0. ^{31}P{^{1}H} NMR ($CDCl_3$, 202 MHz): δ 66.2. HRMS (FAB, M^+) calcd for $C_{36}H_{56}Cl_2N_2P_2Ru^+$: 750.2334. Found m/z = 750.2314.

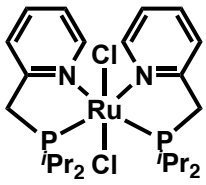

Dichlorobis(diisopropylphosphinomethylpyridine)–ruthenium (II), RUPIP (1b): A morpholine (10 mL) solution of diisopropylphosphinomethylpyridine–borane complex (714.3 mg, 3.2 mmol) was degassed and subsequently filled with Ar, and heated at 130 °C for 2 h under Ar. The solution was cooled to room temperature and morpholine was removed *in vacuo* (*ca.* 10 mmHg, 60 °C). To the residue was added sequentially dichlorotris(triphenylphosphino)ruthenium (II) (1438.2 mg, 1.50 mmol) and an anhydrous toluene (20 mL). The resulting mixture was heated at 110 °C for 2 h under Ar, and was cooled to room temperature. Then to the mixture was added an anhydrous hexane (40 mL) to afford yellow suspension. The mixture of the suspension was stirred at room temperature for 1 h and filtered through a filtration paper. The obtained yellowish orange solid was dried *in vacuo* (*ca.* 0.1 mmHg, room temperature) and dissolved in $CHCl_3$. This solution was purified by column chromatography on silica gel ($CHCl_3$/hexane/EtOAc =4/4/1) to afford RUPIP (**1b**) as orange powder (251.6 mg, 27%). ^{1}H NMR ($CDCl_3$, 500 MHz): δ 1.00–1.45 (m, 24H), 2.41–2.69 (m, 4H), 3.93 (br, 4H), 7.12 (t, J = 6.9 Hz, 2H), 7.48 (d, J = 7.6 Hz, 2H), 7.64 (t, J = 7.6 Hz, 2H), 8.52 (d, J = 5.5 Hz, 2H). ^{13}C NMR ($CDCl_3$, 126 MHz): δ 19.3, 19.9, 26.8, 37.9, 121.6, 122.1, 136.0, 155.1, 165.0. ^{31}P{^{1}H} NMR ($CDCl_3$, 202 MHz): δ 72.8. HRMS (ESI, M^+) calcd for $C_{24}H_{40}Cl_2N_2P_2Ru^+$: 590.1082. Found m/z = 590.1087.

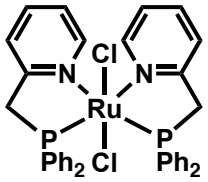

Dichlorobis((diphenylphosphino)methyl)pyridine-ruthenium (II), RUPPH (1c): To an anhydrous toluene (10 mL) solution of 2-[(diphenylphosphino)methyl]pyridine (458 mg, 1.65 mmol) was added dichlorotris(triphenylphosphino)ruthenium (II) (791 mg, 0.83 mmol). The mixture was heated at 110 °C for 12 h under Ar, and was cooled to room temperature. Then to the mixture was added an anhydrous hexane (60 mL) to afford yellow suspension. The mixture of the suspension was stirred at room temperature for 1 h and filtered through a filtration paper. The obtained yellowish orange solid was dried *in vacuo* (*ca.* 0.1 mmHg, room temperature), affording RUPPH (**1c**) as orange powder (140 mg, 23%). The product contains *ca.* 1:1 mixture of diastereomers. ^{1}H NMR (600 MHz, $CDCl_3$): δ 4.02 (dd, J = 11.7 Hz, J = 15.8 Hz, 1H), 4.09 (dd, J = 13.7 Hz, J = 15.8 Hz, 1H), 4.82 (dd, J = 10.3 Hz, J = 15.8 Hz, 1H), 4.89 (dd, J = 10.3 Hz, J = 16.5 Hz, 1H), 5.89–6.76 (m, 6H), 6.90–7.38 (m, 15H), 7.63–7.81 (m, 4H), 8.37 (m, 2H), 9.84 (d, J = 5.52 Hz, 1H). ^{13}C NMR (200 MHz, $CDCl_3$): δ 43.8 (1C), 44.0 (2C), 44.2 (1C), 120.4, 121.2, 121.3, 122.5, 122.6, 122.9, 122.9, 127.2, 127.3,127.7, 127.8, 127.9, 128.0, 128.4, 129.0, 130.0, 130.1, 130.4, 130.5, 131.1, 131.2, 133.2, 133.3, 134.2, 135.6, 135.6, 137.0, 153.5, 153.6. ^{31}P{^{1}H} NMR (200 MHz, $CDCl_3$): δ 62.4, 57.5. HRMS (FAB, [M – Cl]$^{+}$) calcd for $C_{36}H_{32}ClN_2P_2Ru$: 691.0767. Found m/z = 691.0743.

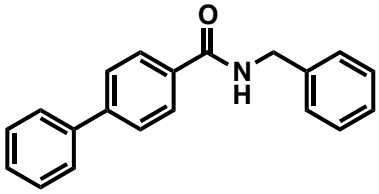

***N*-benzylbiphenyl-4-carboxamide (3f)**: A thionyl chloride (30 mL) solution of biphenyl-4-carboxylic acid (2.97 g, 15 mmol) was refluxed for 5 h under Ar (bath temperature: *ca.* 95 °C), and the solution was cooled to room temperature. The remaining thionyl chloride was removed *in vacuo* (*ca.* 10 mmHg, room temperature). To an anhydrous CH_2Cl_2 (20 mL) solution of the residue were added Et_3N (2.8 mL, 20 mmol) and benzylamine (2.18 mL, 20 mmol). The mixture was stirred at room temperature overnight under N_2, and was quenched by adding a small portion of water (*ca.* <2 mL). The residue was dissolved in CH_2Cl_2 (100 mL), washed with H_2O (100 mL), and extracted with CH_2Cl_2 (100 mL×2). The organic layer was dried over Na_2SO_4 and filtrated. Evaporation of the filtrate gave colorless solid, which was recrystallized from CH_2Cl_2/hexane giving **3f** (2.09 g, 7.27 mmol, 48%). IR (neat): 3324, 3028, 1637, 1549, 1323, 1310, 746, 727, 693 cm^{-1}. ^{1}H NMR ($CDCl_3$, 600 MHz): δ 4.67 (d, J = 5.52 Hz, 2H), 6.46 (s, 1H), 7.33–7.29 (m, 1H), 7.41–7.34 (m, 5H), 7.46 (t,

J = 7.56 Hz, 2H), 7.60 (d, *J* = 8.22 Hz, 2H), 7.65 (d, *J* = 8.22 Hz, 2H), 7.87 (d, *J* = 6.18 Hz, 2H). ^{13}C NMR ($CDCl_3$, 150MHz): δ 44.2, 127.2, 127.3, 127.5, 127.7, 127.9, 128.0, 128.8, 128.9, 133.0, 138.2, 140.0, 144.4, 167.0. HRMS (FAB, MH^+) calcd for $C_{20}H_{18}NO^+$: 288.1388. Found *m*/*z* = 288.1364.

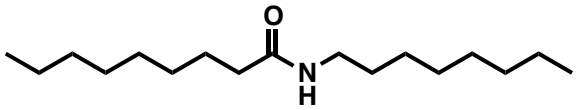

***N*-octylnonanamide (3i)**: To an anhydrous CH_2Cl_2 (15 mL) solution of nonanoyl chloride (3.61 mL, 20 mmol) were added Et_3N (3.3 mL, 24 mmol) and octylamine (3.31 mL, 20 mmol). The mixture was stirred at room temperature overnight under N_2, and was quenched by adding a small portion of water (*ca.* <2 mL). The residue was dissolved into CH_2Cl_2 (100 mL), washed with H_2O (100 mL), and extracted with CH_2Cl_2 (100 mL×2). The organic layer was dried over Na_2SO_4 and filtrated. Evaporation of the filtrate gave colorless solid, which was recrystallized from CH_2Cl_2/hexane giving **3i** (2.42 g, 8.98 mmol, 45%). ^{1}H NMR, ^{13}C NMR ($CDCl_3$, 150MHz) and IR data are consistent with those reported in literature.[5] HRMS (FAB, MH^+) calcd for $C_{17}H_{36}NO^+$: 270.2791. Found *m*/*z* = 270.2772.

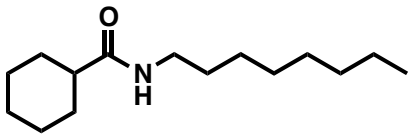

***N*-octylcyclohexanecarboxamide (3j)**: To an anhydrous CH_2Cl_2 (15 mL) solution of cyclohexanecarbonyl chloride (2.68 mL, 20 mmol) were added Et_3N (3.3 mL, 24 mmol) and octylamine (3.31 mL, 20 mmol). The mixture was stirred at room temperature overnight under N_2, and was quenched by adding a small portion of water (*ca.* <2 mL). The residue was dissolved into CH_2Cl_2 (100 mL), washed with H_2O (100 mL), and extracted with CH_2Cl_2 (100 mL×2). The organic layer was dried over Na_2SO_4 and filtrated. Evaporation of the filtrate gave colorless solid, which was recrystallized from CH_2Cl_2/hexane giving **3j** (4.02 g, 16.8 mmol, 86%). IR (neat): 3311, 2927, 2854, 1638, 1540, 1447, 1210 cm^{-1}. ^{1}H NMR ($CDCl_3$, 600 MHz): δ 0.88 (t, *J* = 6.84 Hz, 3H), 1.16–1.34 (m, 13H), 1.43 (q, *J* = 8.94 Hz, 2H), 1.48 (t, *J* = 7.56 Hz, 2H), 1.63–1.70 (m, 1H), 1.78 (d, *J* = 12.36 Hz, 2H), 1.85 (d, *J* = 13.08 Hz, 2H), 2.05 (tt, *J* = 3.48 Hz, *J* = 11.64 Hz, 1H), 3.22 (q, *J* = 6.9 Hz, 2H), 5.49 (s, 1H). ^{13}C NMR ($CDCl_3$, 150MHz): δ 14.0, 22.6, 25.7 (4C), 26.9, 29.1, 29.2, 29.6, 29.7, 31.7, 39.3, 45.6, 175.9. HRMS (FAB, MH^+) calcd for $C_{15}H_{30}NO^+$: 240.2327. Found *m*/*z* = 240.2300.

Representative procedure for hydrogenation of amides: The reaction of *N*-benzylbenzamide (3a).

Under a continuous Ar flow, 2-methyl-2-adamantanol (16.6 mg, 0.1 mmol), NaH (60% oil dispersion, 4.0 mg, 0.1 mmol), anhydrous toluene (1.5 mL) and a magnetic stirring bar were placed in a dried Teflon tube (21 mL capacity). The Teflon tube was stoppered with a rubber septum, and the mixture was stirred at room temperature for 2 h under Ar. After removing the septum, under a continuous Ar flow, to the mixture was added RUPCY (7.50 mg, 0.01 mmol) and *N*-benzylbenzamide (105.6 mg, 0.5 mmol). The Teflon tube was quickly inserted into an autoclave and the inside of the autoclave was purged several times with hydrogen gas (>5 MPa). The autoclave was pressurized with an 8 MPa of hydrogen gas at 25 °C, and heated at 160 °C for 24 h under stirring (800 rpm). The autoclave was cooled to room temperature in an ice–water (0 °C) bath, and the reaction mixture was quenched with NH_4Cl (5.3 mg, 0.1 mmol). The organic phase was removed *in vacuo* (*ca.* 100 mmHg, 40 °C). The residue was diluted with $CDCl_3$, and analyzed by ^1H NMR. The yields of benzyl alcohol (92%) and benzylamine (92%) were calculated based on the integral ratio among the signals of these compounds with respect to an internal standard (1,1,2,2-tetrachloroethane).

Afterward, the reaction mixture was purified by column chromatography on silica gel (silica gel (*ca.* 100 g) was pretreated with Et_3N (small amount)–Et_2O/hexane (vol%: 2/3), eluent; Et_2O/hexane = 2/3, then EtOAc/Et_3N = 100/1) to give *N*-benzylbenzamide (7.7 mg, 0.036 mmol, 7%), benzyl alcohol (47.4 mg, 0.438 mmol, 88%) and benzylamine (44.1 mg, 0.4187 mmol, 82%).

Representative procedure for hydrogenation of amides with preactivated catalyst: The reaction of *N*-benzylbenzamide (3a).

Under a continuous Ar flow, RUPCY (10.01 mg, 0.013 mmol), sodium 2-methyl-2-adamantoxide (5.02 mg, 0.027 mmol), anhydrous toluene (2.0 mL) and a magnetic stirring bar were placed in a dried Teflon tube (21 mL capacity). The Teflon tube was quickly inserted into an autoclave, and the inside of the autoclave was purged several times with hydrogen gas (>5 MPa). The autoclave was pressurized with an 8 MPa of hydrogen gas at 25 °C, and heated at 160 °C for 5 h under stirring (800 rpm). Then the autoclave was cooled to room temperature in an ice–water (0 °C) bath, and hydrogen was blown away under an Ar stream. Under the continuous Ar flow, to

another autoclave, in which a dried Teflon tube charged with *N*-benzylbenzamide (105.63 mg, 0.5 mmol) had been in advance inserted, was transferred the reaction mixture using a gas-tight syringe (2.5 mL). The autoclave was purged (×3 with >5 MPa H_2 gas) and finally charged with 4 MPa of hydrogen gas, and the reaction mixture was heated at 140 °C for 12 h under stirring (800 rpm). The autoclave was cooled to room temperature in an ice–water (0 °C) bath, and the reaction mixture was quenched with NH_4Cl (1.1 mg, 0.02 mmol). The organic phase was removed *in vacuo* (*ca.* 100 mmHg, 40 °C). The residue was diluted with $CDCl_3$, and analyzed by ^1H NMR. The yields of benzyl alcohol (89%) and benzylamine (89%) were calculated based on the integral ratio among the signals of these compounds with respect to an internal standard (1,1,2,2-tetrachloroethane).

X-ray single crystal structure analysis of 1a.

Single crystals of RUPCY suitable for X-ray crystal analysis were obtained by slow diffusion of hexane into a toluene solution of RUPCY. Intensity data were collected at 173 K on a Rigaku Single Crystal CCD X-ray Diffractometer (Saturn 70 with MicroMax-007) with Mo Kα radiation (λ = 0.71070 Å) and graphite monochromater. A total of 12551 reflections were measured at a maximum 2θ angle of 51.0°, of which 6569 were independent reflections (R_{int} = 0.0869). The structure was solved by direct methods (SHELXS-97) and refined by the full-matrix least-squares on F_2 (SHELXL-97). All non-hydrogen atoms were refined anisotropically. All hydrogen atoms were placed using AFIX instructions. The following crystal structure has been deposited at the Cambridge Crystallographic Data Centre and allocated the deposition number CCDC 894187.

The crystal data are as follows: $C_{36}H_{56}Cl_2N_2P_2Ru$; FW = 750.77, crystal size 0.10 × 0.20 × 0.20 mm^3, Triclinic, P-1, a = 11.3882(14) Å, b = 12.763(9) Å, c = 13.21680(10) Å, α = 86.38(19)°, β = 79.81(18)°, γ = 72.19(16)°, V = 1800.0(22) $Å^3$, Z = 2, D_c = 1.385 g cm^{-3}. The refinement converged to R_1 = 0.0616, wR_2 = 0.1350 ($I > 2\sigma(I)$), GOF = 1.021.

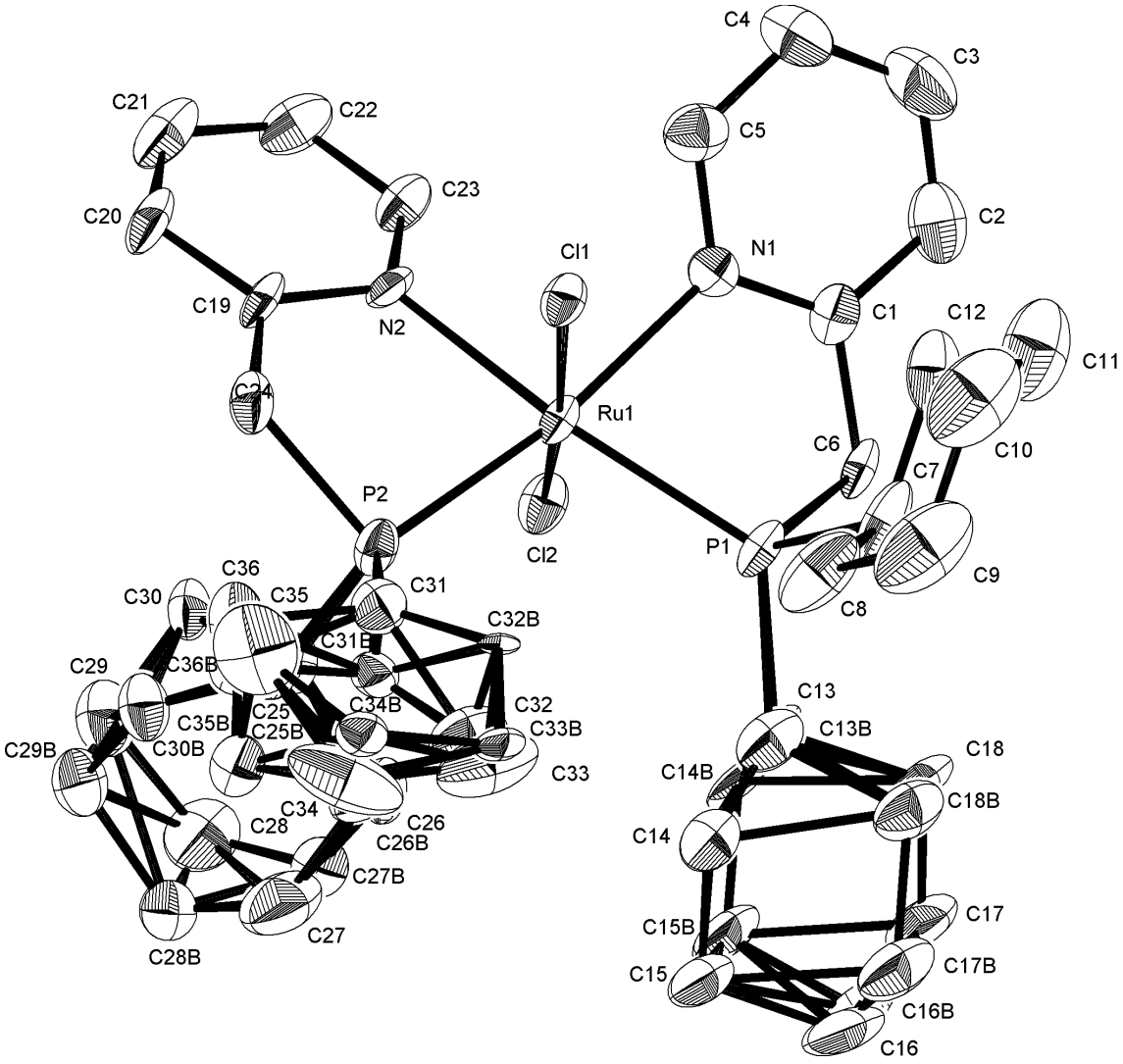

Figure 6. ORTEP drawing of Ru complex **1a**. 50% probability ellipsoids; The hydrogen atoms not involved in hydrogen bonding are omitted for clarity.

1.5. Reference and notes

(1) (a) Challis, B. C.; Challis, J. A. In *The Chemistry of Amides*; Zabicky, J., Patai, S., Eds.; John Wiley & Sons: London, 1970; pp 731–857. (b) Beckwith, A. L. J. In *The Chemistry of Amides*; Zabicky, J., Patai, S., Eds.; John Wiley & Sons: London, 1970; pp 73–1850. (c) Ishihara, K.; Ohara, S.; Yamamoto, H. *J. Org. Chem.* **1996**, *61*, 4196–4197. (d) Ghose, A. K.; Viswanadhan, V. N.; Wendoloski, J. J. *J. Comb. Chem.* **1999**, *1*, 55–68. (e) Bemis, G. W.; Murcko, M. A. *J. Med. Chem.* **1999**, *42*, 5095–5099. (f) Montalbetti, C. A. G. N.; Falque, V. *Tetrahedron* **2005**, *61*, 10827–10852. (g) Carey, J. S.; Laffan, D.; Thomson, C.; Williams, M. T. *Org. Biomol. Chem.* **2006**, *4*, 2337–2347. (h) Goossen, L. J.; Melzer, B. *J. Org. Chem*. **2007**, *72*, 7473–7476. (i) Burk, R. M.; Woodward, D. F. *Drug Dev. Res.* **2007**, *68*, 147–155. (j) Gunanathan, C.; Ben-David, Y.; Milstein, D. *Science* **2007**, *317*, 790–792. (k) Al-Zoubi, R. M.; Marion, O.; Hall, D. G. *Angew. Chem., Int. Ed.* **2008**, *47*, 2876–2879.

(2) (a) Murahashi, S.; Naota, T.; Yonemura, K. *J. Am. Chem. Soc.* **1988**, *110*, 8256–8258. (b) Beller, M.; Zapf, A. *Chem. Eur. J.* **2001**, *7*, 2908–2915. (c) Eldred, S. E.; Stone, D. A.; Gellman, S. H.; Stahl, S. S. *J. Am. Chem. Soc.* **2003**, *125*, 3422–3423. (d) DeBoef, B.; Pastine, S. J.; Sames, D. *J. Am. Chem. Soc.* **2004**, *126*, 6556–6557. (e) Botella, L.; Nájera, C. J. Org. Chem. **2005**, *70*, 4360–4369. (f) Smith, S. M.; Thacker, N. C.; Takacs, J. M. *J. Am. Chem. Soc.* **2008**, *130*, 3734–3735. (g) Nakao, Y.; Idei, H.; Kanyvia, K. S.; Hiyama, T. *J. Am. Chem. Soc.* **2009**, *131*, 5070–5071. (h) Stephenson, N. A.; Zhu, J.; Gellman, S. H.; Stahl, S. S. *J. Am. Chem. Soc.* **2009**, *131*, 10003–10008. (i) Smith, S. M.; Takacs, J. M. *J. Am. Chem. Soc.* **2010**, 132, 1740–1741.

(3) (a) Greenberg, A.; Moore, D. T. *J. Mol. Struct.* **1997**, *413–414*, 477–485; (b) Fersner, A.; Karty, J. M.; Mo, Y. *J. Org. Chem.* **2009**, *74*, 7245–7253.

(4) (a) Núñez Magro, A. A.; Eastham, G. R.; Cole-Hamilton, D. J. *Chem. Commun.* **2007**, 3154–3156. (b) Coetzee, J.; Klankermayer, D. L.; Brosinski, S.; Leitner, W.; Slawin, A. M. Z.; Cole-Hamilton, D. J. *Chem. Eur. J.* **2013**, *19*, 11039–11050. (c) vom Stein, T.; Meuresch, M.; Limper, D.; Schmitz, M.; Hölscher, M.; Coetzee, J.; Cole-Hamilton, D. L.; Klankermayer, J.; Leitner, W. *J. Am. Chem. Soc.* **2014**, *136*, 13217−13225.

(5) (a) Ito, M.; Sakaguchi, A.; Kobayashi, C.; Ikariya, T. *J. Am. Chem. Soc.* **2007**, *129*, 290–291. (b) Ito, M.; Koo, L. W.; Himizu, A.; Kobayashi, C.; Sakaguchi, A.; Ikariya, T. *Angew. Chem., Int. Ed.* **2009**, *48*, 1324–1327. (c) Ito, M.; Kobayashi, C.; Himizu, A.; Ikariya, T. *J. Am. Chem. Soc.* **2010**, *132*, 11414–11415. (d) Ito, M.; Ootsuka, T.; Watari, R.; Shiibashi, A.; Himizu, A.; Ikariya, T. *J. Am. Chem. Soc.* **2011**, *133*, 4240–4242.

(6) (a) Balaraman, E.; Gnanaprakasam, B.; Shimon, L. J. W.; Milstein, D. *J. Am. Chem. Soc.* **2010**, *132*, 16756–16758. carbamate hydrogenaiton: (b) Balaraman, E.; Gunanathan, C.; Zhang, J.; Shimon, L. J. W.; Milstein, D. *Nat. Chem.* **2011**, *3*, 609– 614. urea hydrogenation: (c) Balaraman, E.; Ben-David, Y.; Milstein, D. *Angew. Chem., Int. Ed.* **2011**, *50*, 11702–11705.

(7) (a) Takebayashi, S.; John, J. M.; Bergens, S. H. *J. Am. Chem. Soc.* **2010**, *132*, 12832–12834. (b) John, J. M.; Bergens, S. H. *Angew. Chem., Int. Ed.* **2011**, *50*, 10377–10380.

(8) Significantly higher electrophilicity of the carbonyl carbon of α-alkoxy carbonyl compounds over α-unsubstituted ones due to substituent field/ inductive effects: (a) Das, G.; Thoronton, E. R. *J. Am. Chem. Soc.* **1990**, *112*, 5360– 5362. (b) Das, G.; Thoronton, E. R. *J. Am. Chem. Soc.* **1993**, *115*, 1302–1312.

(9) (a) Hirosawa, C.; Wakasa, N.; Fuchikami, T. *Tetrahedron Lett.* **1996**, *37*, 6749–6752. (b) Stein, M.; Breit, B. *Angew. Chem., Int. Ed.* **2013**, *125*, 2287–2290.

(10) (a) Ashby, M. T.; Halpern, J. *J. Am. Chem. Soc.* **1991**, *113*, 589–594. (b) Brown, J. M.; Maddox, P. J. *Chirality* **1991**, *3*, 345–354. (c) Hadzovic, A.; Song, D.; MacLaughlin, C. M.; Morris, R. H. *Organometallics* **2007**, *26*, 5987–5999. (d) Donald, S. M. A.; Vidal-Ferran, A.; Maseras, F. *Can. J. Chem.* **2009**, *87*, 1273–1279. (e) O, W. W. N.; Lough, A. J.; Morris, R. H. *Organometallics* **2011**, *30*, 1236– 1252.

(11) Alkylphosphines are better than arylphosphines for π back-donation from a metal to the δ^*_{P-C}. The pyridine structure ensures the p back-donation is more effective than that which occurs to $\delta^*_{N(sp3)-C}$. Due to the supplementary interaction with the π^*_{N-C} orbital, a pyridine ligand is twice as strong a pacceptor as the NH_3 ligand. The contribution from π-back-bonding to phosphine ligands is much larger than Py ligands, contributing from 37 to nearly 70% of the total bond energy: (a) Park,

S.-H.; Milletti, M. C.; Gardner, N. *Polyhedron* **1998**, *17*, 1267–1273. (b) Leyssens, T.; Peeters, D.; Orpen, A. G.; Harvey, J. N. *Organometallics* **2007**, *26*, 2637–2645.

(12) A *cis*(P,P) geometry, providing a more sterically demanding environment around the Ru center, is electronically more favored when two phosphanyl donor groups have a strong *trans* influence. Hashimoto, A.; Yamaguchi, H.; Suzuki, T.; Kashiwabara, K.; Kojima, M.; Takagi, H. D. *Eur. J. Inorg. Chem.* **2010**, 39–47.

(13) (a) Saito, S.; Noyori, R.; Miura, T.; Held, I. E.; Suzuki, M.; Iida, K. JP patent Appl. #2011-012316, Filed: Jan. 24, 2011.; (b) Miura, T.; Held, I. E.; Oishi, S.; Naruto, M.; Saito, S. *Tetrahedron Lett.* **2013**, *54*, 2674–2678.

(14) Related structure adopting *trans*(Cl,Cl): Mothes, E.; Sentets, S.; Luquin, M. A.; Mathieu, R.; Lugan, N.; Lavigne, G. *Organometallics* **2008**, *27*, 1193–1206.

(15) Takebayashi, S.; Dabral, N.; Miskolzie, M.; Bergens, S. H. *J. Am. Chem. Soc.* **2011**, *133*, 9666–9669.

(16) At present, $Me_2N(CH_2)_nOH$ (n = 6, 3, 2) have been used worldwide as catalysts for the production of poly(urethane) foam: Imabeppu, M.; Kiyoga, K.; Okamura, S.; Shoho, H.; Kimura, H. *Catal. Commun.* **2009**, *10*, 753–757.

(17) (a) Olah, G. A. *Angew. Chem., Int. Ed.* **2005**, *44*, 2636–2639. (b) Olah, G. A.; Goeppert, A.; Prakash, G. K. S. *J. Org. Chem.* **2009**, *74*, 487–498.

(18) Zhang, J.; Leitus, G.; Ben-David, Y.; Milstein, D. *Angew. Chem., Int. Ed.* **2006**, *45*, 1113–1115.

(19) (a) Whitesides, G. M.; Hackett, M.; Brainard, R. L.; Lavalleye, J.-P. P. M.; Sowinski, A. F.; Izumi, A. N.; Moore, S. S.; Brown, D. W.; Staudt, E. M. *Organometallics* **1985**, *4*, 1819–1830. (b) Jaska, C. A.; Manners, I. *J. Am. Chem. Soc.* **2004**, *126*, 9776–9785. (c) O, W. W. N.; Lough, A. J.; Morris, R. H. *Chem. Commun.* **2010**, 8240–8242.

(20) Direct injection of a similar sample into an ESI-MS instrument under air, skipping the BH_3 treatment, gave an intense signal corresponding to 8 (Found: m/z = 312.2482; Calcd for **8**+H^+: 312.2451). The structure of **7**, **7** · $(BH_3)_2$, and **8** was unambiguously ascertained in reference to $^{31}P\{^1H\}$ NMR and/or ESI-MS data of a set of authentic samples prepared separately. An attempt to purify and to isolate the complex $(RuCl_2)$ · $\mathbf{7}_2$ is unsatisfactory so far; however, a crude mixture of **7** and $[RuCl_2(cod)]_n$ ($[\mathbf{7}]_0$:$[Ru]_0$ = ca. 2:1) also enabled the hydrogenation of **3a**.

(21) ^{1}H NMR (toluene-d_8) of a preactivated catalyst (P_{H2} = 8 MPa, 160 °C, 5 h) showed several signals within a range from δ –7 to –24 ppm, corresponding to RuH species; however, they are variable depending on technical conditions.

(22) When 2 mol % instead of 4 mol % of **2a** was used for the hydrogenation of **3a** under conditions B in Table 2 (160 °C, PH2 = 8 MPa, 36 h), NMR yields of **4a** and **5a** were 9% and 8%, respectively.

(23) Martinelli, J. R.; Clark. T. P.; Watson, D. A.; Munday, R. H.; Buchwald, S. L. *Angew. Chem. Int. Ed.* **2007**, *46*, 8460–8463.

(24) (a) Agwada, V. C. *J. Chem. Eng. Data* **1982**, *27*, 479–481. (b) Huang, Z.; Reilly, J. E.; Buckle, R. N. *Synlett* **2007**, *7*, 1026–1030.

(25) Prosser, A. R.; Banning, J. E.; Rubina, M.; Rubin, M. *Org. Lett.* **2010**, *12*, 3968–3971.

(26) Zou, B.; Dreger, K.; Lichtenfeld, C. M.; Grimme, S.; Schäfer, H. J.; Fuchs, H.; Chi, L. *Langmuir* **2005,** *21,* 1364–1370.

(27) Flapper, J.; Kooijman, H.; Lutz, M.; Spek, A. L.; Van Leeuwen, P. W. N. M.; Cornelis J. Elsevier, C. J.; Kamer, P. C. J. *Organometallics* **2009**, *28*, 1180–1192.

(28) Pasha, M.A.; Jayashankara, V. P. *Synthetic Communications* **2006**, *36*, 1787–1793.

Chapter 2.

Multifaceted Catalytic Hydrogenation of Amides via Diverse Activation of a "Molecular Surface" as Precatalyst

Abstract: Amides are ubiquitous and abundant in nature and our society, but are very stable and reluctant to salt-free, catalytic chemical transformations. Through the activation of a "molecular surface" (a group of 15 planar atoms) incorporated into a ruthenium (Ru) precatalyst, catalytic hydrogenation of amides (formamides through polyamides) is achieved under a wide range of reaction conditions. That is, a diverse set of "catalytic molecular surfaces" (catalyst diversity) is induced by activation of a single molecular surface within the precatalyst when the conditions are varied. The catalysts have different structures and different resting states, but the common structure produced upon reaction with H_2 which catalyzes hydrogenation is "H–Ru–N–H." The molecular surface is a useful precatalyst to generate a diverse set of versatile catalysts for multifaceted amide hydrogenation. This catalytic molecular surface can be described as lying at the interface between homogeneous and heterogeneous hydrogenation catalysis.

2.1. Introduction

As a result of high thermodynamic stability and kinetic inertness,[1–3] amides have been found in natural systems for millennia, as the repeating units of functional polypeptides (proteins), and have more recently become a valuable commodity as the monomer units (e.g., α,β-unsaturated carboxamides, caprolactams) of synthetic polymers including poly(acrylamide), nylons, and Kevlar produced on an enormous scale. Rapidly emerging C(sp^3)–H and C(sp^2)–H bond activation strategies that lead to C–N[4,5] and C–C[6,7] bond formation frequently utilize amides as directing groups. Were it possible to develop an effective method for the catalytic hydrogenation of amides (formally, a hydrogenolysis–hydrogen addition sequence) that leads to selective C–N bond cleavage in preference to C=O bond cleavage, alcohols and amines would be generated. Both are useful platform chemicals or intermediate building blocks for organic synthesis. Alcohol and amine monomer units could also be regenerated/recycled from waste polyamides, which would otherwise be disposed of via combustion, resulting in the emission of CO_2 and NO_x. For example, the hydrogenation leading to effective C–N bond cleavage in *N,N*-dimethyl formamide (DMF) produces CH_3OH. This method, if it can be developed, would be potentially useful for enhancing the "anthropogenic chemical carbon cycle (methanol economy)," as suggested by Olah,[8] in conjunction with the elegant DMF synthesis reported by Noyori[9] involving the reaction of supercritical CO_2 with H_2 and Me_2NH, catalyzed by a Ru complex with an extremely high turnover number (substrate/catalyst ratio: S/C = 370,000).

Recently, Cole-Hamilton[10,11]/Leitner,[11] Ikariya,[12–15] Milstein[16–19] and Bergens[20,21] reported the use of different ruthenium (Ru) complexes which hydrogenate a range of strongly or moderately activated amides, including *N*-aryl-, *N*-acyl-, and α-alkoxy amides and morpholino ketones, as well as relatively small amides. Very recently, Mashima[22] reported the use of a combination of a Ru complex (2 mol %) bearing two bidentate ligands ($Ph_2P(CH_2)_2NH_2$), KO^{t}Bu (20 mol %) and Zn salts (4 mol %), which promoted the hydrogenation of *N*-methyl amides, but the reactivity of sterically more demanding amides and primary amides was scant to moderate, and could not be improved, since the catalysis did not seem to be sustainable under harsher reaction conditions. Thus, the development of a new catalytic system generally applicable for the hydrogenation of different classes of amides such as those found in DMF, oligopeptides

and artificial polyamides remains a significant challenge; however, there is a lack of basic knowledge concerning the molecular design of a catalyst competent under both the mild and harsh conditions necessary to achieve such multifaceted amide hydrogenation.

The author recently reported preliminary research on the molecular design of Ru complexes including RUPCY (**2a**, Cy = C_6H_{11}),[23,24] which was shown to be effective for the hydrogenation of unactivated amides (Scheme 1a).[23] Unfortunately, however, the catalyst system is only viable under harsh reaction conditions (substrate/catalyst ratio (S/C) = 50; hydrogen pressure (P_{H2}) = 4–8 MPa; reaction temperature (T) = 140–180 °C, reaction time (t) = 24–216 h). Herein is reported a greatly improved method for the hydrogenation of unactivated amides (Scheme 1b), realized by introducing an incredibly versatile "molecular surface (molecularly well-designed surface)". These molecular surfaces are hidden within the structures of Ru complexes RUPIP2 (**1a**, ^{i}Pr = $(CH_3)_2CH$) and RUPCY2 (**1b**), which serve as precatalysts, from which catalytically active (catalytic) surfaces within the molecules are generated by incorporation of multiple hydrogen atoms. Through simple but rational structural modification of **2a** to **1a** and **1b**, catalyst performance has been significantly advanced under both mild (P_{H2} = 0.5–2 MPa; T = 60–120 °C) and harsh (P_{H2} = 3–8 MPa; T = 130–160 °C) conditions.

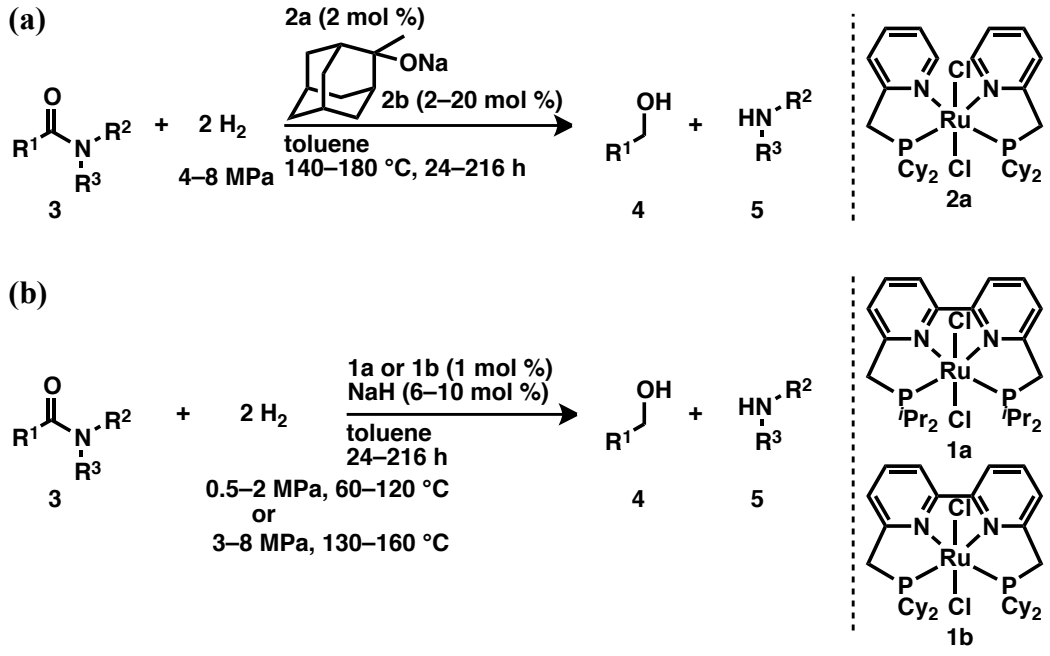

Scheme 1. General schemes of amide hydrogenation: (a) previous method; (b) present method.

2.2. Results and discussion

2.2.1. Strategy and design of ruthenium catalyst.

In our previous study,[23] it was shown that a plausible catalyst, either **cat$_A$** or **cat$_B$**, was likely induced upon treatment of precatalyst **2a** with bulky base **2b** and H_2 (Figure 1). Under the pre-activation conditions, full hydrogenation of the pyridines of **2a** gave a new bidentate ligand **2c** incorporating the piperidine (N–H) unit. It is therefore likely that hydrogen(s) transfer takes place from the four-centered "H–Ru–N–H" unit to an amide carbonyl group (Noyori's bifunctional mechanism),[25–27] affording $R^1CH(OH)(NR^2R^3)$ (Figure 3 right). Thus, this amide hydrogenation mechanism may involve an outer-sphere, rather than inner-sphere, mechanism that involves a two-step pathway, wherein the Ru catalyst having an H–Ru–N–H functionality is generated in the first step, followed by the amide carbonyl group interacting with both of the H of the H–Ru–N–H component to facilitate the hydrogen (H^- and H^+) transfer. However, the question as to which catalyst (**cat$_A$** or **cat$_B$**) is more active for hydrogenation has yet to be answered. To probe this, Ru complex **1b** bearing a tetradentate bipyridine (bpy) analog ligand was synthesized, in which the two bidentate ligands of **2a** are connected. This simple ligand manipulation rules out the possibility of facile detachment of the ligand from the Ru center, which the bidentate ligand **2c** of **cat$_A$** or **cat$_B$** underwent.

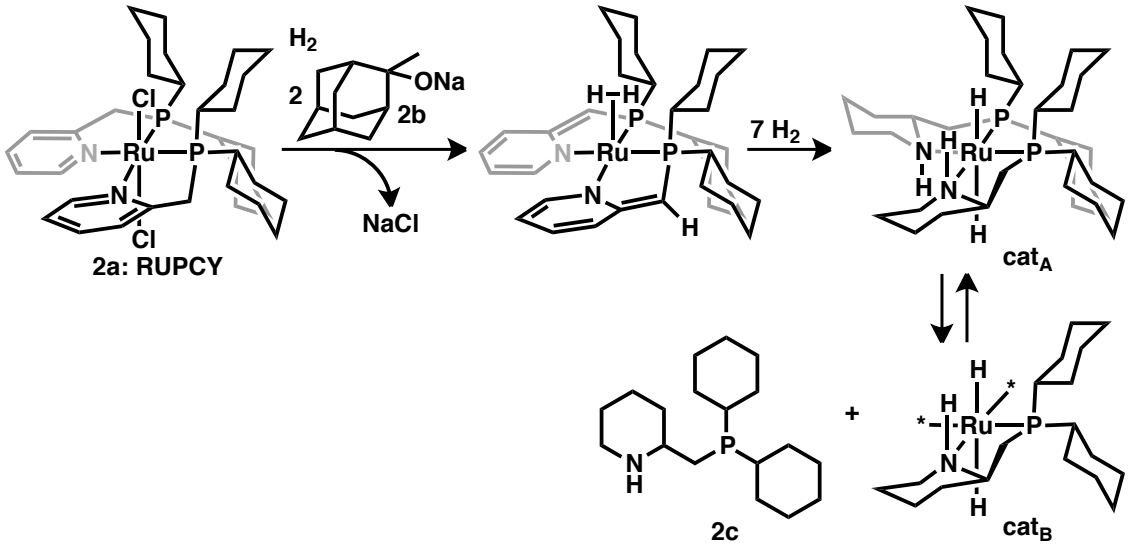

Figure 1. Earlier work: possible catalysts **cat$_A$** and **cat$_B$** derived from **2a**, which were modified to new Ru complexes **1a** and **1b**.

According to the X-ray single crystal structure analysis of **1b** (Figure 2), there are fifteen (non-H) atoms (the bpy, Ru, and two phosphorus atoms) in a planar orientation constituting a "molecular surface," with four sterically bulky cyclohexyl (Cy) architectures on top and bottom. The catalytic molecular surface (Figure 3 right) resembles what would serve as a catalytic solid surface (Figure 3 left), but differs in the sense that the former could provide customized structural diversity, tailor-made for any situation, in that the X group can be freely chosen at the element/molecular level. This exciting catalytic molecular surface therefore lies at the interface between homogeneous and heterogeneous hydrogenation catalysis.

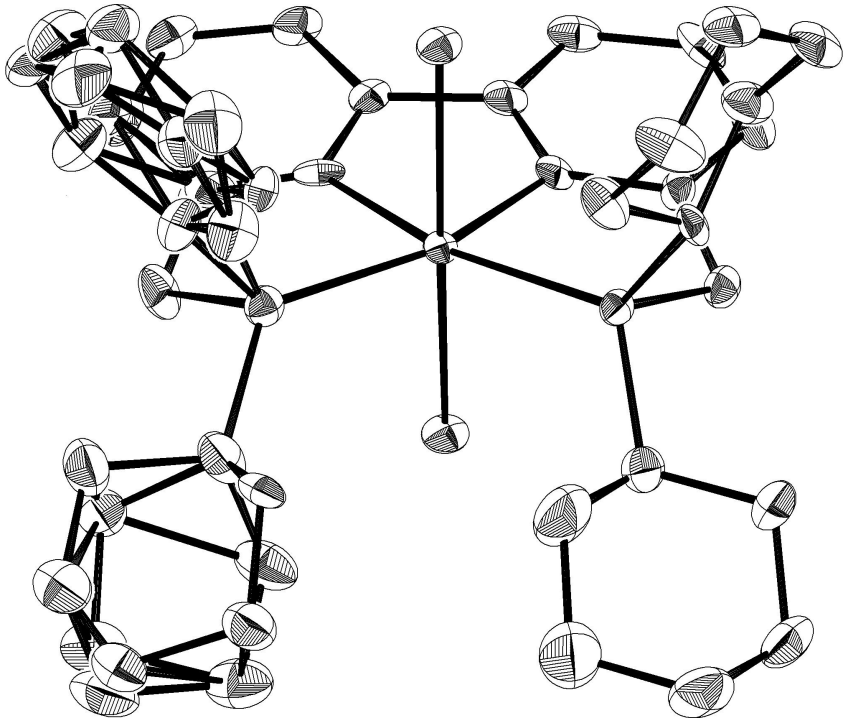

Figure 2. ORTEP drawing of Ru complex **1b**. 50% probability ellipsoids; The hydrogen atoms not involved in hydrogen bonding are omitted for clarity.

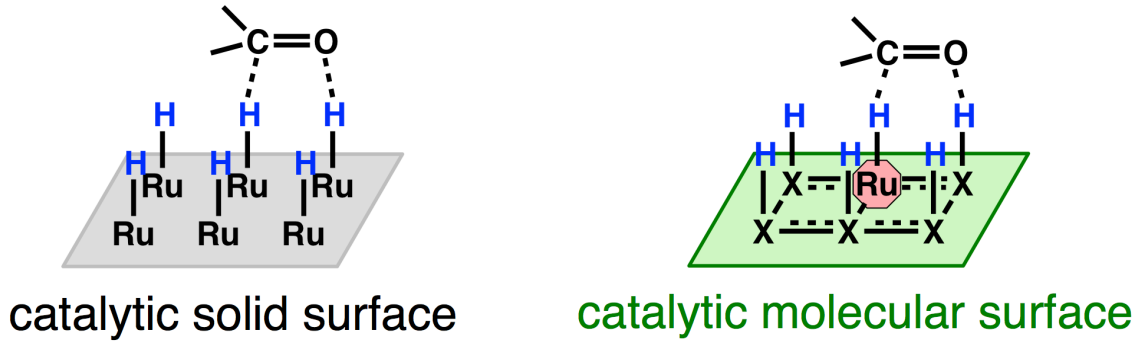

Figure 3. Solid and molecular surface for hydrogenation transfer to carbonyl group.

2.2.2. Relationship between structure and catalytic activity of Ru complexes.

At the outset, the catalyst performance of **1b** was compared with that of **2a** (Table 1): toluene solutions of each Ru complex (1 mol %), amide **3a** (100 mol %), and NaH (6 mol %) were reacted under identical reaction conditions ($[Ru]_0$ = 3.3 mM, S/C = 100; P_{H2} = 1 MPa, T = 110 °C, t = 15 h). The apparent reaction rate obtained using **1b** (**4a**: 82%) was more than 40-fold faster than that with **2a** (**4a**: <2%) under mild conditions (entries 1 and 4). By replacing **1b** with **1a**, the initial load of the Ru complex can be reduced to not less than 0.25 mol % (S/C = 400; NaH: 5 mol %), giving a turnover number (TON) of ca. 300 (calculated as the number of moles of H_2 molecules added to the amide per the initial amount of **1a** (mol)) ($[\mathbf{1a}]_0$ = 0.83 mM, P_{H2} = 1 MPa, T = 110 °C, t = 24 h) (entry 3). The catalytic performance of **1a** and **1b** exceed the best reported values by a wide margin (**4a**: 57%: S/C = 100, P_{H2} = 1 MPa, T = 110 °C, t = 48 h, TON = 57).[16] From this, the turnover frequency (TOF = TON•h^{-1}) can be roughly estimated to be more than 10-fold greater in this new system.

In order to find a more competent catalyst, several derivatives of **1** (**1c**,[28] **1d**, **1e**, and **1f**[29]) were synthesized as different molecular surface precatalysts and tested in the hydrogenation of **3a** under similar conditions ($[\mathbf{1}]_0$ = 3.3 mM, S/C = 100; **1**:NaH:**3a** (mol %) = 1:6:100; P_{H2} = 1 MPa, T = 110 °C, t = 15 h) (Table 1).[30] The phenanthroline series **1d–f**, which has a more extended π-conjugation system resulting in seventeen elements in the molecular surface, was totally ineffective (entries 6–8). The sterically more bulky **1c** (R = ^{t}Bu) also showed less promising results (entry 5). In order to minimize steric repulsion between the catalyst and the incoming substrate, including less reactive, sterically bulky amides, **1a** was chosen for further investigation.

Table 1. Hydrogenation of **3a** using different Ru complexes **1a**–**f** and **2a** ($[Ru]_0$ = 3.3 mM) as precatalysts.

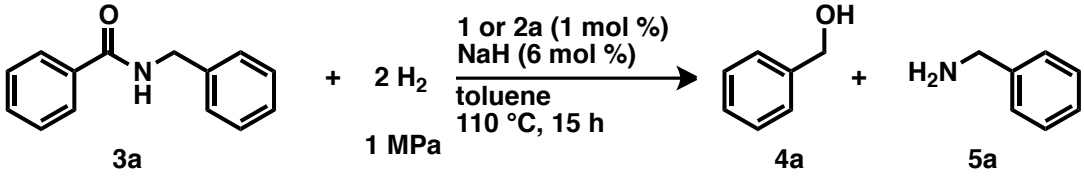

entry	Ru complex	result[a] (%)		
		conv.	4a	5a
1	2a	<2	<2	<2
2	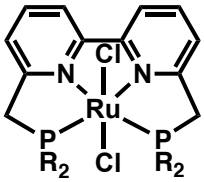 1a (R = ^{i}Pr)	81	81	81
3[b]	1a (R = ^{i}Pr)	72	73	74
4	1b (R = Cy)	82	82	80
5	1c (R = ^{t}Bu)	57	57	56
6	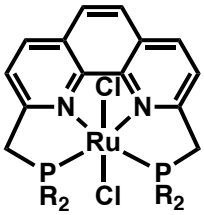 1d (R = ^{i}Pr)	4	4	<2
7	1e (R = Cy)	6	6	4
8	1f (R = ^{t}Bu)	<2	<2	<2

[a] Determined by ^{1}H NMR. [b] 1a (0.25 mol %), NaH (5 mol %), 24 h.

2.2.3. ESI-MS study of preactivated catalyst.

Bulky base **2b** (Figure 1), which was used previously[23] as an additive for the preactivation of **2a** in the absence of amide, was as effective as NaH for the amide hydrogenation catalyzed by **1a** and **1b**. It turned out, however, that this preactivation step in the absence of amide could be eliminated using NaH. The resting state of a matured catalyst generated under preactivation conditions in the presence or in the absence of amide **3a** ($[\mathbf{1a}]_0$ = 3.3 mM in toluene; **1a**:NaH (mol %) = 1:10; $[\mathbf{3a}]_0$ = 5.0 mM or 0; P_{H2} = 1 MPa, T = 110 °C, t = 5 h) was thus evaluated. Solutions of pre-activated catalyst with and without **3a** were prepared separately, and the samples were measured directly via electrospray ionization-mass spectroscopy (ESI-MS) (Figures 5, 6). Both samples showed a Ru species that retained a tetradentate ligand-incorporated structure during the induction period of the catalyst: organic frameworks comprised of a Ru with slightly different molecular weights (m/z = 519.1626±0.0052 (strong intensity), 565.1317±0.0021 ($\mathbf{I_C}$ –2H + 3O: small to moderate

intensity)) were consistently detected. Both signals correspond to structures less the two Cl groups from the original **1a**. The former intense signal corresponds to $\mathbf{I_{C1}}$–$\mathbf{I_{C3}}$ (^{1}H NMR (ppm): δ –8.62 (t (dd), J = 29.7 Hz, RuH)), produced by deprotonation of two methylene groups (CH_2–bpy–CH_2) of **1a** (with two NaCl formation), followed by H_2 adsorption (Figure 4). The deprotonation[16] and subsequent capture of one H_2 molecule was confirmed using D_2 instead of H_2 (Figure 7). The ^{1}H NMR signal at δ –8.62 became significantly weaker, and the ESI-MS signal of $\mathbf{I_{C1}}$–$\mathbf{I_{C3}}$ disappeared; instead, a signal at 521.1752±0.0070 ($\mathbf{I_C}$ –H_2 +D_2) was observed as the only intense signal. In contrast, when preactivation was carried out under the identical conditions, except for P_{H2} = 8 MPa and T = 160 °C or P_{H2} = 4 MPa and T = 140 °C being used, the base peak (m/z = 429.1603±0.0016) was consistent with $\mathbf{I_E}$ (or its tautomers): fully hydrogenated bipyridine with concurrent cleavage of one C–P bond (Figures 8, 9).[31,32] The corresponding $\mathbf{I_E}$-d_{16} (m/z = 445.2608±0.0090) was also detected using D_2 instead of H_2, suggesting hydrogenolysis of the C–P bond. Under milder conditions (P_{D2} = 1 MPa, T = 160 °C), $\mathbf{I_D}$ (m/z = 534.2661±0.0019 or its tautomers) was also detected as a major product (Figures 10, 11) which would correspond to an intermediate during the structural changes from $\mathbf{I_C}$ to $\mathbf{I_E}$, during which time deuterium atoms from multiple D_2 (one to eight molecules) are in turn incorporated. The oxygenation of $\mathbf{I_E}$ likely occurred during aerobic sample injection into the ESI-MS instrument,[23] so that any oxygen atom-incorporating processes affecting the hydrogenation steps could be fully ruled out. These experiments show that different catalyst resting states, in which the common structure produced upon reaction with H_2 is "H–Ru–N–H," are necessary to catalyze hydrogenation, depending on the range of P_{H2} and T. Hydride- and proton-transfer to an amide carbonyl most likely occurs from a "H(δ^-)–Ru–N–H(δ^+)" fragment, in which both the Ru–H and N–H face the same direction due to the catalytic molecular surface. The scant catalytic activity derived from phenanthroline series **1d–f** could partly be explained by a more acidic nature of the NH group of aniline structures in the catalytic molecular surface induced by preactivation of **1d–f** (Figure 12; Table 2, entry 3). In any event, the molecular surface is non-innocent and undergoes meaningful structural changes via multiple hydrogen additions before producing the diverse, active forms of the catalyst. The features resemble those of a catalytic solid surface of bulk metal, which also adsorbs numerous hydrogen atoms upon reaction with $n$$H_2$. These results further suggest that a Ru complex bearing a (P,bpy,P) ligand is more versatile in the

production of diverse catalysts than precatalysts bearing simple bidentate (*P*,*N*)[21–23] or tridentate (*P*,*N*,*N*)[16–19] ligand(s).

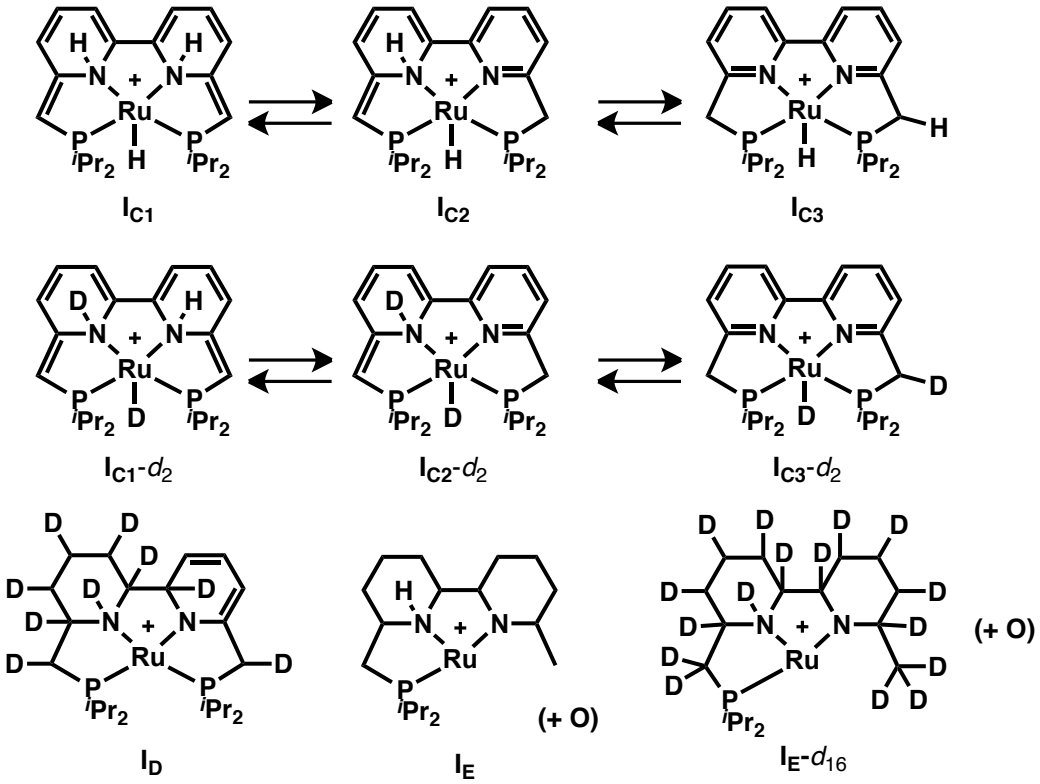

Figure 4. Major resting states of catalysts. Calculated exact masses: $\mathbf{I_{C1}}$– $\mathbf{I_{C3}}$ (519.1626), $\mathbf{I_C}$-d_2 (521.1752), $\mathbf{I_D}$ (534.2661), $\mathbf{I_E}$ (429.1603) and $\mathbf{I_E}$-d_{16} (455.2608).

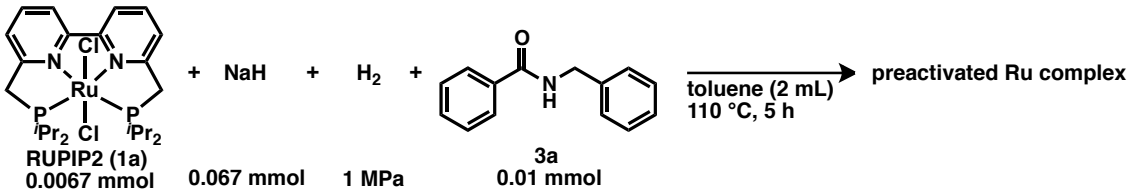

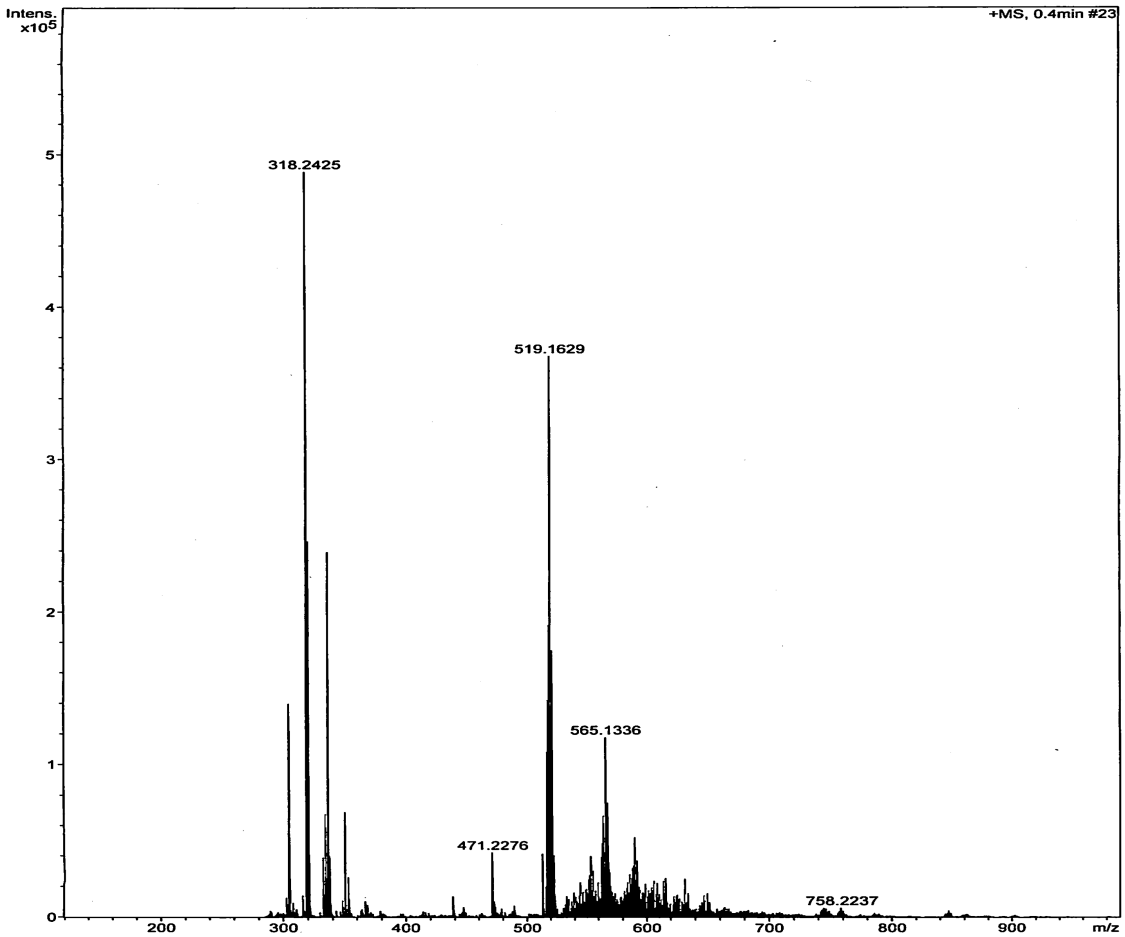

Plausible tautomers

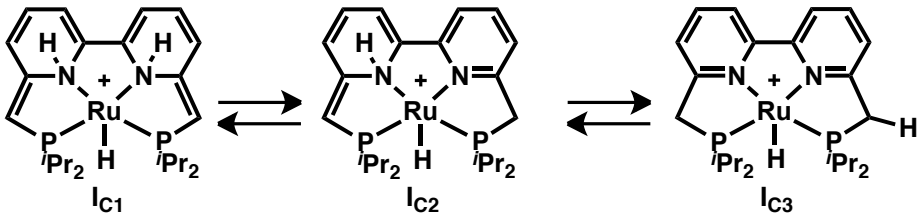

Exact Mass: 519.1626; found: 519.1629

Figure 5. ESI-MS data of a preactivated catalyst: with *N*-benzylbenzamide (**3a**) ([**1a**]$_0$ = 3.3 mM, P_{H2} = 1 MPa, T = 110 °C).

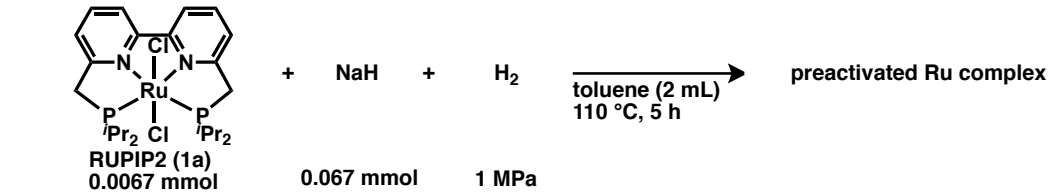

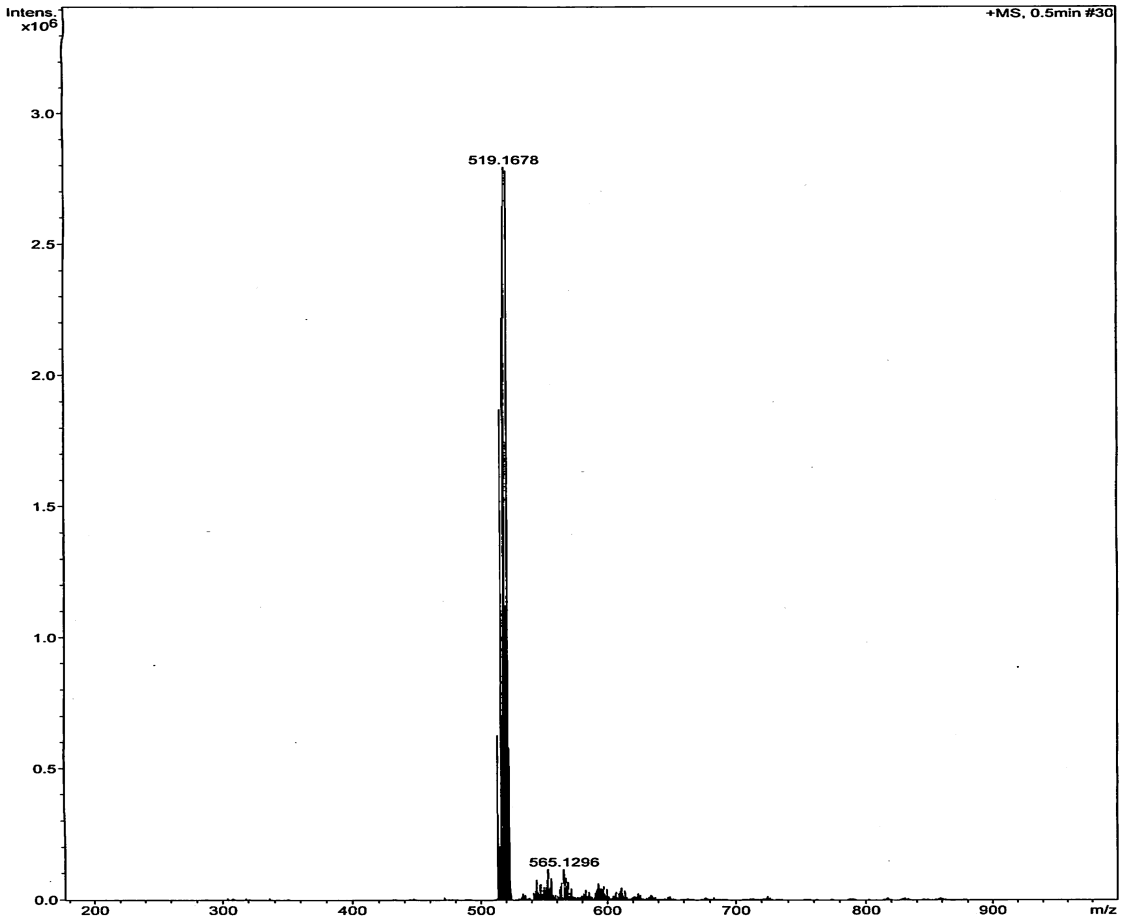

Plausible tautomers

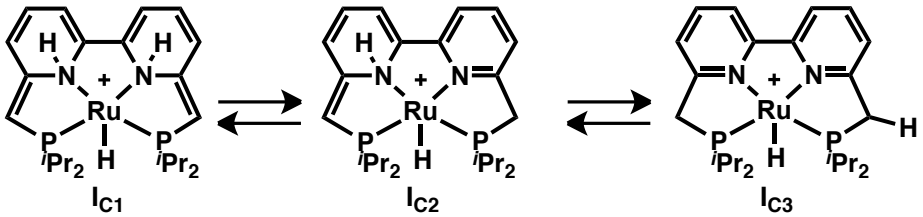

Exact Mass: 519.1626; found: 519.1678

Figure 6. ESI-MS data of a preactivated catalyst: without *N*-benzylbenzamide (**3a**) ([**1a**]$_0$ = 3.3 mM, P_{H2} = 1 MPa, T = 110 °C).

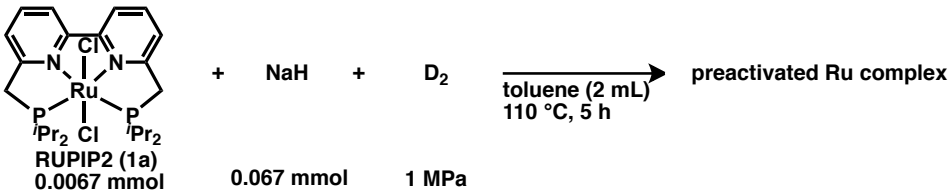

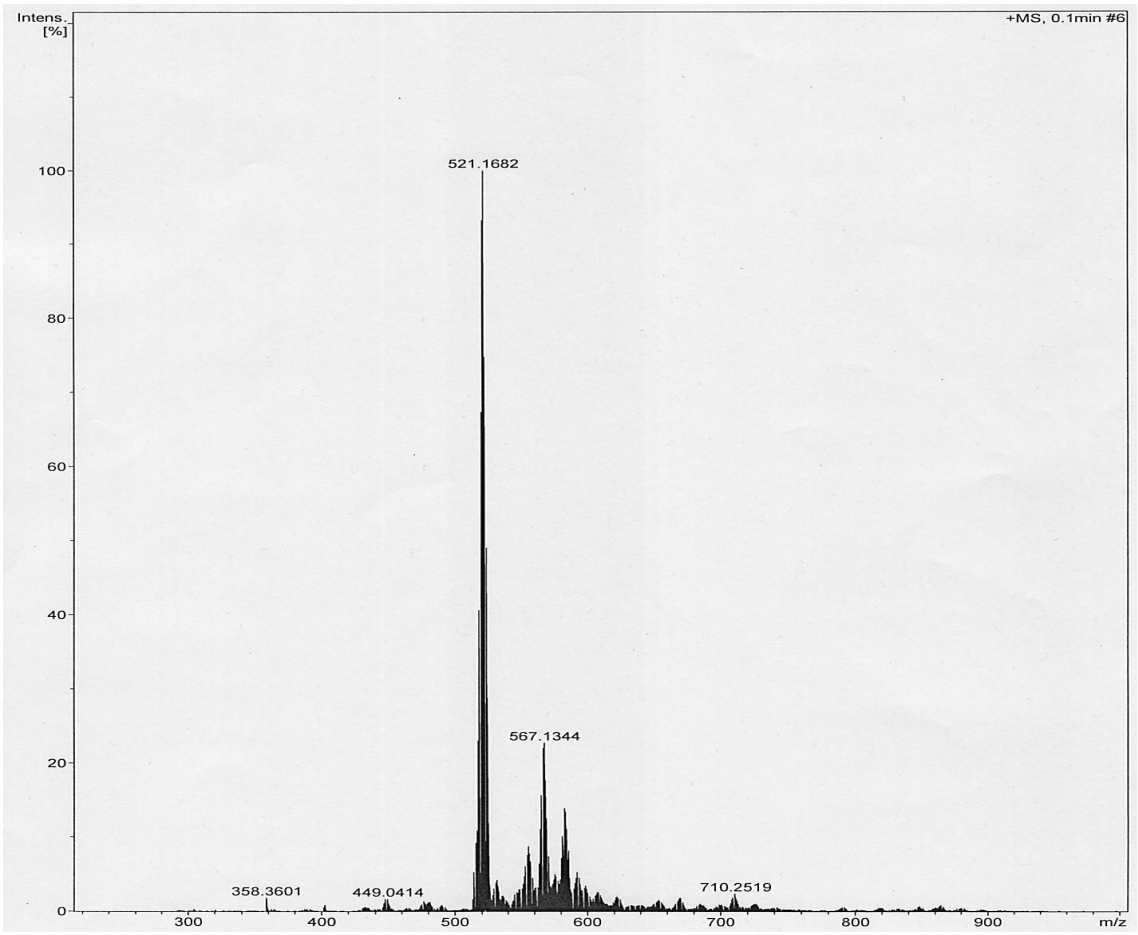

Plausible tautomers

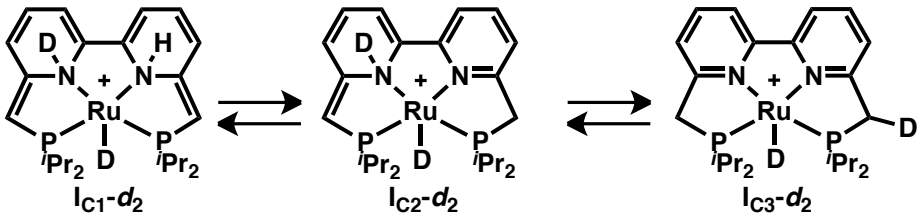

Figure 7. ESI-MS data of a preactivated catalyst: without *N*-benzylbenzamide (**3a**) ([**1a**]$_0$ = 3.3 mM, P_{D2} = 1 MPa, T = 110 °C).

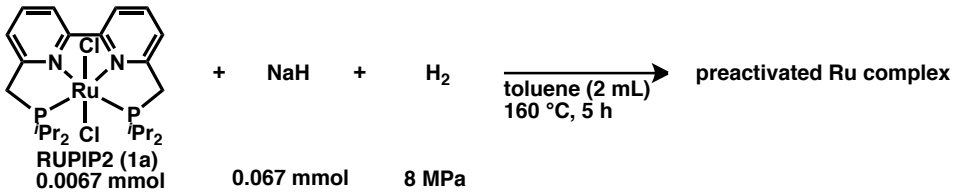

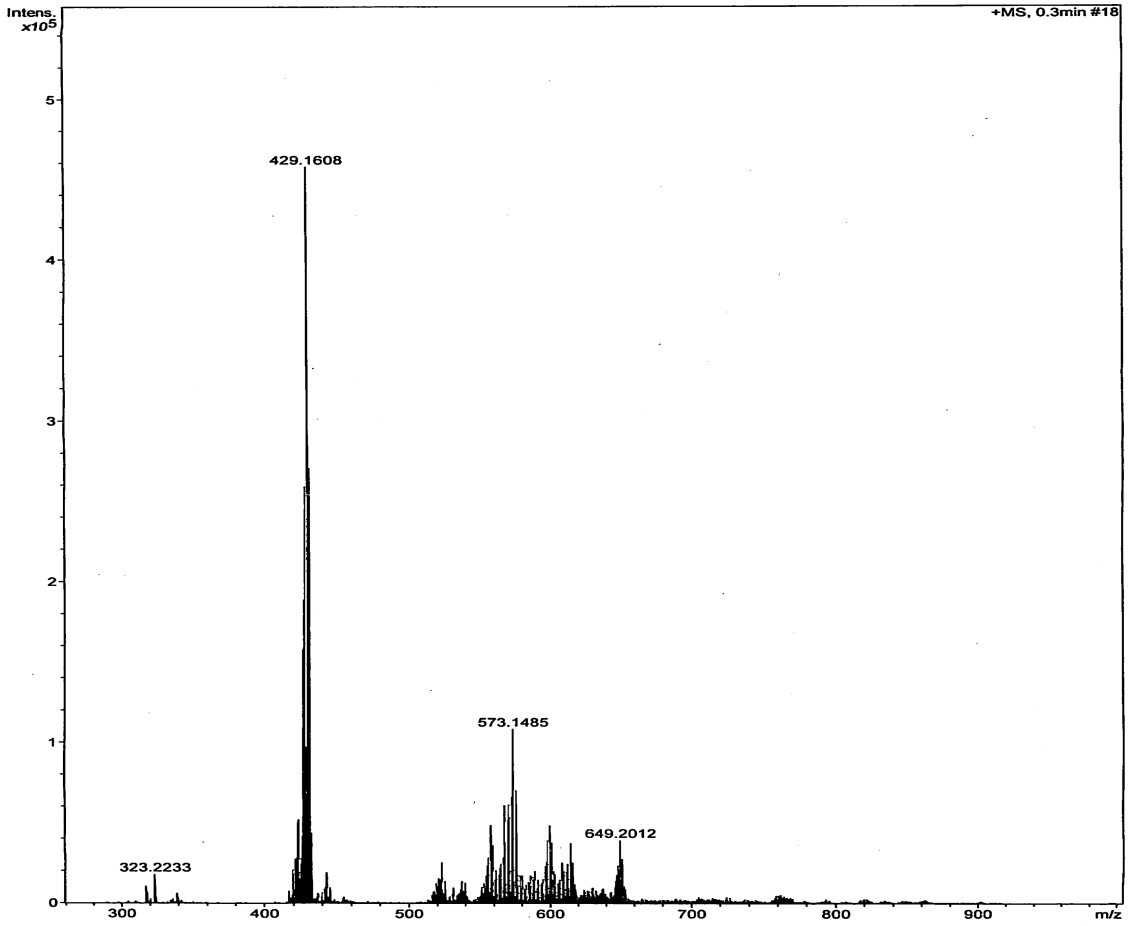

Plausible tautomers

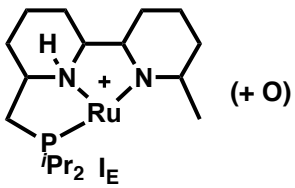

(+ O)

Exact Mass: 429.1603; found: 429.1608

Figure 8. ESI-MS data of a preactivated catalyst: without *N*-benzylbenzamide (**3a**) ([**1a**]$_0$ = 3.3 mM, P_{H2} = 8 MPa, T = 160 °C).

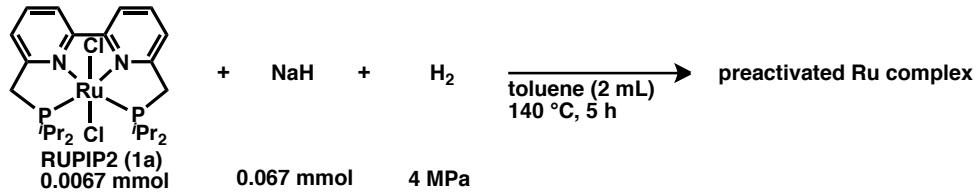

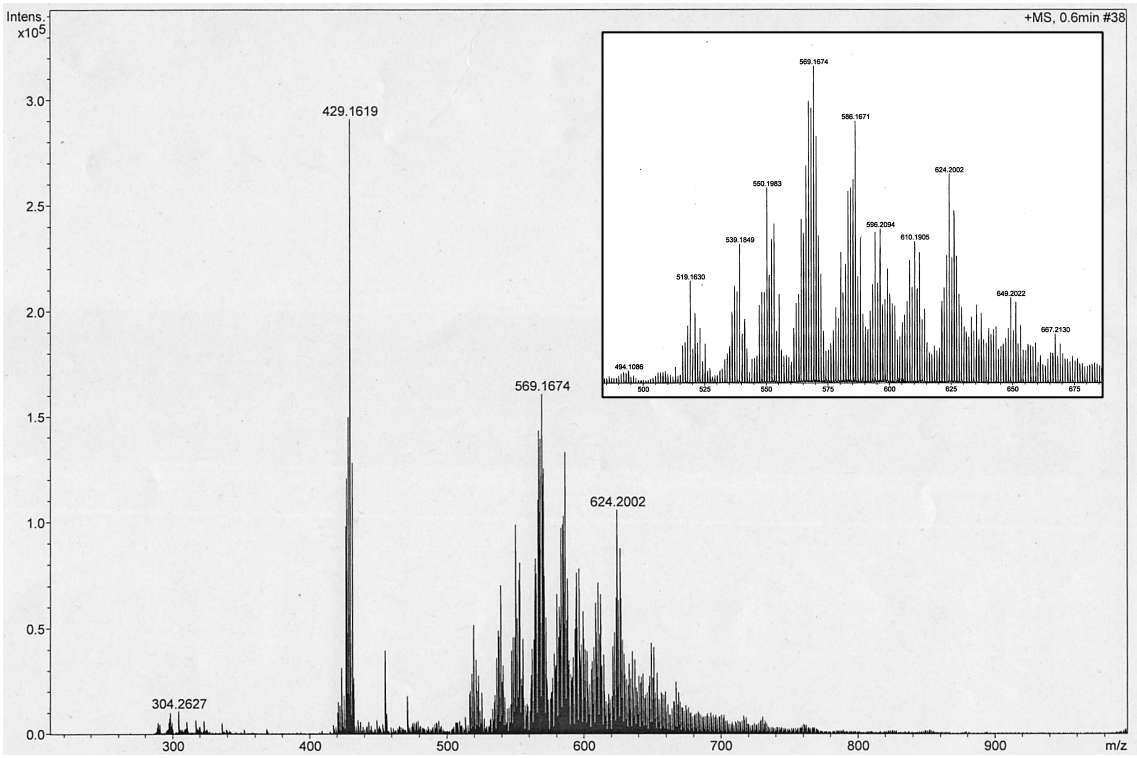

Plausible tautomers

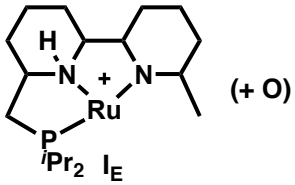

Figure 9. ESI-MS data of a preactivated catalyst: without *N*-benzylbenzamide (**3a**) ([**1a**]$_0$ = 3.3 mM, P_{H2} = 4 MPa, T = 140 °C).

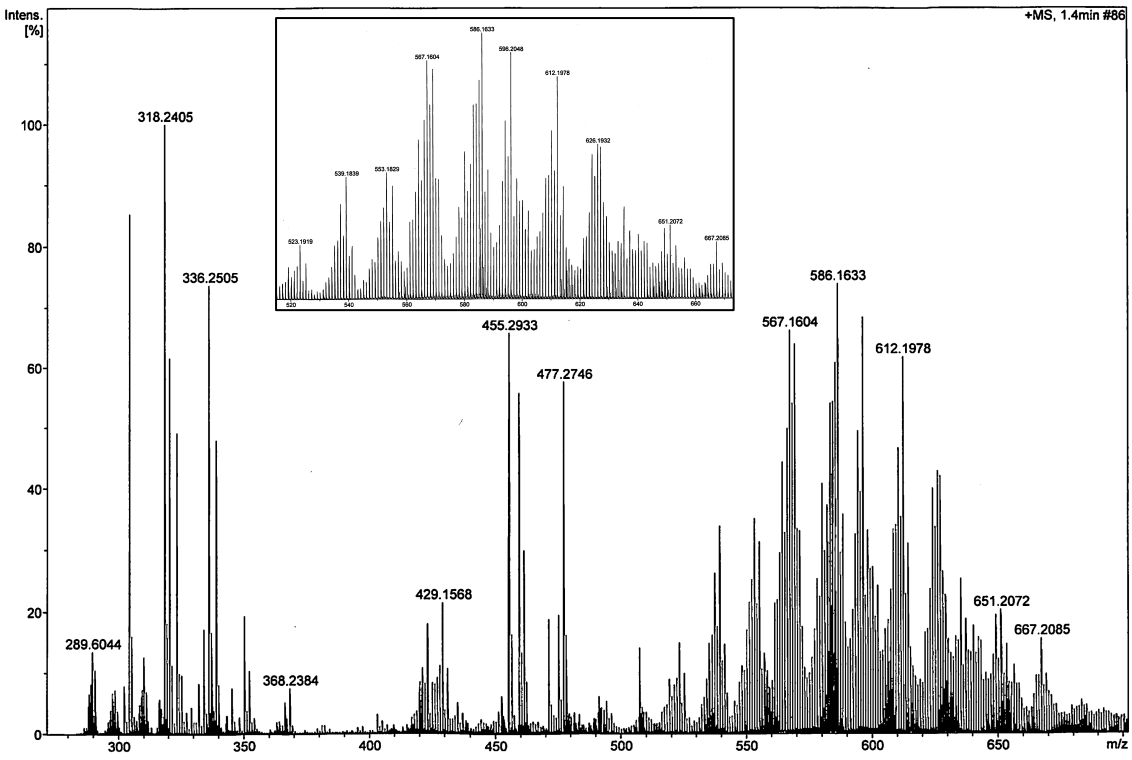

Plausible tautomers

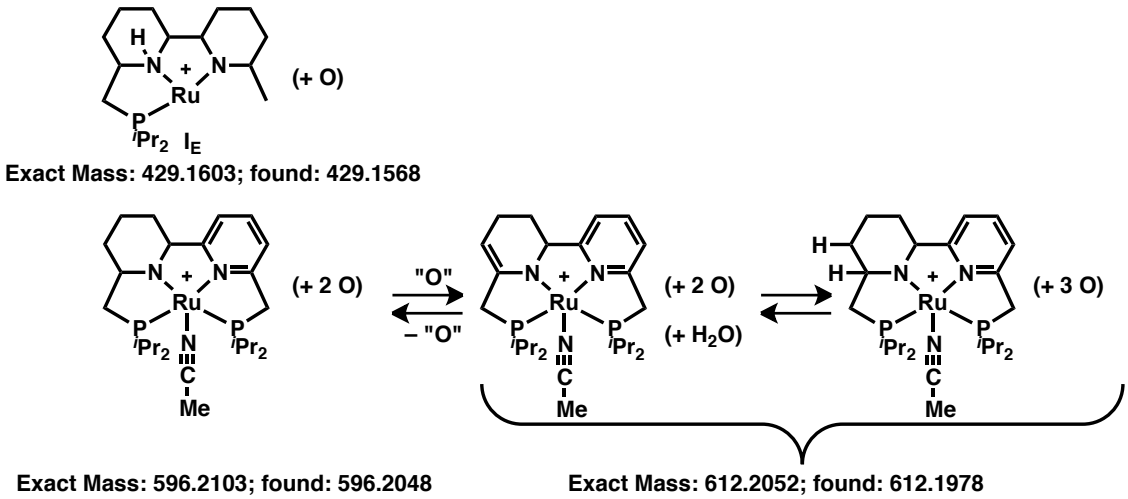

Figure 10. ESI-MS data of a preactivated catalyst: without *N*-benzylbenzamide (**3a**) ([**1a**]$_0$ = 3.3 mM, P_{H2} = 1 MPa, T = 160 °C).

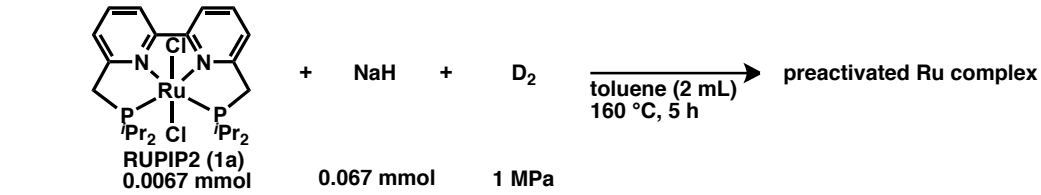

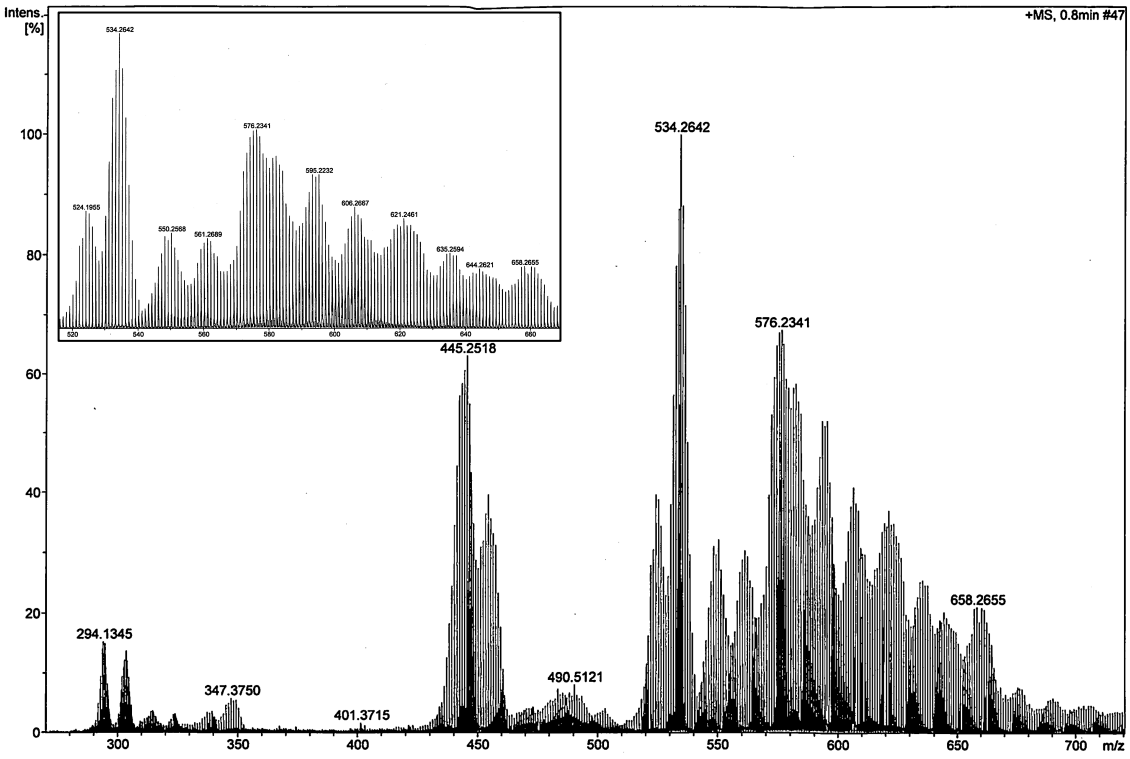

Plausible tautomers

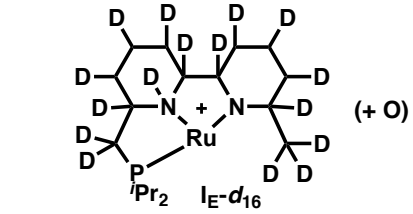

Exact Mass: 445.2608; found: 445.2518

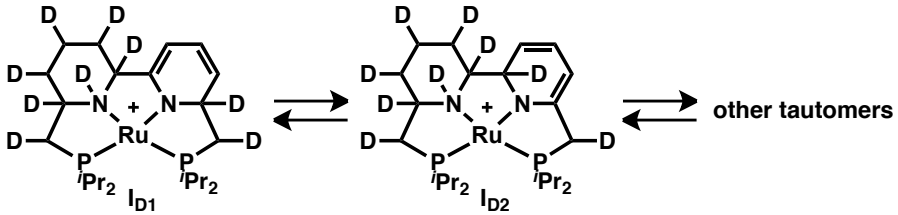

Exact Mass: 534.2661; found: 534.2642

Figure 11. ESI-MS data of a preactivated catalyst: without *N*-benzylbenzamide (**3a**) ([**1a**]$_0$ = 3.3 mM, P_{D2} = 1 MPa, T = 160 °C).

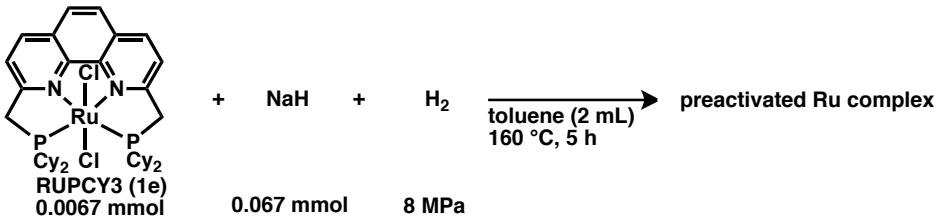

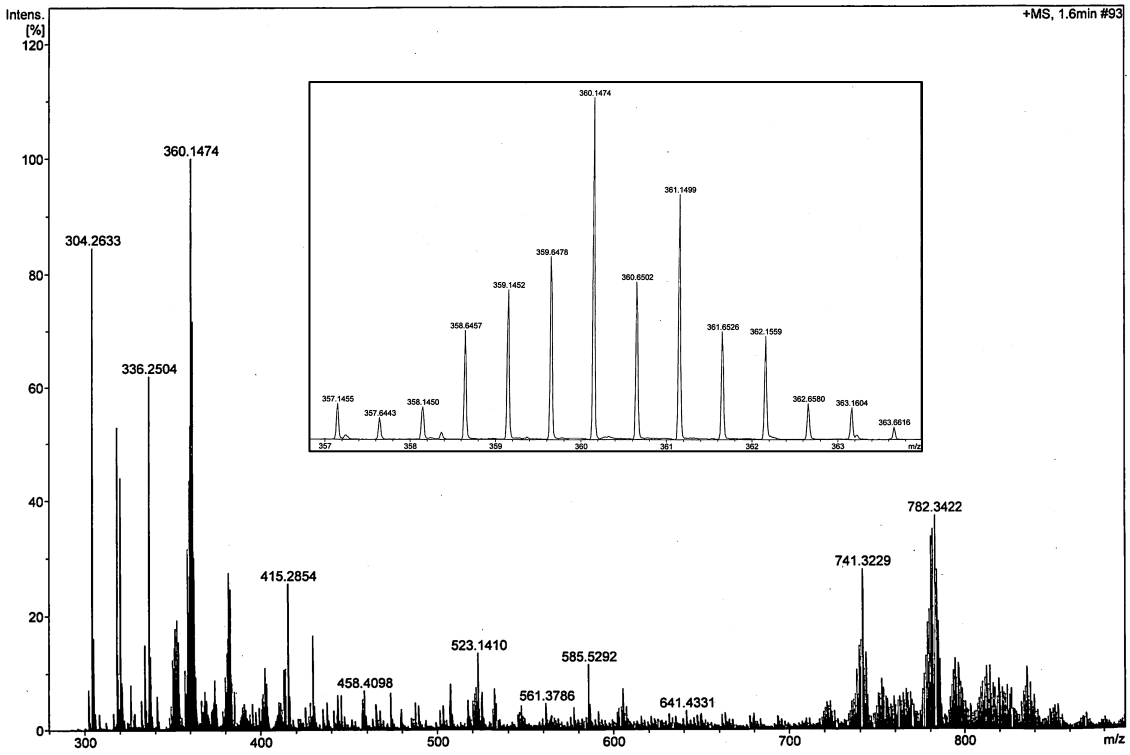

Plausible tautomers

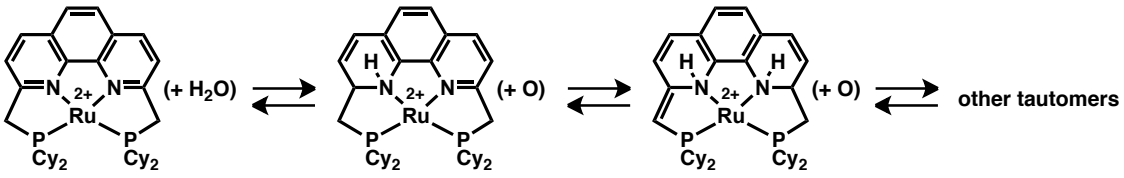

Exact Mass: 720.2900 (*m/z* = 360.1450); found: 360.1474

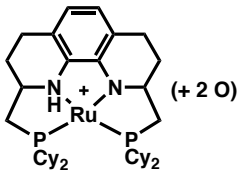

Exact Mass: 741.3246; found: 741.3229

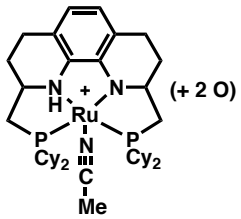

Exact Mass: 782.3512; found: 782.3422

Figure 12. ESI-MS data of a preactivated catalyst: without *N*-benzylbenzamide (**3a**) ([**1e**]$_0$ = 3.3 mM, P_{H2} = 8 MPa, T = 160 °C).

2.2.4. Substrate scope.

Hydrogenation can be started conveniently by mixing air-stable **1a**, amide **3**, and NaH together, followed by pressurizing the reaction vessel with H_2 and then elevating *T*. Catalyst preactivation procedures in a separate reaction vessel is not necessarily needed. The hydrogenation of various unactivated amides under different conditions was tested, and the results are given in Table 2. Primary, secondary, and tertiary amides showed excellent compatibility with the same precatalyst, regardless of steric demands or whether aromatic/aliphatic. In order to shorten the reaction time for practical application, it is better to slightly increase the *T* (120–130 °C) and P_{H2} (2–3 MPa) (entries 1–11). The hydrogenation of ε-caprolactam (**3h**), a cyclic amide which serves as the monomer of nylon-6, showed a similar pattern of C–N bond cleavage, giving the amino alcohol $HO(CH_2)_6NH_2$ (**6h**) predominantly (azepane: 1%). Products $HO(CH_2)_6NH_2$ (**6h**) (entry 10) and $HO(CH_2)_6NHMe$ (**6i**) (entry 11) are synthetic precursors of *N,N*-dimethyl-6-amino-1-hexanol, a polymerization initiator in polyurethane synthesis.[33]

Hydrogenation of the more sterically demanding amides **3k**, **3m**, and **3n** also took place, capitalizing on the structural robustness (negligible ligand detachment) of the catalyst even under harsher reaction conditions (P_{H2} = 3–8 MPa, *T* = 130–160 °C) (entries 12–16). The mercury test[23] was also employed, in which Hg(0) (150 mol %) was added during the hydrogenation of **3n** to probe the possibility of catalysis by a Ru nanoparticle under the harshest reaction conditions (P_{H2} = 8 MPa, *T* = 160 °C, *t* = 96 h) (entry 17). The catalytic activity was not perturbed during the course of the reaction (**4n**: 71%; **5n**: 92%). This is in good contrast to previous results using the less stable precatalyst **2a**,[23] in which only marginal hydrogenation of **3m** and **3n** took place. In general, the more sterically demanding the amide, the less reactive the amide.

The hydrogenation rate of urea **3p** with **1b** was comparable to that obtained with **1a**, while urethane derivative **3q** was hydrogenated more effectively using **1b** than **1a** (entries 19 and 20). Methanol was produced in ca. 60–70% yield in both cases, along with **4a** and **5a** in almost quantitative yields. These reactions are vitally important to the methanol economy,[8,17,18] as urea specifically is an excellent chemical reservoir and carrier of CO_2. Compared with **3p** and **3q**, hydrogenation of another CO_2 derivative, DMF, proceeded far more smoothly, giving full conversion at 60 °C with P_{H2} = 8 MPa (Figure 13), and at 120 °C with P_{H2} = 2 MPa, producing CH_3OH in ca. 60% yield in

both cases (entries 22 and 23). To hydrogenate tertiary amides DMF, **3j** and **3k**, and acetamide **3g**, preactivation of the catalyst was required (P_{H2} = 1 MPa, T = 160 °C, t = 5 h) before addition of the corresponding **3** to the catalyst mixture (entries 9, 12, 13, 22, and 23). Since the chemical immobilization of CO_2 as DMF has well been investigated,[9] a combination of the previous and present methods could provide an alternative route that benefits the methanol economy at low T and/or P_{H2}, in a future effort to improve the method of recovering/recycling Me_2NH (Figure 13). To the best of our knowledge, the selective and stepwise cleavage of the different C–N bonds in oligoamides such as diamide **3s** and triamide **3t** (a dipeptide with protection at the N-terminus) was successfully accomplished for the first time (entries 24, 25). The chiral centers epimerized, giving a racemic mixture of phenylalaninol (**6s**) and leucinol (**6t**). More intricately functionalized, commercial polyamides available from Toray Co. (AQ nylon P-70 and T-70 (105–120 mg each)) were also hydrogenated (**1a**, 2.9 mg; P_{H2} = 8 MPa, T = 160 °C, t = 48 h), giving different monomer units, where the mass balance before and after the reaction was ca. 80% consistent (the structures of the two monomer units cannot be disclosed here due to a confidentiality agreement with Toray).

Table 2. Catalytic hydrogenation of various amides **3**.

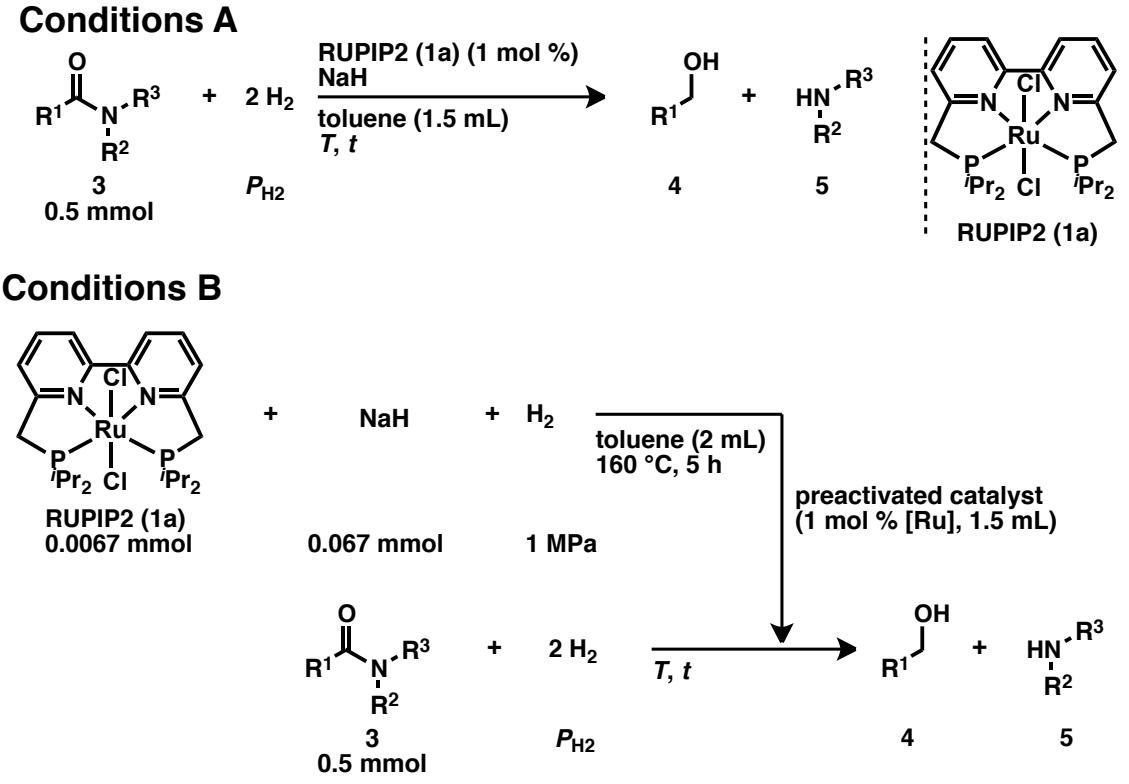

entry	3	conditions	NaH /mol %	P_{H2} /MPa	T /°C	t /h	result[a] (%) conv.	4	5
1	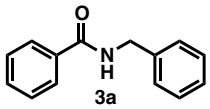 3a	A	10	1	110	24	87	86	86
2		A[b]	5	1	110	24	72	73	74
3		B[c]	10	1	110	15	18	18	14
4	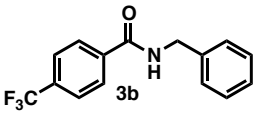 3b	A	10	0.5	80	24	95	94	92
5	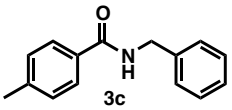 3c	A	10	2	110	39	90	93	89
6	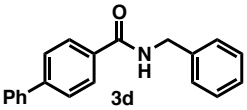 3d	A	6	2	120	24	94	93	82
7	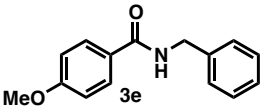 3e	A	10	2	120	24	84	84	82
8	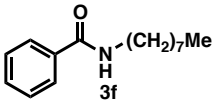 3f	A	6	2	120	24	84	84	86
9	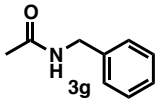 3g	B	10	2	120	24	85	—	84
10	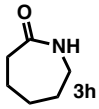 3h	A	6	3	130	39	88	86[d]	1[e]
11	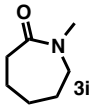 3i	A	6	3	130	48	65	66[d]	—
12	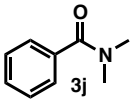 3j	B	10	1	110	24	98	95	—
13	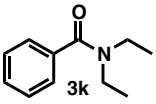 3k	B	10	3	130	24	99	94	—
14	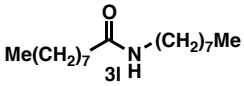 3l	A	6	3	130	39	92	89	86
15	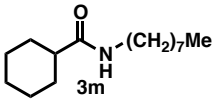 3m	A	10	4	140	96	96	96	94

[a] NMR analysis (mesitylene was used as internal standard). [b] RUPIP2 (1a) (0.25 mol %) was used.

[c] RUPCY3 (1e) was used. Catalyst was preactivated: P_{H2} = 8 MPa, T = 160 °C, t = 5 h.

[d] Yield of aminoalcohol.

[e] Yield of azepane ($C_6H_{13}N$).

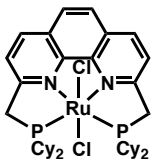

RUPCY3 (1e)

entry	3	conditions	NaH /mol %	P_{H2} /MPa	*T* /°C	*t* /h	result[a] (%) conv.	4	5
16	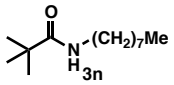 3n	A	10	8	160	96	97	70	87
17		A[f]	10	8	160	96	93	71	92
18	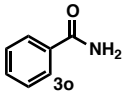 3o	A	6	8	160	39	99	92	—
19	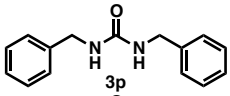 3p	B[g,h]	6	6	160	24	99	57	91
20	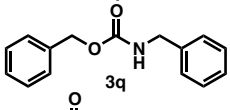 3q	B[g,i]	6	6	160	24	99	4a 99 MeOH 64	99
21	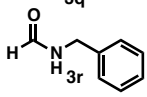 3r	A	6	8	60	24	99	71	95
22		B	10	8	60	15	99	52	—
23		B	10	2	120	27	99	56	—
24	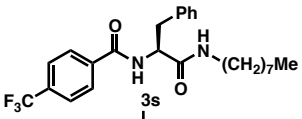 3s	A[j]	12	8	160	24	99	4b 93 6s 96	93
25	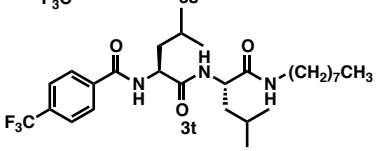 3t	A[j]	20	8	160	72	99	4b 99 6t 83	89
26	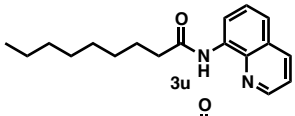 3u	B	10	3	130	24	99	93	5u 99
27	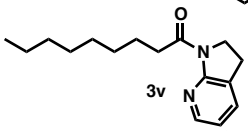 3v	B	10	3	130	24	99	99	99
28	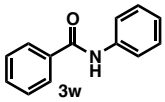 3w	A[b]	6	0.5	80	48	99	93	88

[a] NMR analysis (mesitylene or DMF was used as internal standard).

[b] RUPIP2 (1a) (0.25 mol %) was used.

[f] Hg (150 mol %) was used.

[g] RUPCY2 (1b) was used.
Catalyst was preactivated: P_{H2} = 8 MPa, *T* = 160 °C, *t* = 2 h.

[h] $[Ru]_0$ =10 mM. [i] $[Ru]_0$ =5 mM.

[j] RUPIP2 (1a) (2 mol %) was used.

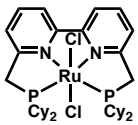
RUPCY2 (1b)

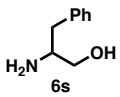
6s

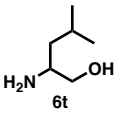
6t

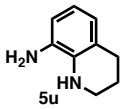
5u

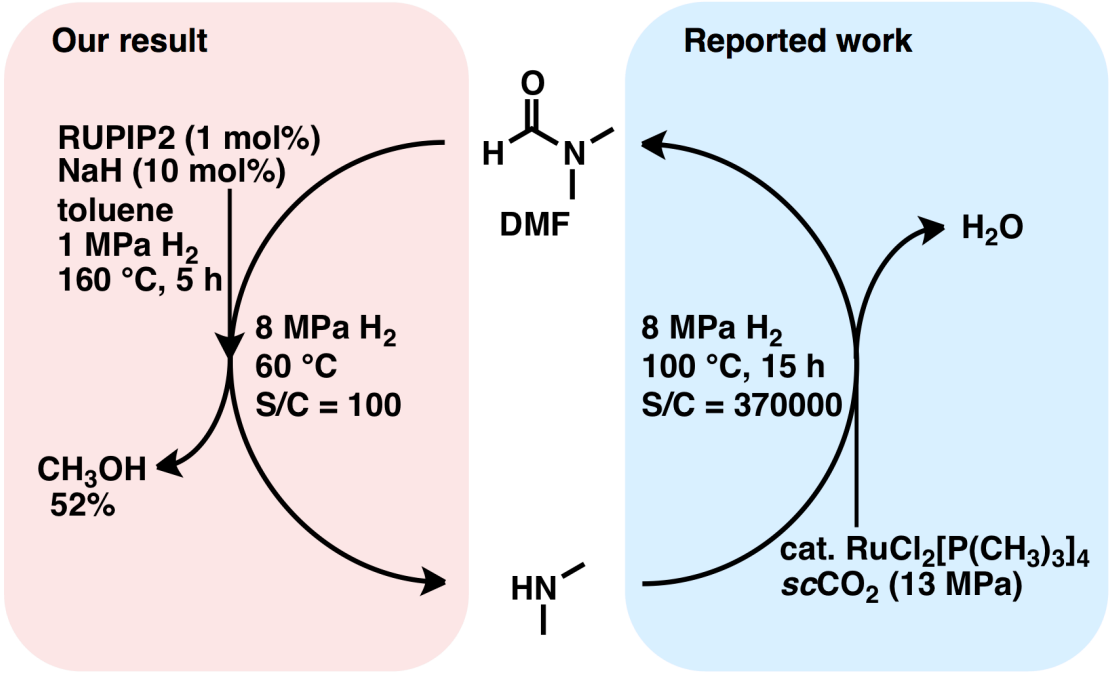

Figure 13. DMF hydrogenation.

Finally, the synthetic potential, including the chemoselectivity, of the hydrogenation was investigated. The directing groups of C–H bond functionalization[6] and a catalytic amide aldol reaction[7] were obtained in high yields, accompanied with undesirable hydrogenation of the pyridine moiety of **3u** (entry 26). Although the directing groups could be expected to strongly coordinate with a transition metal, H_2 reacts even more favorably with the Ru center. A more activated amide, anilide **3w**, was hydrogenated rapidly, giving near quantitative yields of **4a** and aniline with 0.25 mol % of **1a** and 6 mol % of NaH (P_{H2} = 0.5 MPa, T = 80 °C, t = 48 h; TON = ~400) (entry 28). Furthermore, the amide group of **3w** was hydrogenated (P_{H2} = 1 MPa, T = 80 °C, t = 27 h) preferentially even in the presence of a tri- and di-substituted olefins **4x** and **4y** (Scheme 2). Since olefins are more likely to be hydrogenated via an inner-sphere mechanism[34] (through direct interaction of the olefin with a metal center), these results again justify an outer-sphere mechanism[12–15,20,21,25–27,34] that operates specifically for the hydrogenation of amides in preference to olefins, at least under mild conditions.

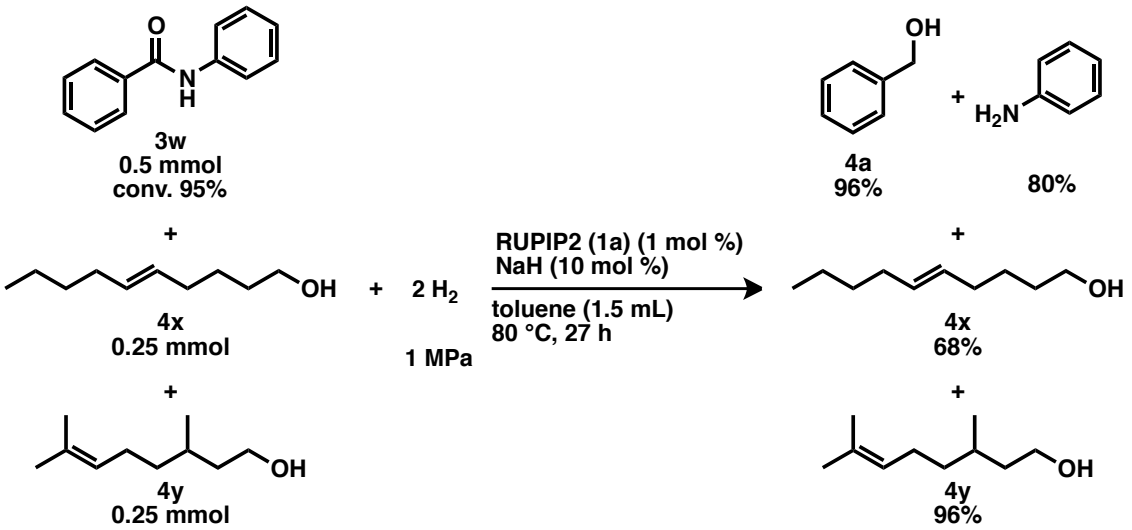

Scheme 2. Chemoselective hydrogenation of **3w**.

2.3. Conclusion

In conclusion, the effectiveness of a versatile "molecular surface" for the hydrogenation of a variety of amides (from DMF to polyamides including diamides, triamides, and the synthetic polymers) under both mild and harsh reaction conditions has been demonstrated. Chemoselective amide hydrogenation, as well as hydrogenation of compounds potentially useful for the "methanol economy" under mild conditions, was also accomplished. A set of 15 atoms including bpy, Ru and phosphorus are the unique constituents of the molecular surface, and are cooperative and crucial for inducing diverse catalytic molecular surfaces. Further improvement of the precatalyst molecular surface, including adopting a coordinatively-saturated Ru center, may significantly benefit the development of a better-performing catalytic molecular surface for amide hydrogenation producing nonstandard peptides of pharmaceutically great importance, and even for facilitating the selective C=O bond cleavage of amide bonds.

2.4. Experimental section

2.4.1. General

All experiments were performed under an Ar atmosphere unless otherwise noted. ^{1}H NMR spectra were measured on JEOL ECA–600 (600 MHz), JEOL ECA–500 (500 MHz) at ambient temperature. Data were recorded as follows: chemical shift in ppm from internal tetramethylsilane on the δ scale, multiplicity (br = broad, s = singlet, d = doublet, t = triplet, q = quartet, quin = quintet m = multiplet), coupling constant (Hz), integration, and assignment. ^{13}C NMR spectra were measured on JEOL ECA–600 (150 MHz), JEOL ECA–500 (126 MHz) at ambient temperature. Chemical shifts were recorded in ppm from the solvent resonance employed as the internal standard (chloroform-*d* at 77.00 ppm or tetramethylsilane at 0 ppm). ^{31}P NMR spectra were measured on JEOL ECA–600 (243 MHz), JEOL ECA–500 (202 MHz) at ambient temperature. Chemical shifts were recorded in ppm from the solvent resonance employed as the external standard (phosphoric acid (85 wt% in H_2O) at 0.0 ppm). High–resolution mass spectra (HRMS) were obtained from JEOL JMS700 (FAB), PE Biosystems QSTAR (ESI). IR spectra were obtained from JASCO FT/IR6100. For thin–layer chromatography (TLC) analysis through this work, Merck precoated TLC plates (silica gel 60 GF254 0.25 mm) were used. The products were purified by preparative column chlomatography on silica gel 60 N (spherical, neutral) (40–100 μm; Kanto).

2.4.2. Materials

Benzylamine, 4-methoxybenzoyl chloride, benzoyl chloride, 2,3-dihydro-7-azaindole, urea, β-citronellol, diisopropylamine, (*L*)-phenylalanine, octylamine, *N,N*-dimethylbenzamide (**3j**), HCl (2.0 M Et_2O solution) and ε-caprolactam (**3h**) were purchased from Aldrich. Biphenyl-4-carboxylic acid, $NaHCO_3$, $RuCl_2(PPh_3)_3$, chlorodicyclohexylphosphine, chlorodiisopropylphosphine, chlorodi-*tert*-butylphosphine, BH_3–THF complex (1.0 M in THF), (*L*)-leucine, *N*-benzylacetamide (**3g**), 1-(3-Dimethylaminopropyl)-3-ethylcarbodiimide hydrochloride (EDCI), EtOAc and hexane were purchased from Wako Pure Chemical industries, Ltd. *n*-Nonanoyl chloride, I_2, $Na_2S_2O_3$•$5H_2O$, pyridine, *N,N*-dimethyl formamide, benzanilide (**3u**), Et_2O, trifluoroacetic acid, NaH (55% oil dispersion),

mesitylene, MeCN (anhydrous), THF (anhydrous), dichloromethane (anhydrous), hexane (anhydrous), toluene (anhydrous), dichloromethane, Na_2SO_4, Et_3N, Et_2NH, *N*-methylmorpholine, Bu^{n}Li (1.5 M in hexane), morpholine, pivaloyl chloride, NaOH, K_2CO_3 and aq. HCl were purchased from Kanto Chemicals, Ltd. 4-(Trifluoromethyl)benzoyl chloride, 4-methylbenzoyl chloride, thionyl chloride, neocuproine hemihydrate, *N*-methylcaprolactam (**3i**), benzyl chloroformate, *N*-benzylformamide (**3r**), *trans*-5-decen-1-ol (**4x**), geraniol (**4y**), 6,6'-bi-2-picoline, 1,2,3-benzotriazol-1-ol monohydrate (HOBt · H_2O), 1,1,2,2-tetrachloroethane, 2-methyl-2-adamantanol, 8-aminoquinoine, benzamide (**3o**) and cyclohexanecarbonyl chloride were purchased from TCI, Ltd. Boc–(*L*)-leucine–OH · H_2O was purchased from Watanabe Chemical Industries, Ltd. *N*-benzylbenzamide (**3a**) was purchased from Across Organics, Ltd. $CDCl_3$ was purchased from Cambridge Isotope Laboratories, Inc. Hydrogen gas was purchased from Alpha System. These chemicals were used without further purification. *N*-benzyl-4-(trifluoromethyl)benzamide (**3b**),[35] *N*-benzyl-4-methylbenzamide (**3c**),[36,37] *N*-benzylbiphenyl-4-carboxamide (**3d**),[23] *N*-benzyl-4-methoxybenzamide (**3e**),[38] *N*-octylbenzamide (**3f**),[39] *N,N*-diethylbenzamide (**3k**),[40] *N*-octylnonanamide (**3l**),[23,41] *N*-octylcyclohexanecarboxamide (**3m**),[23] *N*-octylpivalamide (**3n**),[23] *N,N'*-dibenzylurea (**3p**),[42] *N,O*-dibenzyl carbamate (**3q**),[43] dichloro(6,6'-bis((di-*tert*-butylphosphino)methyl)-2,2'-bipyridine)–ruthenium (II) (**1c**),[28] dichloro(2,9-bis((di-*tert*-butylphosphino)methyl)-1,10-phenanthroline)–ruthenium (II) (**1f**)[29] and 8-amino-1,2,3,4-tetra-hydroquinoline (**5u**)[44] are all known compounds and synthesized according to the literature.

2.4.3. Experimental procedure.

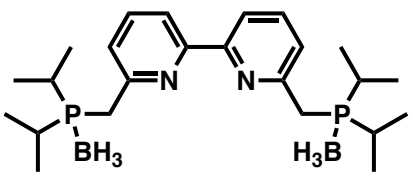

6,6'-bis((diisopropylphosphino)methyl)-2,2'-bipyridine –diborane complex: To an anhydrous THF (10 mL) solution of 6,6'-bi-2-picoline (184.2 mg, 1.0 mmol) was added a THF solution of lithium diisopropylamide {prepared by mixing diisopropylamine (0.85 mL, 6.0 mmol) and 1.5 M hexane solution of Bu^{n}Li (4.0 mL, 6.0 mmol) in THF (10 mL), followed by being stirred for 10 min at 0 °C under Ar} by cannula at 0 °C (H_2O-ice) under Ar, and the mixture was stirred at room temperature for 1 h. To the bluish-purple suspension was added chlorodiisopropylphosphine (314.6 μL, 2.0 mmol) dropwise at the same

temperature, and it was stirred for 4 h. To the reaction mixture was added BH_3–THF complex (1 M in THF, 10 mL, 10 mmol) at room temperature, and the mixture was stirred for 12 h. The mixture was quenched by adding a small portion of water (*ca.* <5 mL) at 0 °C, and the organic phase was removed *in vacuo* (*ca.* 50 mmHg, 40 °C). The residue was dissolved into CH_2Cl_2 (20 mL), washed with H_2O (40 mL), and extracted with CH_2Cl_2 (20 mL×5) and then washed with brine. The organic layer was dried over Na_2SO_4 and filtrated. The evaporation of the filtrate gave a yellow crude oil, which was purified by column chromatography on silica gel (CH_2Cl_2/hexane = 8/1) to afford the target compound (244.3 mg, 55%) as white solid. IR (KBr): 3423, 3068, 2969, 2934, 2876, 2366, 2253, 1572, 1436 cm^{-1}. ^1H NMR (600 MHz, $CDCl_3$): δ 8.24 (d, 2H, J = 7.6 Hz, $C_{10}H_6N_2$), 7.76 (t, 2H, J = 7.6 Hz, $C_{10}H_6N_2$), 7.34 (d, 2H, J = 7.6 Hz, $C_{10}H_6N_2$), 3.33 (d, 4H, J = 11.0 Hz, PCH_2), 2.12–2.23 (m, 4H, $CH(CH_3)_2$), 1.17–1.27 (m, 24H, $CH(CH_3)_2$). 0.10–0.70 (br, 6H, BH_3). ^{13}C NMR (151 MHz, $CDCl_3$): δ 155.3, 154.2 (d, $^2J_{PC}$ = 7.2 Hz), 137.3, 124.9, 118.8, 30.6 (d, $^1J_{PC}$ = 26.0 Hz), 21.8 (d, $^1J_{PC}$ = 31.8 Hz), 17.0 (d, $^2J_{PC}$ = 5.8 Hz). $^{31}P\{^1H\}$ NMR (243 MHz, $CDCl_3$): δ 36.1 (d, $^1J_{PB}$ = 72.4 Hz), HRMS (ESI, $(M+H)^+$) Calcd for $C_{24}H_{44}B_2N_2P_2^+$: 445.3247; Found: m/z = 445.3247.

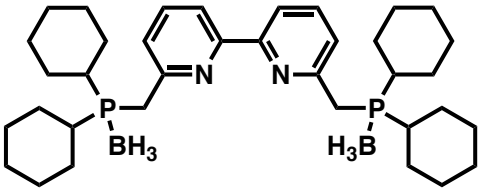

6,6'-bis((dicyclohexylphosphino)methyl)-2,2'-bipyridine−diborane complex: To an anhydrous THF (60 mL) solution of 6,6'-bi-2-picoline (1850.0 mg, 10 mmol) was added a THF solution of lithium diisopropylamide {prepared by mixing diisopropylamine (8.41 mL, 60 mmol) and 1.5 M hexane solution of Bu^nLi (40 mL, 60 mmol) in THF (30 mL), followed by being stirred for 10 min at 0 °C under Ar} by cannula at 0 °C (H_2O-ice) under Ar, and the mixture was stirred at room temperature for 1 h. To the bluish-purple suspension was added chlorodicyclohexylphosphine (4.4 mL, 20 mmol) dropwise at the same temperature, and it was stirred for 2 h. To the reaction mixture was added BH_3–THF complex (1 M in THF, 100 mL, 100 mmol) at room temperature, and the mixture was stirred for 12 h. The mixture was quenched by adding a small portion of water (*ca.* <5 mL) at 0 °C, and the organic phase was removed *in vacuo* (*ca.* 50 mmHg, 40 °C). The residue was dissolved into CH_2Cl_2 (50 mL), washed with H_2O (100 mL), and extracted with CH_2Cl_2 (50 mL×4) and then washed with brine. The organic layer was dried over Na_2SO_4 and filtrated. The evaporation of the filtrate

gave a yellow residue, which was suspended by a small portion of THF (*ca.* <10 mL), and slurry was filtrated to afford the target compound (2417.6 mg, 40%) as white solid. IR (KBr): 3435, 2931, 2849, 2378, 2332, 1572, 1437 cm^{-1}. ^{1}H NMR (600 MHz, $CDCl_3$): δ 8.29 (d, 2H, J = 8.3 Hz, $C_{10}H_6N_2$), 7.75 (t, 2H, J = 8.3 Hz, $C_{10}H_6N_2$), 7.31 (d, 2H, J = 7.6 Hz, $C_{10}H_6N_2$), 3.31 (d, 4H, J = 11.0 Hz, PCH_2), 1.60–2.00 (m, 24H, C_6H_{11}), 1.11–1.50 (m, 20H, C_6H_{11}). ^{13}C NMR (151 MHz, $CDCl_3$): δ 155.2, 154.5 (d, $^{2}J_{PC}$ = 7.2 Hz), 137.2, 125.0, 118.7, 31.5 (d, $^{1}J_{PC}$ = 30.3 Hz), 30.5 (d, $^{1}J_{PC}$ = 27.5 Hz), 27.0 (d, $^{2}J_{PC}$ = 11.6 Hz), 26.9 (d, $^{2}J_{PC}$ = 11.6 Hz), 26.7, 26.6, 26.0. $^{31}P\{^{1}H\}$ NMR (243 MHz, $CDCl_3$): δ 28.8 (d, $^{1}J_{PB}$ = 39.2 Hz), HRMS (ESI, $(M+H)^+$) Calcd for $C_{36}H_{60}B_2N_2P_2^+$: 605.4502; Found: *m/z* = 605.4502.

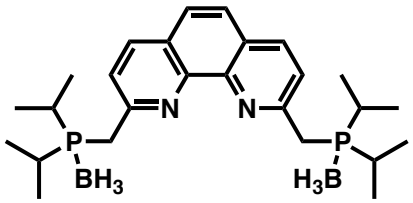

2,9-bis((diisopropylphosphino)methyl)-1,10-phenanthroline−diborane complex: To an anhydrous THF (100 mL) solution of neocuproine hemihydrate (1041.5 mg, 5.0 mmol) was added a THF solution of lithium diisopropylamide {prepared by mixing diisopropylamine (4.2 mL, 30 mmol) and 1.5 M hexane solution of Bu^nLi (20.0 mL, 30.0 mmol) in THF (50 mL), followed by being stirred for 10 min at 0 °C under Ar} by cannula at 0 °C (H_2O-ice) under Ar, and the mixture was stirred at room temperature for 1 h. To the bluish-purple suspension was added chlorodiisopropylphosphine (1.59 mL, 10 mmol) dropwise at the same temperature, and it was stirred for 12 h. To the reaction mixture was added BH_3–THF complex (1 M in THF, 50 mL, 50 mmol) at room temperature, and the mixture was stirred for 12 h. The mixture was quenched by adding a small portion of water (*ca.* <5 mL) at 0 °C, and the organic phase was removed *in vacuo* (*ca.* 50 mmHg, 40 °C). The residue was dissolved into CH_2Cl_2 (50 mL), washed with H_2O (100 mL), and extracted with CH_2Cl_2 (50 mL×5) and then washed with brine. The organic layer was dried over Na_2SO_4 and filtrated. The evaporation of the filtrate gave a yellow crude oil, which was purified by column chromatography on silica gel ($CHCl_3$/EtOAc/hexane = 1/1/3) to afford the target compound (1248 mg, 53%) as pale yellow solid. ^{1}H NMR (600 MHz, $CDCl_3$): δ 8.19 (d, 2H, J = 8.3 Hz, $C_{12}H_6N_2$), 7.76 (d, 2H, J = 7.6 Hz, $C_{12}H_6N_2$), 7.76 (s, 2H, $C_{12}H_6N_2$), 3.63 (d, 4H, J = 11.7 Hz, PCH_2), 2.18-2.26 (m, 4H, $CH(CH_3)_2$), 1.16-1.24 (m, 24H, $CH(CH_3)_2$). ^{13}C NMR (151 MHz, $CDCl_3$): δ 155.3 (d, $^{2}J_{PC}$ = 4.3 Hz), 145.3, 136.2, 127.5, 126.1, 124.7, 31.9 (d, $^{1}J_{PC}$ = 24.6Hz), 22.2 (d, $^{1}J_{PC}$ =

31.8 Hz), 17.1 (d, $^{2}J_{PC}$ = 4.3 Hz). $^{31}P\{^{1}H\}$ NMR (243 MHz, $CDCl_3$): δ 36.2 (d, $^{1}J_{PB}$ = 65.9 Hz). (ESI, $(M+H)^+$) Calcd for $C_{26}H_{44}B_2N_2P_2^+$: 469.3247; Found: m/z = 469.3235.

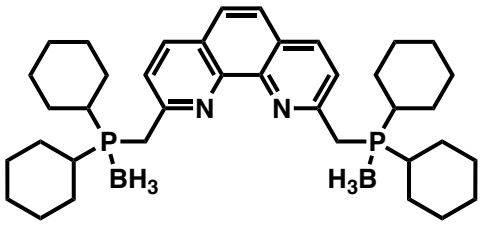

2,9-bis((dicyclohexylphosphino)methyl)-1,10-phenanthroline−diborane complex: To an anhydrous THF (100 mL) solution of neocuproine hemihydrate (1041.5 mg, 5.0 mmol) was added a THF solution of lithium diisopropylamide {prepared by mixing diisopropylamine (4.2 mL, 30 mmol) and 1.5 M hexane solution of Bu^{n}Li (20.0 mL, 30.0 mmol) in THF (50 mL), followed by being stirred for 10 min at 0 °C under Ar} by cannula at 0 °C (H_2O-ice) under Ar, and the mixture was stirred at room temperature for 1 h. To the bluish-purple suspension was added chlorodicyclohexylphosphine (2.2 mL, 10 mmol) dropwise at the same temperature, and it was stirred for 12 h. To the reaction mixture was added BH_3–THF complex (1 M in THF, 50 mL, 50 mmol) at room temperature, and the mixture was stirred for 12 h. The mixture was quenched by adding a small portion of water (*ca.* <5 mL) at 0 °C, and the organic phase was removed *in vacuo* (*ca.* 50 mmHg, 40 °C). The residue was dissolved into CH_2Cl_2 (50 mL), washed with H_2O (100 mL), and extracted with CH_2Cl_2 (50 mL×5) and then washed with brine. The organic layer was dried over Na_2SO_4 and filtrated. The evaporation of the filtrate gave a pale red residue, which was suspended by a small portion of EtOAc (*ca.* <10 mL), and slurry was filtrated with acetone to afford the target compound (1580 mg, 50%) as pale red solid. ^{1}H NMR (600 MHz, $CDCl_3$): δ 8.16 (d, 2H, *J* = 8.3 Hz, $C_{12}H_6N_2$), 7.75 (s, 2H, $C_{12}H_6N_2$), 7.7 (d, 2H, *J* = 8.3 Hz, $C_{12}H_6N_2$), 3.57 (d, 4H, *J* = 11.3 Hz, PCH_2), 1.60-2.03 (m, 24H, C_6H_{11}), 1.13-1.57 (m, 20H, C_6H_{11}). ^{13}C NMR (149 MHz, $CDCl_3$): δ 155.3 (d, $^{2}J_{PC}$ = 5.8 Hz), 145.5, 136.0, 127.4, 126.1, 124.6, 31.9 (d, $^{1}J_{PC}$ = 31.5 Hz), 31.5 (d, $^{1}J_{PC}$ = 25.8 Hz), 27.1 (d, $^{2}J_{PC}$ = 11.6 Hz), 27.0 (d, $^{2}J_{PC}$ = 11.6 Hz), 26.8, 26.6, 25.9. $^{31}P\{^{1}H\}$ NMR (243 MHz, $CDCl_3$): δ 28.5. (ESI, $(M+H)^+$) Calcd for $C_{38}H_{60}B_2N_2P_2^+$: 629.4503; Found: m/z = 629.4503.

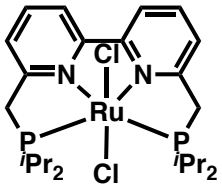

Dichloro(6,6'-bis((diisopropylphosphino)methyl)-2,2'-bipyridine)–ruthenium (II), RUPIP2 (1a): A degassed morpholine (10 mL) solution of 6,6'-bis((diisopropylphosphino)methyl)-2,2'-bipyridine–diborane complex (300.0 mg, 0.68 mmol) was heated at 130 °C for 2 h under Ar. The solution was cooled to room temperature and morpholine was removed *in vacuo* (*ca.* 1 mmHg, room temperature). To the residue was added sequentially dichlorotris(triphenylphosphino)ruthenium (II) (648.6 mg, 0.68 mmol) and an anhydrous toluene (15 mL). The resulting mixture was heated at 110 °C for 2 h under Ar, and was cooled to room temperature. Then to the mixture was added an anhydrous hexane (40 mL) to afford the purple suspension. The mixture of the suspension was stirred at room temperature for 1 h and filtered through a filtration paper. The obtained purple solid was dried *in vacuo* (*ca.* 0.1 mmHg, room temperature). This solid was purified by column chromatography on silica gel ($CHCl_3$/EtOAc = 5/1) to afford RUPIP2 (**1a**) as purple solid (204.3 mg, 51%). ^{1}H NMR (600 MHz, $CDCl_3$): δ 7.89 (d, 2H, J = 8.3 Hz, $C_{10}H_6N_2$), 7.69 (t, 2H, J = 7.6 Hz, $C_{10}H_6N_2$), 7.59 (d, 2H, J = 8.3 Hz, $C_{10}H_6N_2$), 3.89 (d, 4H, J = 7.6 Hz, PCH_2), 2.67–2.78 (m, 4H, $CH(CH_3)_2$), 1.35–1.43 (m, 24H, $CH(CH_3)_2$). ^{13}C NMR (151 MHz, $CDCl_3$): δ 163.3, 158.3, 134.4, 121.9, 120.0, 42.1 (d, $^1J_{PC}$ = 20.2 Hz), 25.4, 20.5, 19.4. ^{31}P{^{1}H} NMR (243MHz, $CDCl_3$): δ 60.4. HRMS (ESI, $(M–Cl)^+$) Calcd for $C_{24}H_{38}ClN_2P_2Ru^+$: 553.1242; Found: m/z = 553.1240.

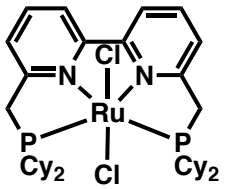

Dichloro(6,6'-bis((dicyclohexylphosphino)methyl)-2,2'-bipyridin e)–ruthenium (II), RUPCY2 (1b): A degassed morpholine (20 mL) solution of 6,6'-bis((dicyclohexylphosphino)methyl)-2,2'-bipyridine−diborane complex (604.4 mg, 1.0 mmol) was heated at 130 °C for 2 h under Ar. The solution was cooled to room temperature and morpholine was removed *in vacuo* (*ca.* 1 mmHg, room temperature). To the residue was added sequentially dichlorotris(triphenylphosphino)ruthenium (II) (958.8 mg, 1.0 mmol) and an anhydrous toluene (20 mL). The resulting mixture was heated at 110 °C for 3 h under Ar, and was cooled to room temperature. Then to the mixture was added an anhydrous hexane (40 mL) to afford the purple suspension. The mixture of the suspension was stirred at room temperature for 1 h and filtered through a filtration paper. The obtained purple solid was dried *in vacuo* (*ca.* 0.1 mmHg, room temperature). This solid was purified by column

chromatography on silica gel ($CHCl_3$/ EtOAc = 5/1) to afford RUPCY2 (**1b**) as purple solid (435.1 mg, 58%). ^{1}H NMR (500 MHz, $CDCl_3$): δ 7.86 (d, 2H, J = 7.4 Hz, $C_{10}H_6N_2$), 7.66 (t, 2H, J = 7.5 Hz, $C_{10}H_6N_2$), 7.56 (d, 2H, J = 7.5 Hz, $C_{10}H_6N_2$), 3.87 (d, 4H, J = 8.1 Hz, PCH_2), 2.41 (br, 4H, C_6H_{11}), 2.18 (d, 4H, J = 12.1 Hz Hz, C_6H_{11}), 2.05 (d, 4H, J = 10.9 Hz, C_6H_{11}), 1.54–1.81 (m, 20H, C_6H_{11}), 1.20–1.34 (m, 20H, C_6H_{11}). ^{13}C NMR (126 MHz, $CDCl_3$): δ 163.3, 158.3, 134.1, 122.0, 119.9, 40.5 (d, $^1J_{PC}$ = 12.8 Hz), 36.3, 30.3, 29.4, 27.7, 27.5, 26.4. ^{31}P{^{1}H} NMR (159 MHz, $CDCl_3$): δ 54.2. HRMS (ESI, $(M–Cl)^+$) Calcd for $C_{36}H_{54}ClN_2P_2Ru^+$: 713.2494; Found: m/z = 713.2476.

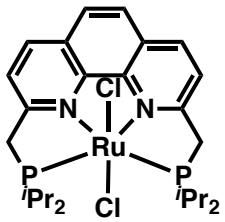

Dichloro(2,9-bis((diisopropylphosphino)methyl)-1,10-phenanthroline)–ruthenium (II), RUPIP3 (1d): A degassed morpholine (15 mL) solution of 2,9-bis((diisopropylphosphino)methyl)-1,10-phenanthroline−diborane complex (362.2 mg, 0.77 mmol) was heated at 120 °C for 2 h under Ar. The solution was cooled to room temperature and morpholine was removed *in vacuo* (*ca.* 1 mmHg, room temperature). To the residue was added sequentially dichlorotris(triphenylphosphino)ruthenium (II) (738.2 mg, 0.77 mmol) and an anhydrous toluene (15 mL). The resulting mixture was heated at 110 °C for 12 h under Ar, and was cooled to room temperature. Then to the mixture was added an anhydrous hexane (40 mL) to afford the purple suspension. The mixture of the suspension was stirred at room temperature for 1 h and filtered with Et_2O through a filtration paper. The obtained purple solid was dried *in vacuo* (*ca.* 0.1 mmHg, room temperature). This solid was purified by column chromatography on silica gel ($CHCl_3$/acetone = 3/1) to afford RUPIP3 (**1d**) as purple solid (180.4 mg, 38%). ^{1}H NMR (600 MHz, $CDCl_3$): δ 8.13 (d, 2H, J = 8.3 Hz, $C_{12}H_6N_2$), 7.88 (d, 2H, J = 8.3 Hz, $C_{12}H_6N_2$), 7.81 (s, 2H, $C_{12}H_6N_2$), 4.07 (d, 4H, J = 8.2 Hz, PCH_2), 2.75-2.85 (m, 4H, $CH(CH_3)_2$), 1.38-1.52 (m, 24H, $CH(CH_3)_2$). ^{13}C NMR (151 MHz, $CDCl_3$): δ 163.6, 149.3, 132.9, 128.7, 125.4, 121.7 (d, $^2J_{PC}$ = 5.8 Hz), 43.0 (dd, $^1J_{PC}$ = 17.3 Hz, $^2J_{CC}$ = 7.2 Hz), 25.6 (dd, $^1J_{PC}$ = 8.6 Hz, $^2J_{CC}$ = 7.2 Hz), 20.9, 19.4. ^{31}P{^{1}H} NMR (243 MHz, $CDCl_3$): δ 62.9. HRMS (ESI, $(M–Cl)^+$) Calcd for $C_{26}H_{38}ClN_2P_2Ru^+$: 577.1242; Found: m/z = 577.1210.

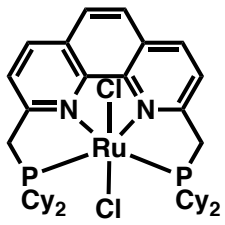

Dichloro(2,9-bis((dicyclohexylphosphino)methyl)-1,10-phenanthroline)–ruthenium (II), RUPCY3 (1e): A degassed morpholine (15 mL) solution of 2,9-bis((dicyclohexylphosphino)methyl)-1,10-phenanthroline−diborane complex (628.5 mg, 1.0 mmol) was heated at 120 °C for 2 h under Ar. The solution was cooled to room temperature and morpholine was removed *in vacuo* (*ca.* 1 mmHg, room temperature). To the residue was added sequentially dichlorotris(triphenylphosphino)ruthenium (II) (958.8 mg, 1.0 mmol) and an anhydrous toluene (20 mL). The resulting mixture was heated at 110 °C for 12 h under Ar, and was cooled to room temperature. Then to the mixture was added an anhydrous hexane (40 mL) to afford the purple suspension. The mixture of the suspension was stirred at room temperature for 1 h and filtered with Et_2O through a filtration paper. The obtained purple solid was dried *in vacuo* (*ca.* 0.1 mmHg, room temperature). This solid was purified by column chromatography on silica gel ($CHCl_3$/THF = 10/1) to afford RUPCY3 (**1e**) as purple solid (563.7 mg, 73%). ^{1}H NMR (600 MHz, $CDCl_3$): δ 8.12 (d, 2H, J = 8.3 Hz, $C_{12}H_6N_2$), 7.86 (d, 2H, J = 8.2 Hz, $C_{12}H_6N_2$), 7.80 (s, 2H, $C_{12}H_6N_2$), 4.05 (d, 4H, J = 6.8 Hz, PCH_2), 2.42-2.51 (br, 4H, C_6H_{11}), 2.31 (d, 4H, J = 11.0 Hz C_6H_{11}), 2.12 (d, 4H, J = 12.4 Hz, C_6H_{11}), 1.61-1.94 (m, 20H, C_6H_{11}), 1.18-1.37 (m, 12H, C_6H_{11}). ^{13}C NMR (151 MHz, $CDCl_3$): δ 163.6, 149.3, 132.6, 128.6, 125.3, 121.8, 41.4 (dd, $^1J_{PC}$ = 15.8 Hz, $^2J_{CC}$ = 7.2 Hz), 36.6 (dd, $^1J_{PC}$ = 7.2 Hz, $^2J_{CC}$ = 7.2 Hz), 30.7, 29.4, 27.8, 27.6, 26.4. $^{31}P\{^1H\}$ NMR (243 MHz, $CDCl_3$): δ 56.8. HRMS (ESI, $(M–Cl)^+$) Calcd for $C_{38}H_{54}ClN_2P_2Ru^+$: 737.2494; Found: m/z = 737.2483.

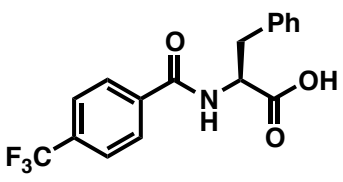

(*S*)-3-phenyl-2-(4-(trifluoromethyl)benzamido)propanoic acid: To a pure H_2O (250 mL) solution of NaOH (1800 mg, 45 mmol) was added (*L*)-phenylalanine (2477.9 mg, 15 mmol), and the mixture was stirred at 0 °C for 15 min under N_2. To the reaction mixture was added 4-(trifluoromethyl)benzoyl chloride (2.23 mL, 15 mmol) dropwise at same temperature, and it was stirred at room temperature for 2.5 h. The mixture was quenched by adding 1.0 N aqueous solution of HCl (100 mL, 100 mmol) at 0 °C, and white precipitate was appeared. The precipitate was washed with H_2O to afford the wet white solid. The slurry was dissolved into CH_2Cl_2 (100 mL), washed with H_2O (200 mL), and extracted with CH_2Cl_2 (100 mL×3). The organic layer

was dried over Na_2SO_4 and filtrated. Evaporation of the filtrate gave white solid (3.93 g). However 4-(trifluoromethyl)benzoic acid was included as impurity (*ca.* 22% impurity: based on the molar ratio). So desired product was obtained in ca. 67% yield (*ca.* 10.1 mmol, 78% purity). This compound was used for following reactions without further purification.

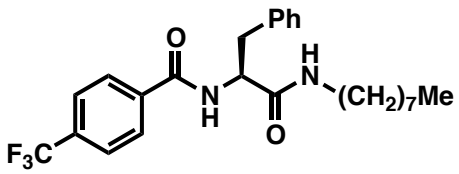

(*S*)-*N*-(1-(octylamino)-1-oxo-3-phenylpropan-2-yl)-4-(trifluoromethyl)benzamide (3s): To an anhydrous THF (75 mL) solution of (*S*)-3-phenyl-2-(4-(trifluoromethyl)benzamido)propanoic acid (78% purity) (5.06 g, 13.0 mmol) were added 1-(3-Dimethylaminopropyl)-3-ethylcarbodiimide hydrochloride (EDCI) (6.90 mg, 36 mmol), 1,2,3-benzotriazol-1-ol monohydrate (HOBt·H_2O) (2.71 mg, 17.7 mmol) and *N*-methylmorpholine (7.92 mL, 72 mmol). The mixture was stirred at 0 °C for 30 min under N_2. To the reaction mixture was added octylamine (12.43 mL, 75 mmol) dropwise at same temperature, and was stirred at room temperature overnight. The reaction mixture was quenched by adding a small portion of water (*ca.* <2 mL) at 0 °C, and the organic phase was removed *in vacuo* (*ca.* 1 mmHg, room temperature). The residue was dissolved into CH_2Cl_2 (300 mL), washed with HCl (aq) (1N, 200 mL×2), $NaHCO_3$ (aq) (saturated, 200 mL×2), brine (aq) (saturated, 100 mL×1), and extracted with CH_2Cl_2 (300 mL×2). The organic layer was dried over Na_2SO_4 and filtrated. Evaporation of the filtrate gave colorless solid, which was recrystallized from CH_2Cl_2 giving **3s** (4.31 g, 9.61 mmol, 64%) as colorless solid. IR (neat): 3306, 2925, 2854, 1637, 1538, 1327, 1171, 1131 cm^{-1}. ^1H NMR ($CDCl_3$, 600 MHz): δ 0.87 (t, J = 6.90 Hz, 3H), 1.12–1.40 (m, 12H), 3.03–3.14 (m, 2H), 3.17–3.26 (m, 2H), 4.80 (q, J = 6.18 Hz, 1H), 5.83 (d, J = 4.80 Hz, 1H), 7.21–7.30 (m, 5H), 7.33 (dd, J = 6.90 Hz, J = 2.10 Hz, 1H), 7.67 (d, J = 8.28 Hz, 2H), 7.87 (d, J = 8.28 Hz, 2H). ^{13}C NMR ($CDCl_3$, 150 MHz): δ 14.0, 22.6, 26.8, 29.12, 29.18, 29.23, 31.7, 38.8, 39.7, 55.4, 123.6 (q, $^1J_{CF}$ = 270 Hz), 125.48, 125.51, 127.0, 127.7 (2C), 128.6 (2C), 129.3 (2C), 133.4 (q, $^2J_{CF}$ = 31.6 Hz), 136.7, 137.0, 165.9, 170.7. HRMS (FAB, MH^+) calcd for $C_{25}H_{32}F_3N_2O_2^+$: 449.2410; Found: m/z = 449.2400.

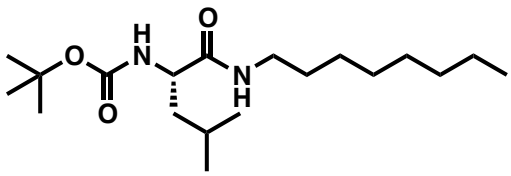

(*S*)-*tert*-butyl (4-methyl-1-(octylamino)-1-oxopentan-2-yl)carbamate: To an anhydrous THF (100 mL) solution of Boc–(*L*)-leucine–OH・H_2O (3739.7 mg, 15 mmol) were added 1-(3-Dimethylaminopropyl)-3-ethylcarbodiimide hydrochloride (EDCI) (9968.4 mg, 52 mmol), 1,2,3-benzotriazol-1-ol monohydrate (HOBt・H_2O) (2710.6 mg, 17.7 mmol) and *N*-methylmorpholine (7.92 mL, 72 mmol). The mixture was stirred at 0 °C for 30 min under N_2. To the reaction mixture was added octylamine (12.43 mL, 75 mmol) dropwise at same temperature, and was stirred at room temperature overnight. The reaction mixture was quenched by adding a small portion of water (*ca.* <2 mL) at 0 °C, and the organic phase was removed *in vacuo* (*ca.* 1 mmHg, room temperature). The residue was dissolved into Et_2O (200 mL), washed with citric acid (aq) (5%, 50 mL×2), $NaHCO_3$ (aq) (saturated, 50 mL×1), brine (aq) (saturated, 50 mL×1), and extracted with CH_2Cl_2 (100 mL×3). The organic layer was dried over Na_2SO_4 and filtrated. Evaporation of the filtrate gave as a colorless solid (3.33 g, 10.15 mmol, 67%). This compound was used for following reactions without further purification.

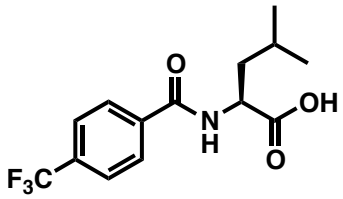

(*S*)-4-methyl-2-(4-(trifluoromethyl)benzamido)pentanoi c acid: To a pure H_2O (500 mL) solution of NaOH (3600 mg, 90 mmol) were added (*L*)-leucine (3935.1 mg, 30 mmol), and the mixture was stirred at 0 °C for 15 min under N_2. To the reaction mixture was added 4-(trifluoromethyl)benzoyl chloride (4456.4 μL, 30 mmol) dropwise at same temperature, and it was stirred at room temperature for 2.5 h. The mixture was quenched by adding 1.0 N aqueous solution of HCl (200 mL, 200 mmol) at 0 °C, and white precipitate was appeared. The precipitate was washed with H_2O to afford the wet white solid. The slurry was dissolved into CH_2Cl_2 (200 mL), washed with H_2O (400 mL), and extracted with CH_2Cl_2 (100 mL×3). The organic layer was dried over Na_2SO_4 and filtrated. Evaporation of the filtrate gave white solid (9.07 g). However 4-(trifluoromethyl)benzoic acid was included as impurity (*ca.* 29% impurity: based on the molar ratio). So desired product was obtained in ca. 79% yield (*ca.* 23.8 mmol, 71% purity). This compound was used for following reactions without further purification.

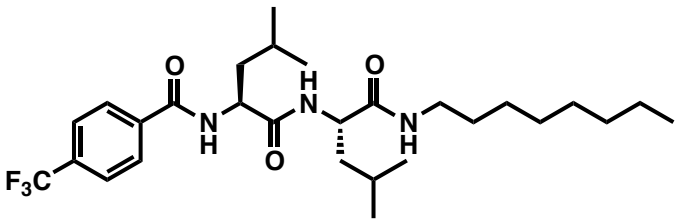

***N*-((*S*)-4-methyl-1-(((*S*)-4-methyl-1-(octylamino)-1-oxopentan-2-yl)amino)-1-oxopentan-2-yl)-4-(trifluoromethyl)benzamide (3t)**: To an anhydrous CH_2Cl_2 (7.0 mL) solution of (*S*)-*tert*-butyl (4-methyl-1-(octylamino)-1-oxopentan-2-yl)carbamate (2397.6 mg, 7.0 mmol) was added trifluoroacetic acid (TFA) (7.0 mL, 91.4 mmol). The mixture was stirred at room temperature for 1 h under N_2, and the organic phase was removed *in vacuo* (*ca.* 1 mmHg, room temperature). To the residue were added THF (50 mL), 1-(3-Dimethylaminopropyl)-3-ethylcarbodiimide hydrochloride (EDCI) (3450.6 mg, 18 mmol), 1,2,3-benzotriazol-1-ol monohydrate (HOBt·H_2O) (1531.4 mg, 10 mmol), *N*-methylmorpholine (4.40 mL, 40 mmol) and (*S*)-4-methyl-2-(4-(trifluoromethyl)benzamido)pentanoic acid (71% purity) (2122.9 mg, 5.6 mmol) at 0 °C, and stirred at room temperature overnight. The reaction mixture was quenched by adding a small portion of water (*ca.* <2 mL) at 0 °C, and the organic phase was removed *in vacuo* (*ca.* 1 mmHg, room temperature). The residue was dissolved into CH_2Cl_2 (100 mL), washed with HCl (aq) (1 N, 100 mL×2), $NaHCO_3$ (aq) (saturated, 50 mL×1), brine (aq) (saturated, 50 mL×1), and extracted with CH_2Cl_2 (100 mL×3). The organic layer was dried over Na_2SO_4 and filtrated. The evaporation of the filtrate gave a yellow crude oil, which was purified by column chromatography on silica gel (hexane/EtOAc = 4/1 and only EtOAc) to afford the target compound (**3t**) (2099.8 mg, 3.98 mmol, 57%) as white solid. IR (neat): 3289, 3078, 2957, 2930, 2858, 1639, 1550, 1328, 1170, 1134, 1067 cm^{-1}. ^1H NMR (600 MHz, $CDCl_3$): δ 0.81–0.96 (m, 15H), 1.17–1.32 (m, 10H), 1.37–1.80 (m, 8H), 3.10 (m, 0.4H, *J* = 7.6 Hz), 3.16 (m, 1H, *J* = 5.5 Hz), 3.26 (m, 0.6H, *J* = 7.6 Hz), 4.49 (q, 0.4H, *J* = 5.5 Hz), 4.54 (q, 0.6H, *J* = 8.3 Hz), 4.72 (q, 0.4H, *J* = 6.9 Hz), 4.87 (q, 0.6H, *J* = 8.3 Hz), 6.69 (t, 0.4H, *J* = 5.5 Hz), 6.76 (t, 0.6H, *J* = 11 Hz), 7.13 (d, 0.4H, *J* = 8.3 Hz), 7.43 (d, 0.6H, *J* = 8.28 Hz), 7.48 (t, 1H, *J* = 8.9 Hz), 7.63 (t, 2H, *J* = 8.9 Hz), 7.92 (t, 2H, *J* = 8.9 Hz). ^{13}C NMR ($CDCl_3$, 150 MHz): *δ* 14.0, 22.1 (0.4C), 22.4, 22.52 (2C), 22.55 (2C), 22.8 (0.6C), 24.87 (0.6C), 24.92, 24.96 (0.4C), 26.9 (0.4C), 27.0 (0.6C), 29.15 (0.4C), 29.18 (0.6C), 29.24 (0.4C), 29.28 (0.6C), 29.34 (0.4C), 29.38 (0.6C), 31.7 (0.4C), 31.8 (0.6C), 39.6 (0.6C), 39.7 (0.4C), 41.4 (0.6C), 41.5, 41.8 (0.4C), 51.9 (0.6C), 52.0 (0.6C), 52.1 (0.4C), 52.8 (0.4C),

123.7 (q, $^1J_{CF}$ = 264 Hz), 125.1 (1.2C), 125.2 (0.8C), 128.0 (0.8C), 128.1 (1.2C), 133.1 (q, $^2J_{CF}$ = 34.5 Hz), 137.0 (0.4C), 137.5 (0.6C), 166.0 (0.6C), 166.2 (0.4C), 171.6 (0.6C), 172.1, 172.5 (0.4C). HRMS (FAB, MH^+) calcd for $C_{28}H_{45}F_3N_3O_3^+$: 528.3408; Found: *m*/*z* = 528.3385.

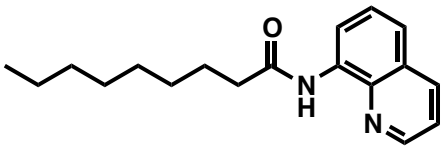

***N*-(quinolin-8-yl)nonanamide (3u)**: To an anhydrous CH_2Cl_2 (20 mL) solution of nonanoyl chloride (2.70 mL, 15 mmol) were added Et_3N (2.80 mL, 20 mmol) and 8-aminoquinoine (2.88 mL, 20 mmol). The mixture was stirred at room temperature overnight under Ar, and was quenched by adding a small portion of water (*ca.* <2 mL). The residue was dissolved into CH_2Cl_2 (100 mL), washed with HCl (aq) (1M, 100 mL×1), $NaHCO_3$ (aq) (saturated, 100 mL×1), brine (aq) (saturated, 100 mL×1), and extracted with CH_2Cl_2 (100 mL×2). The organic layer was dried over Na_2SO_4 and filtrated. Evaporation of the filtrate gave dark brown oil, which was distilled by Kugel-Rohr (230 °C/0.006 mmHg) to give **3u** as pale yellow oil (3.43 g, 12.04 mmol, 80%). IR (neat): 3357, 3048, 2925, 2854, 1686, 1523, 1485, 1325, 1163, 1106 cm^{-1}. ^1H NMR ($CDCl_3$, 600 MHz): δ 0.87 (t, *J* = 6.84 Hz, 3H), 1.21–1.40 (m, 8H), 1.43 (quin, *J* = 7.56 Hz, 2H), 1.82 (quin, *J* = 7.56 Hz, 2H), 2.56 (t, *J* = 7.56 Hz, 2H), 7.45 (dd, *J* = 8.25 Hz, *J* = 4.14 Hz, 1H), 7.49 (dd, *J* = 8.28 Hz, *J* = 1.38 Hz, 1H), 7.54 (t, *J* = 8.22 Hz, 1H), 8.16 (dd, *J* = 8.28 Hz, *J* = 2.04 Hz, 1H), 8.77–8.82 (m, 2H), 9.81 (s, 1H). ^{13}C NMR ($CDCl_3$, 150 MHz): δ 14.1, 22.6, 25.7, 29.2, 29.3, 29.4, 31.8, 38.3, 116.4, 121.3, 121.5, 127.5, 127.9, 134.6, 136.3, 138.4, 148.1, 171.9. HRMS (FAB, MH^+) calcd for $C_{18}H_{25}N_2O^+$: 285.1961; Found: *m*/*z* = 285.1952.

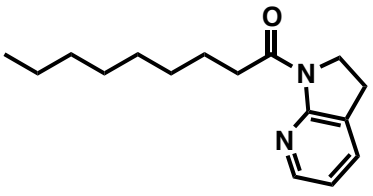

1-(2,3-dihydro-1*H*-pyrrolo[2,3-*b*]pyridin-1-yl)nonan-1-one (3v): To an anhydrous THF (20 mL) solution of nonanoyl chloride (1.08 mL, 6 mmol) were added K_2CO_3 (1382 mg, 10 mmol) and 2,3-dihydro-7-azaindole (600 mg, 5 mmol). The mixture was stirred at room temperature overnight under Ar, and was quenched by adding a small portion of water (*ca.* <5 mL). The residue was dissolved into CH_2Cl_2 (50 mL), washed with $NaHCO_3$ (aq) (saturated, 100 mL), brine (aq) (saturated, 100 mL), and extracted with CH_2Cl_2 (50

mL×3). The organic layer was dried over Na_2SO_4 and filtrated. Evaporation of the filtrate gave yellow oil, which was distilled by Kugel-Rohr (180 °C/0.006 mmHg) to give **3v** as colorless oil (697 mg, 2.68 mmol, 54%). IR (neat): 3509, 3303, 3053, 2925, 2854, 1652, 1587, 1417, 1243 cm^{-1}. ^1H NMR ($CDCl_3$, 600 MHz): δ 0.88 (t, J = 6.84 Hz, 3H), 1.23–1.37 (m, 8H), 1.41 (quin, J = 7.56 Hz, 2H), 1.71 (quin, J = 7.56 Hz, 2H), 3.04 (t, J = 8.28 Hz, 2H), 3.13 (t, J = 7.56 Hz, 2H), 4.10 (t, J = 8.22 Hz, 2H), 6.85 (dd, J = 7.56 Hz, J = 4.80 Hz, 1H), 7.44 (dd, J = 7.56 Hz, J = 1.38 Hz, 1H), 8.11 (d, J = 3.42 Hz, 1H). ^{13}C NMR ($CDCl_3$, 150 MHz): δ 14.1, 22.6, 24.2, 25.0, 29.2, 29.4 (2C), 31.8, 36.5, 45.5, 117.7, 126.0, 133.2, 146.1, 156.1, 173.4. HRMS (FAB, MH^+) calcd for $C_{16}H_{25}N_2O^+$: 261.1961; Found: m/z = 261.1968.

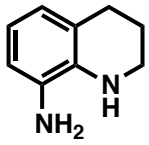

1,2,3,4-tetrahydroquinolin-8-amine (5u)[13] : Compound **5u** is rather easily oxidized by air.[13] ^1H NMR ($CDCl_3$, 600 MHz): δ 1.91 (quin, J = 5.52 Hz, 2H), 2.76 (t, J = 6.18 Hz, 2H), 3.1–3.3 (br, 3H), 3.32 (t, J = 4.86 Hz, 2H), 6.52–6.60 (m, 3H). ^{13}C NMR ($CDCl_3$, 150 MHz): δ 22.4, 27.0, 42.5, 114.0, 118.0, 121.1, 123.2, 133.8, 133.9. HRMS (ESI, MH^+) calcd for $C_9H_{13}N_2^+$: 149.1073; Found: m/z = 149.1067.

Representative procedure for hydrogenation of amides (conditions A): The reaction of *N*-benzylbenzamide (3a).

Under a continuous Ar flow, RUPIP2 (**1a**) (2.94 mg, 0.005 mmol), sodium hydride (55% oil dispersion, 2.18 mg, 0.05 mmol), anhydrous toluene (1.5 mL), *N*-benzylbenzamide (**3a**) (105.6 mg, 0.5 mmol) and a magnetic stirring bar were placed in a dried Teflon tube (21 mL capacity). The Teflon tube was quickly inserted into an autoclave, and the inside of the autoclave was purged 10 times with hydrogen gas (1 MPa). The autoclave was pressurized with a 1 MPa of hydrogen gas at 25 °C, and heated at 110 °C for 24 h under stirring (800 rpm). The autoclave was cooled to room temperature in an ice–water (0 °C) bath, and the reaction mixture was quenched with 2.0 M Et_2O solution of HCl (25 μL, 0.05 mmol). The organic phase was removed *in vacuo* (*ca.* 100 mmHg, 40 °C). The residue was diluted with $CDCl_3$, and analyzed by ^1H NMR. The yields of benzyl alcohol (**4a**) (86%) and benzylamine (**5a**) (86%) were calculated based on the integral ratio among the signals of these compounds with respected to an internal standard (mesitylene). Afterward, the reaction mixture was

diluted with CH_2Cl_2, and HCl (2 M in Et_2O, 250 μL, 0.5 mmol) was added dropwise. White precipitate was generated and purified by filtration to give benzylamine hydrochloride (52.1 mg, 0.364 mmol, 73%). Then the filtrate was purified by column chromatography on silica gel (eluent; Et_2O/hexane = 2/3) to give *N*-benzylbenzamide (9.5 mg, 0.045 mmol, 9%) and benzyl alcohol (44.7 mg, 0.413 mmol, 83%).

Representative procedure for hydrogenation of amides 3 with preactivated catalyst (conditions B): The reaction of *N,N'*-dimethylbenzamide (3j).

Under a continuous Ar flow, RUPIP2 (**1a**) (3.98 mg, 0.0067 mmol), sodium hydride (55% oil dispersion, 2.91 mg, 0.067 mmol), anhydrous toluene (2.0 mL) and a magnetic stirring bar were placed in a dried Teflon tube (21 mL capacity). The Teflon tube was quickly inserted into an autoclave, and the inside of the autoclave was purged 10 times with hydrogen gas (1 MPa). The autoclave was pressurized with a 1 MPa of hydrogen gas at 25 °C, and heated at 160 °C for 5 h under stirring (800 rpm). Then the autoclave was cooled to room temperature in an ice–water (0 °C) bath, and hydrogen was blown away under an Ar stream. Under the continuous Ar flow, to another autoclave, in which a dried Teflon tube charged with *N,N'*-dimethylbenzamide (**3j**) (74.6 mg, 0.5 mmol) had been in advance inserted, was transferred the reaction mixture (1.5 mL, 1 mol % Ru) using a gas-tight syringe (2.5 mL). The autoclave was purged (×10 with 1 MPa H_2 gas) and finally charged with 1 MPa of hydrogen gas, and the reaction mixture was heated at 110 °C for 24 h under stirring (800 rpm). The autoclave was cooled to room temperature in an ice–water (0 °C) bath, and the reaction mixture was quenched with 2.0 M Et_2O solution of HCl (25 μL, 0.05 mmol). The organic phase was removed *in vacuo* (*ca.* 100 mmHg, 40 °C). The residue was diluted with $CDCl_3$, and analyzed by ^1H NMR. The yield of benzyl alcohol (**4a**) (95%) was calculated based on the integral ratio among the signals of these compounds with respect to an internal standard (mesitylene).

X-ray single crystal structure analysis of RUPCY2 (1b).

Single crystals of RUPCY2 suitable for X-ray crystal analysis were obtained by slow diffusion of hexane into a chloroform solution of RUPCY2. Intensity data were collected at 103 K on a Rigaku Single Crystal CCD X-ray Diffractometer (Saturn 70 with MicroMax-007) with Mo Kα radiation (λ = 0.71075 Å) and graphite monochromater. A total of 21375 reflections were measured at a maximum 2θ angle of

49.96°, of which 6042 were independent reflections (R_{int} = 0.1018). The structure was solved by direct methods (SHELXS-97) and refined by the full-matrix least-squares on F_2 (SHELXL-97). All non-hydrogen atoms were refined anisotropically. All hydrogen atoms were placed using AFIX instructions. The following crystal structure has been deposited at the Cambridge Crystallographic Data Centre and allocated the deposition number CCDC1022649.

The crystal data are as follows: $C_{36}H_{54}Cl_2N_2P_2Ru$; FW = 748.72, crystal size 0.20 × 0.20 × 0.20 mm^3, monoclinic, C2/c, a = 34.191(16) Å, b = 13.813(6) Å, c = 14.856(6) Å, α = 90.00°, β = 93.164(9)°, γ = 90.00°, V = 7006(5) $Å^3$, Z = 8, D_c = 1.420 g cm^{-3}. The refinement converged to R_1 = 0.0885, wR_2 = 0.2118 ($I > 2\sigma(I)$), GOF = 1.081.

2.5. Reference and notes

(1) Smith, A. M.; Whyman, R. *Chem. Rev.* **2014**, *114*, 5477–5510.

(2) Werkmeister, S.; Junge, K.; Beller, M. *Org. Process Res. Dev.* **2014**, *18*, 289–302.

(3) Dub, P. A.; Ikariya, T. *ACS Catal. 2*, **2012**, 1718–1741.

(4) He, G.; Zhao, Y.; Zhang, S.; Lu, C.; Chen, G. *J. Am. Chem. Soc.* **2012**, *134*, 3–6.

(5) Nadres, E. T.; Daugulis, O. *J. Am. Chem. Soc.* **2012**, *134*, 7–10.

(6) Ano, Y.; Tobisu, M.; Chatani, N. *J. Am. Chem. Soc.* **2011**, *133*, 12984–12986.

(7) Weidner, K.; Kumagai, N.; Shibasaki, M. *Angew. Chem. Int. Ed.* **2014**, *53*, 6150–6154.

(8) Olah, G. A.; Prakash, G. K. S.; Goeppert, A. *J. Am. Chem. Soc.* **2011**, *133*, 12881–12898.

(9) Jessop, P. G.; Hsiao, Y.; Ikariya, T.; Noyori R. *J. Am. Chem. Soc.* **1996**, *118*, 344–355.

(10) Núñez Magro, A. A.; Eastham, G. R.; Cole-Hamilton, D. J. *Chem. Commun*. **2007**, 3154–3156.

(11) Coetzee, J.; Dodds, D. L.; Klankermayer, J.; Brosinski, S.; Leitner, W.; Slawin, A. M. Z.; Cole-Hamilton, D. J. *Chem. Eur. J.* **2013**, *19*, 11039–11050.

(12) Ito, M.; Sakaguchi, A.; Kobayashi, C.; Ikariya, T. *J. Am. Chem. Soc.* **2007**, *129*, 290–291.

(13) Ito, M.; Koo, L. W.; Himizu, A.; Kobayashi, C.; Sakaguchi, A.; Ikariya, T. *Angew. Chem. Int. Ed.* **2009**, *48*, 1324–1327.

(14) Ito, M.; Kobayashi, C.; Himizu, A.; Ikariya, T. *J. Am. Chem. Soc.* **2010**, *132*, 11414–11415.

(15) Ito, M.; Ootsuka, T.; Watari, R.; Shiibashi, A.; Himizu, A.; Ikariya, T. *J. Am. Chem. Soc.* **2011**, *133*, 4240–4242.

(16) Balaraman, E.; Gnanaprakasam, B.; Shimon, L. J. W.; Milstein, D. *J. Am. Chem. Soc.* **2010**, *132*, 16756–16758.

(17) Balaraman, E.; Gunanathan, C.; Zhang, J.; Shimon, L. J. W.; Milstein, D. *Nat. Chem.* **2011**, *3*, 609–614.

(18) Balaraman, E.; Ben-David, Y.; Milstein, D. *Angew. Chem. Int. Ed.* **2011**, *50*, 11702–11705.

(19) Barrios-Francisco, R.; Balaraman, E.; Diskin-Posner, Y.; Leitus, G.; Shimon, L. J. W.; Milstein, D. *Organometallics* **2013**, *32*, 2973–2982.

(20) Takebayashi, S.; John, J. M.; Bergens, S. H. *J. Am. Chem. Soc.* **2010**, *132*, 12832–12834.

(21) John, J. M.; Bergens, S. H. *Angew. Chem. Int. Ed.* **2011**, *50*, 10377–10380.

(22) Kita, Y.; Higuchi, T.; Mashima, K. *Chem. Commun.* **2014**, *50*, 11211–11213.

(23) Miura, T.; Held, I. E.; Oishi, S.; Naruto, M.; Saito, S. *Tetrahedron Lett.* **2013**, *54*, 2674–2678.

(24) Iida, K.; Miura, T.; Ando, J.; Saito, S. *Org. Lett.* **2013**, *15*, 1436–1439.

(25) Sandoval, C. A.; Ohkuma, T.; Muñiz, K.; Noyori, R. *J. Am. Chem. Soc.* **2003**, *125*, 13490–13503.

(26) Noyori, R.; Ohkuma, T. *Angew. Chem. Int. Ed.* **2001**, *40*, 40–73.

(27) Yamakawa, M.; Ito, H.; Noyori, R. *J. Am. Chem. Soc.* **2000**, *122*, 1266–1478.

(28) Li, W.; Xie, J.-H.; Yuan M.-L.; Zhou, Q.-L. *Green Chem.* **2014**, *16*, 4081–4085.

(29) Langer, R.; Fuchs, I.; Vogt, M.; Balaraman, E.; Diskin-Posner, Y.; Shimon, L. J. W.; Ben-David, Y.; Milstein, D. *Chem. Eur. J.* **2013**, *19*, 3407–3414.

(30) Preliminary results of this report (including Ru complexes **1a**–**e**) were used in application for a patent: Saito, S.; Noyori, R.; Miura, T.; Naruto, M.; Iida, K.; Takada, Y.; Toda, K.; Nimura, S.; Agrawal, S.; Lee, S. JP patent, Appl. #2013–42385, Filed: Mar 4, 2013.

(31) Sergeev A. G.; Hartwig, J. F. *Science* **2011**, *332*, 439–443.

(32) Garrou, P. E. *Chem. Rev.* **1985**, *85*, 171–185.

(33) Imabeppu, M.; Kiyoga, K.; Okamura, S.; Shoho, H.; Kimura, H. *Catal. Commun.* **2009**, *10*, 753–757.

(34) Ohkuma, T.; Ooka, H.; Ikariya, T.; Noyori R. *J. Am. Chem. Soc.* **1995**, *117*, 10417–10418.

(35) Prosser, A. R.; Banning, J. E.; Rubina, M.; Rubin, M. *Org. Lett.* **2010**, ***12***, 3968–3971.

(36) Agwada, V. C. *J. Chem. Eng. Data* **1982**, *27*, 479–481.

(37) Huang, Z.; Reilly, J. E.; Buckle, R. N. *Synlett*, **2007**, *7*, 1026–1030.

(38) Martinelli, J. R.; Clark. T. P.; Watson, D. A.; Munday, R. H.; Buchwald, S. L. *Angew. Chem. Int. Ed.* **2007**, *46*, 8460–8463.

(39) Iranpoor, N.; Firouzabadai, H.; Khalili, D. *Bull. Chem. Soc. Jpn.* **2010**, *83*, 923–934.

(40) Zhang, L.; Su, S.; Wu, H.; Wang, S. *Tetrahedron* **2009**, *65*, 10022–10024.

(41) Zou, B.; Dreger, K.; Lichtenfeld, C. M.; Grimme, S.; Schäfer, H. J.; Fuchs, H.; Chi, L. *Langmuir* **2005**, *21,* 1364–1370.

(42) Pasha, M.A.; Jayashankara, V. P. *Synthetic Communications* **2006**, *36*, 1787–1793.

(43) Kung, C.-H.; Kwon, C.-H. *Med. Chem. Res.* **2010**, *19*, 498–513.

(44) Benincori, T.; Pagani, S. B.; Fusco, R.; Sannicolo, F. J. *Chem. Soc. Perkin Trans.* **1988**, 2721–2728.

Chapter 3.

Hydrogenation of Unsaturated Compounds on Catalytic Molecular Surface

Abstract: A high competence of the ruthenium catalysts for hydrogenation reported in Chapter 1 and 2 are reinvestigated by expanding substrate scope to a range of different unsaturated bonds. Since versatile "catalytic molecular surface" can be generated via different activation methods of ruthenium complex precatalysts (molecular surface), selective reduction of substrates other than amides were examined and the primary results are summarized in this chapter. General hydrogenation of a wide range of unsaturated compounds was succeeded. Chemoselective hydrogenation of one out of two different substrates was also observed. The concept and vast usefulness of versatile "molecular surface" is fully demonstrated and supported herein.

3.1. Introduction

A precatalyst for hydrogenation with coordinatively saturated Ru center was designed based on the concept of "molecular surface".[1] The effectiveness of this concept was confirmed by the application of versatile "catalytic molecular surface" in hydrogenation of amides, which is the least reactive amongst the carbonyl family. The catalyst is structurally robust and is sustainable under harsh conditions. Further studies using ESI-MS (Chapter 2) revealed that different preactivation methods apply for precatalysts may lead to the formation of a different set of catalytic molecular surfaces having different catalytic activities. Hence, catalyst precursors are expected to have an ability to hydrogenate diverse types of functional groups. In order to clarify a number of potential application of catalytic molecular surfaces, hydrogenation of a variety of unsaturated compounds were screened through. The outcomes are encouraging, where eleven types of substrates are hydrogenated (Figure 1); This nature is different from the classical hydrogenation catalyst where usually only one or a few kind of functional groups is hydrogenated.[2]

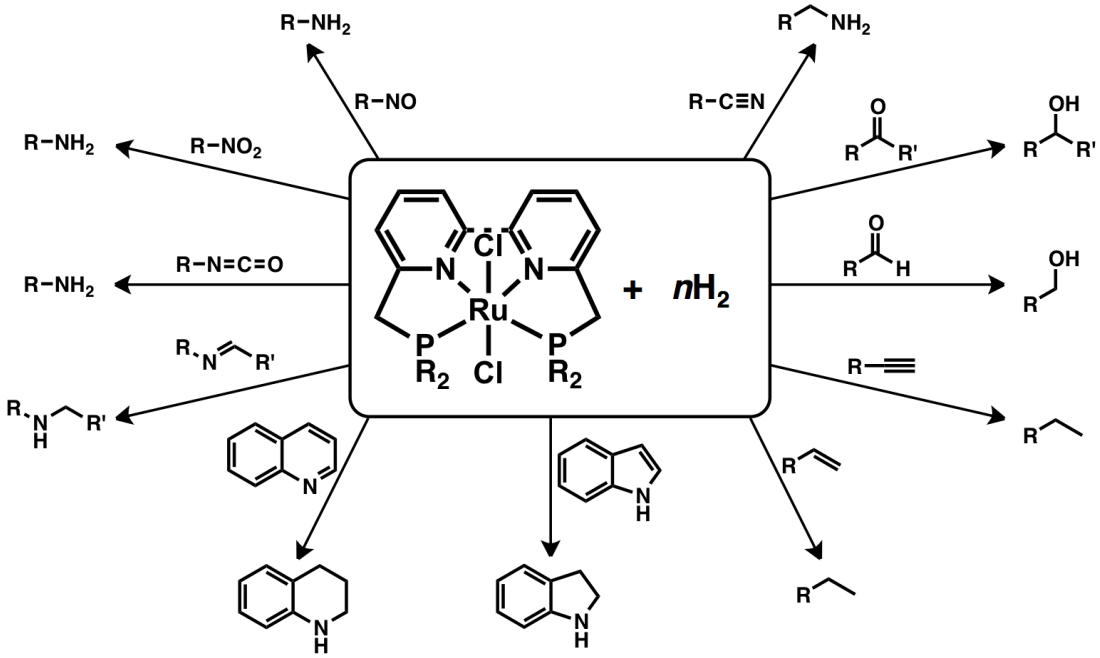

Figure 1. Multifaceted hydrogenation of unsaturated compounds with single precursor.

3.2. Results and discussion

3.2.1. Hydrogenation of unsaturated compounds by same catalyst precursor.

In order to figure out wide applicability of the concept of catalytic molecular surface in different hydrogenation, a series of eleven substrates (**6a–k**) (except amide) was screened through. RUPCY (**2a**) or RUPIP2 (**1a**) was used as precatalyst and sodium 2-methyl-2-adamantoxide (**2b**) was used as base initiator. Bulky **2b** (Chapter 1) was chosen as additive, because it can activate the precatalysts, thereafter giving near neutral pH conditions; a 1:2 ratio of **2a** and **2b** can generate catalytically active species. During the preactivation, base **2b** is completely consumed by reaction with H_2 and precatalysts **1a** or **2a**, thereby ruling out a possibility of undesirable side reactions that may occur after the preactivation. The results are shown in Table 1. To our delight, ketone **6a** and alkene **6c** were readily hydrogenated using RUPIP2 (**1a**), and quantitative yields of 2° alcohol **7a** and alkane **7c** were obtained under P_{H2} = 0.1 MPa (~1 atm) with T = 100 °C (entries 2 and 6). Aldehyde **6b** and alkyne **6d** may coordinate to a Ru center, partly working as catalyst-inhibitor,[3] so that the yields of products, 1° alcohol **7b** and alkane **7c**, would be lower than those obtained from ketone **6a** and alkene **6c** under mild reaction conditions. In contrast, substrates **6b** and **6d** were fully hydrogenated at a higher temperature and/or pressure using RUPCY (**2a**) (P_{H2} = 1 MPa, T = 100–160 °C) (entries 3 and 7) and RUPIP2 (**1a**) (P_{H2} = 2 MPa, T = 120 °C) (entries 4 and 8). These results demonstrate that potential catalyst-inhibitors, aldehyde **6b** and alkyne **6d**, can be hydrogenated easily by slightly increasing T and P_{H2}. Similarly, nitrogen-containing substrates may work as catalyst-inhibitor because of their highly coordinating ability.[4] Hydrogenation of the unsaturated compounds **6e–k** that have nitrogen–oxygen or nitrogen–carbon multiple bonds required rather higher T and P_{H2} to obtain high yields of the corresponding saturated compounds (**7e–k**) using RUPCY (**2a**) (P_{H2} = 1–8 MPa, T = 160 °C) (entries 9, 11, 13 and 15) and RUPIP2 (**1a**) (P_{H2} = 2 MPa, T = 120 °C) (entries 10, 12, 14 and 16). In contrast, hydrogenation of phenyl isocyanate (**6h**) (entries 15 and 16) and benzonitrile (**6i**) (entries 17 and 18) were rather problematic: *N*-phenylformamide (**7h**) and dibenzylamine (**7e**) were obtained, respectively, as side products in both cases using RUPCY (**2a**) and RUPIP2 (**1a**) (entries 15–18). Even heteroaromatic rings of qunoline (**6j**) and indole (**6k**), i.e. pyridine- and pyrrole rings, are converted effectively into the corresponding saturated *N*-heterocyclic rings, giving

1,2,3,4-tetrahydroquinoline (**7j**) and indoline (**7k**) using RUPIP2 (**1a**) (P_{H2} = 2 MPa, T = 120 °C) (entries 20 and 22). However, when RUPCY (**2a**) instead of RUPIP2 (**1a**) was used as precatalyst in the hydrogenation of **6j**, 5,6,7,8-tetrahydroquinoline (**7j'**) was obtained as a side product (P_{H2} = 8 MPa, T = 160 °C) (entry 19). These results indicate that RUPCY (**2a**) is fragile and might be decomposed under the reaction conditions. It may be possible to generate ruthenium nanoparticles from decomposed RUPCY (**2a**), thereby catalyzing the hydrogenation of less reactive benzene rings.

Table 1. Hydrogenation of unsaturated compounds.

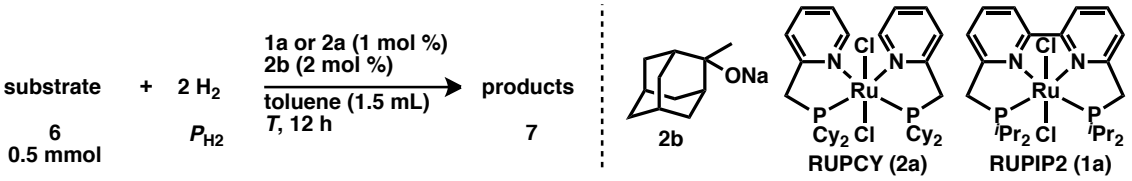

entry	Ru complex	P_{H2} /MPa	T /°C	substrate 6 /conv.	result [a] (%) product 1/yield	product 2/yield
1	2a	1	100	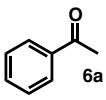 6a	/>99	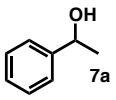 7a />99	
2	1a	0.1	100		/>99	/>99	
3	2a	1	160	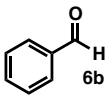 6b	/>99	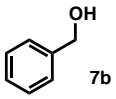 7b />99	
4	1a	2	120		/>99	/>99	
5[b]	2a	0.1	100	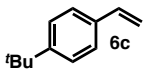 6c	/>99	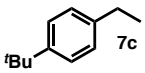 7c />99	
6	1a	0.1	100		/>99	/>99	
7[c]	2a	1	100	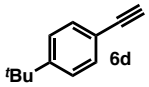 6d	/>99	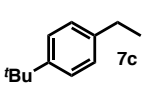 7c />99	
8	1a	2	120		/>99	/80	
9	2a	1	160	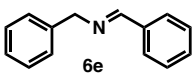 6e	/>99	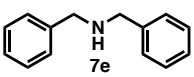 7e />99	
10[d]	1a	2	120		/>99	/>99	
11	2a	6	160	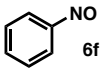 6f	/>99	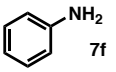 7f /63	
12	1a	2	120		/>99	/58	
13[e]	2a	6	160	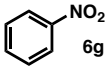 6g	/>99	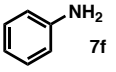 7f /91	
14	1a	2	120		/95	/84	
15	2a	8	160	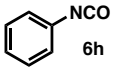 6h	/>99	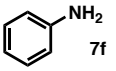 7f /54	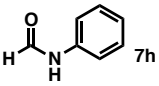 7h /12
16	1a	2	120		/>99	/58	/20
17[d]	2a	6	160	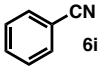 6i	/>99	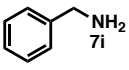 7i /83	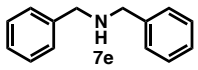 7e /8
18	1a	2	120		/>99	/66	/21
19[f]	2a	8	160	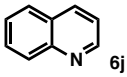 6j	/>99	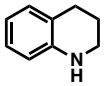 7j /69	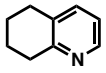 7j' /26
20	1a	2	120		/>99	/>99	/0
21[f]	2a	8	160	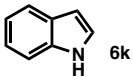 6k	/90	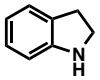 7k /91	
22	1a	2	120		/89	/90	

[a] NMR analysis (mesitylene was used as internal standard) [b] Styrene was used as substrate.

[c] Phenylacetylene was used as substrate. [d] 24 h reaction.

[e] $NaBH_4$ (10 mol %) and THF were used. [f] 2a (2 mol %) and NaOAd (4 mol %) were used.

3.2.2. Hydrogenation reaction with coexistence of different substrates

It turned out that many unsaturated substrates are able to be hydrogenated using RUPIP2 (**1a**) (Table 1). Selective hydrogenation of one out of two different substrates and a possibility of substrate inhibition of catalyst derived from RUPIP2 (**1a**) were also investigated by mixing two different unsaturated compounds in an equimolar amount and subjected to relatively mild reaction conditions (P_{H2} = 0.5 MPa, T = 100 °C, t = 12 h) (Table 2). Since, ketone **6a** and alkene **6c** did not detract the inherent performance of catalyst (Table 1, entries 1, 2, 5, and 6), 2° alcohol **7a** and alkane **7c** are similarly obtained in high yields (entry 2). On the other hand, when aldehyde **6b** and alkyne **6d** are co-present, reactivity of each counterpart compound, is consistently low (entries 1, 3 and 6); this trend is also observed in the case where bulky aldehyde **6l** and internal alkyne **6m** are used (entries 4 and 8). Ketone **6a** was hydrogenated perfectly without being inhibited by alkyne **6m** when sterically more bulky RUPCY2 (**1b**) was used instead of RUPIP2 (**1a**) (entry 5). The bulky Cy groups of RUPCY2 (**1b**) might be preventing substrate inhibition caused by the direct coordination of these substrates to the Ru center and more favorably allow the coordination of small molecules including molecular hydrogen. On the other hand, catalyst inhibition by aldehyde **6b** was somehow resolved using preactivated RUPIP2 (entry 7). This result indicates that aldehyde **6b** might be preventing the formation step of catalytically active species when catalyst preactivation was followed by hydrogenation of substrate in the same reaction vessel (entry 6). No aldol product **7ab** was observed when the preactivated catalyst was used; this fact provides indirect evidence that the pH of the reaction mixture is near neutral when a 1:2 molar mixture of RUPIP2 and **2b** was used. Interestingly, imine **6e** might be accelerating the maturing of active catalyst (entries 9 and 10). This is because when ketone **6a** or aldehyde **6b** was added as a counterpart of **6e**, hydrogenation of **6a** and **6b** proceeded smoothly, albeit imine **6e** itself was not being hydrogenated. These C=O/C=N chemoselectivities are totally different from reduction system reported to date, such as hydrogenation,[5a] transfer hydrogenation,[5b] stoichiometric reduction,[5c,d] which took place nicely with imine in preference to ketone.

Table 2. Hydrogenation reaction under coexistence of two different substrates.

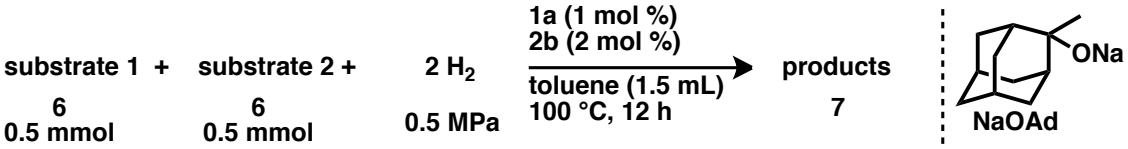

entry	result [a] (%)					
	substrate 1 /conv.	substrate 2 /conv.	product 1 /yield	product 2 /yield	product 3 yield	
1	6b /32	6c /12	7b /3	7c /10		
2	6a />99	6c />99	7a />99	7c />99		
3	6a /trace	6d /50	7a /trace	6c /19	7c /16	
4	6a /5	6m /trace	7a /3	7m /0		
5[b]	6a />99	6m /23	7a />99	7m /23		
6	6a /29	6b /50	7a /trace	7b /3	7ab /11	
7[c]	6a /36	6b />99	7a /39	7b />99	7ab /0	
8	6a /5	6l /20	7a /trace	7l /2		
9	6a />99	6e /8	7a />99	7e /5		
10	6b />99	6e /2	7b />99	7e /2		

[a] NMR analysis (mesitylene was used as internal standard)

[b] RUPCY2 (1b) was used instead of RUPIP2 (1a).

[c] Preactivated catalyst was used: RUPIP2 (1 mol %), NaOAd (2 mol %), 1 MPa H_2, 160 °C, 5 h.

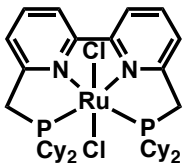

RUPCY2 (1b)

Based on the results obtained through the screening of a number of substrates differently functionalized, hydrogenation of a mixture of eleven different unsaturated compounds (**6a–k**) was carried out (Scheme 1). All substrates were fully or partially hydrogenated into the corresponding hydrogenated products (**7a–c**, **7e**, **7f** and **7i–k**). This result demonstrates that the catalyst is not effectively deactivated by substrate- or product inhibition during the course of the catalytic reaction. However, **6i** and **6k** were not effectively hydrogenated by the catalyst derived under rather harsh conditions (P_{H2} = 8 MPa, T = 160 °C).

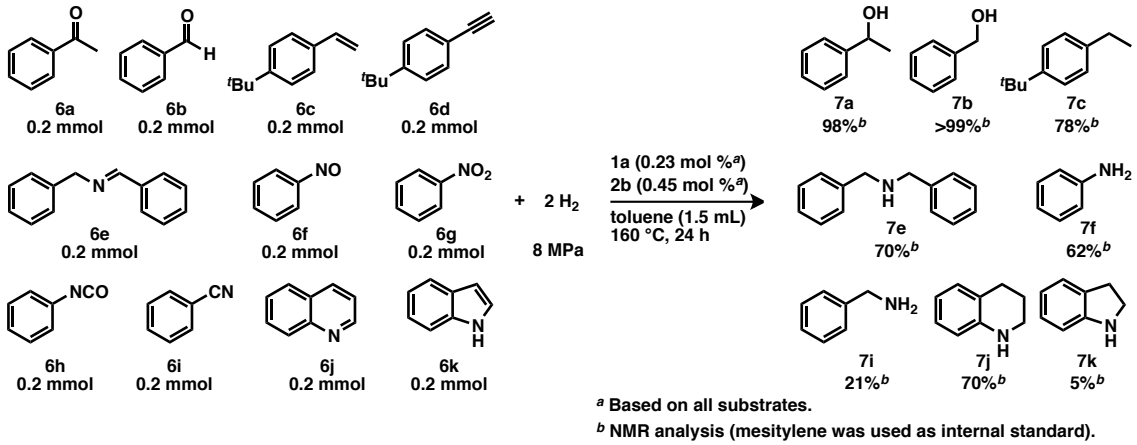

Scheme 1. Hydrogenation of 11 different of unsaturated compounds **6a–k** in one pot.

3.2.3. Competition reaction: hydrogenation of unsaturated compounds in the presence of amide.

Based on the aforementioned results, some compounds promote the preactivation/hydrogenation, while the others are detrimental to either one of the both steps (P_{H2} = 0.5 MPa, T = 100 °C). Whether amide could promote or retard catalyst preactivation and/or hydrogenation catalysis is of great interest. Hence, a series of competition experiments using an equimolar mixture of benzanilide (**3a**) and unsaturated compounds (**6a**, **6b**, **6e** and **6l**) under mild reaction conditions (P_{H2} = 1 MPa, T = 80 °C, t = 24 h) was conducted (Table 3). Without any counterpart compounds, **3a** was hydrogenated in high yield (entry 1). Based on the previous studies, aldehyde **6b** and **6l** should have inhibited the formation step of catalytically active species (Table 2, entries 6–8), and hydrogenation of **6b** required rather harsh reaction conditions (P_{H2} = 2 MPa, T = 120 °C) (Table 1, entry 4). However, with the coexistence of amide **3a**, although hydrogenation of amide was slowed down, aldehydes **6b** and **6l** were hydrogenated preferentially to the corresponding 1° alcohols **7a** and **7l** (entries 2 and 3). These results indicate that 2° amide strongly influences the catalyst preactivation step and preactivation was not started only with aldehyde under milder conditions (P_{H2} = 1 MPa, T = 80 °C). Anionic ($R^1N{=}C(R^2){-}O^-$) species induced by deprotonation of the amide NH hydrogen atom may work as a promoter of catalyst preactivation because amide NH proton is more acidic than the conjugate acid of adamantanoxide **2b**, 2-methyl-2-adamantanol (Scheme 2). Deprotonation of amide NH hydrogen may be important for starting the hydrogenation catalysis. This result might have some relevance with the hydrogenation of 3° amides, which required preactivating RUPIP2 (**1a**) using **2b** and H_2 in a separate reaction vessel under P_{H2} = 1 MPa with T = 160 °C, t = 5 h (Chapter 2, Table 2, entries 12, 13, 22 and 23). In other words, 3° amides do not have a NH hydrogen atom, so that catalyst is not preactivated effectively during hydrogenation reaction under P_{H2} = 1–8 MPa with T = 60–130 °C. In addition, aldehyde may reduce the catalytic activity, because only more reactive substrate, aldehyde, was hydrogenated (entries 2 and 3), even though amide **3a** was hydrogenated in high yields under otherwise the same reaction conditions without counterpart compounds (entry 1). In contrast, amide hydrogenation is not inhibited by the presence of ketone **6a** (entry 4); both amide **3a** and ketone **6a** were hydrogenated in quantitative yields under mild conditions (P_{H2} = 1 MPa, T = 80 °C). Amide **3a** and imine **6e** is suspected to have an

ability to promote the preactivation (Table 3, entries 2 and 3; Table 2, entry 10). However, when imine **6e** was mixed with benzanilide (**3a**), hydrogenation of amide and imine did not proceed effectively under the conditions (entry 5). These results indicate that imine **6e** reduced the catalytic activity for hydrogenation of amide **3a**. In contrast, imine **6e** was hydrogenated slowly in the presence of **3a**.

Table 3. Selective hydrogenation of amide **3a** in the presence of unsaturated compounds.

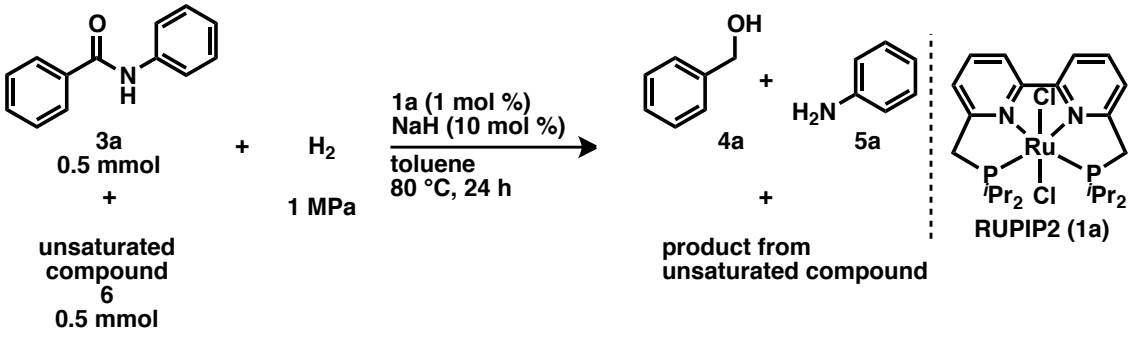

entry	unsaturatedcompound 6 /conv.		result[a] (%) conv. of 3a	4a	5a	product from 6 /yield	
1	none	/—	96	93	86		/—
2	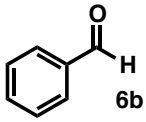 6b	/>99	trace	trace	trace	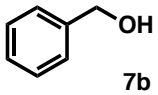 7b	/98
3	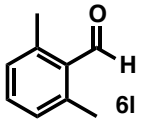 6l	/>99	trace	trace	trace	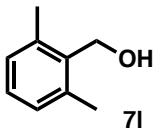 7l	/95
4	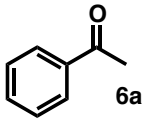 6a	/>99	97	99	90	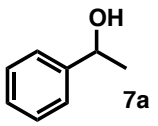 7a	/>99
5	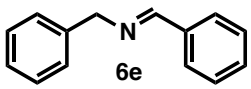 6e	/33	12	8	7	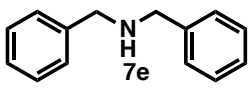 7e	/34

[a] Determined by ^{1}H NMR.

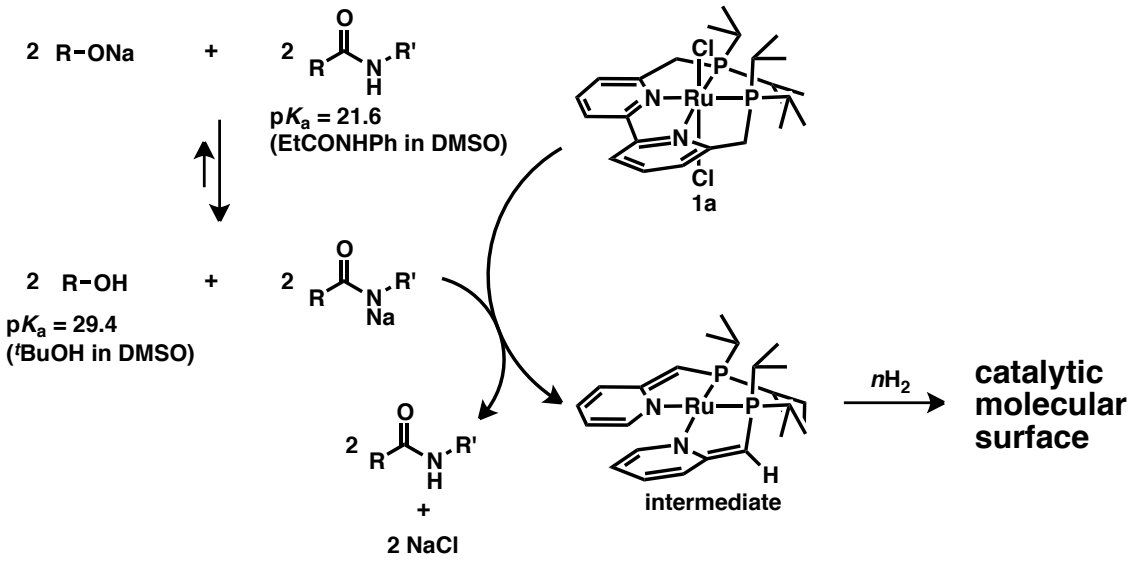

Scheme 2. One of the plausible effect of amide for activation of catalyst.

3.3. Conclusion

The application of molecularly well designed, versatile precatalysts based on the concept of "molecular surface" and "catalytic molecular surface" for hydrogenation has been extended to eleven unsaturated compounds, each bearing a different functional group. Based on the outcome of the screenings, amide and imine show positive effects for preactivation step, while aldehyde and alkyne show negative effects, and ketone and alkene showed neutral effects (Figure 2). In addition, imine, aldehyde and alkyne show positive effects for hydrogenation step, and amide, ketone and alkene show neutral effect. However, the problem of deactivation can be resolved by slightly increase the reaction temperature (T) and hydrogen pressure (P_{H2}). Since the catalyst retains as structurally robust, significant deactivation of catalyst was not observed even under harsher reaction conditions. Some advantages over previous hydrogenation methods and the general applicability of the concept of molecular surface for many hydrogenation systems are demonstrated to a higher extent in this study.

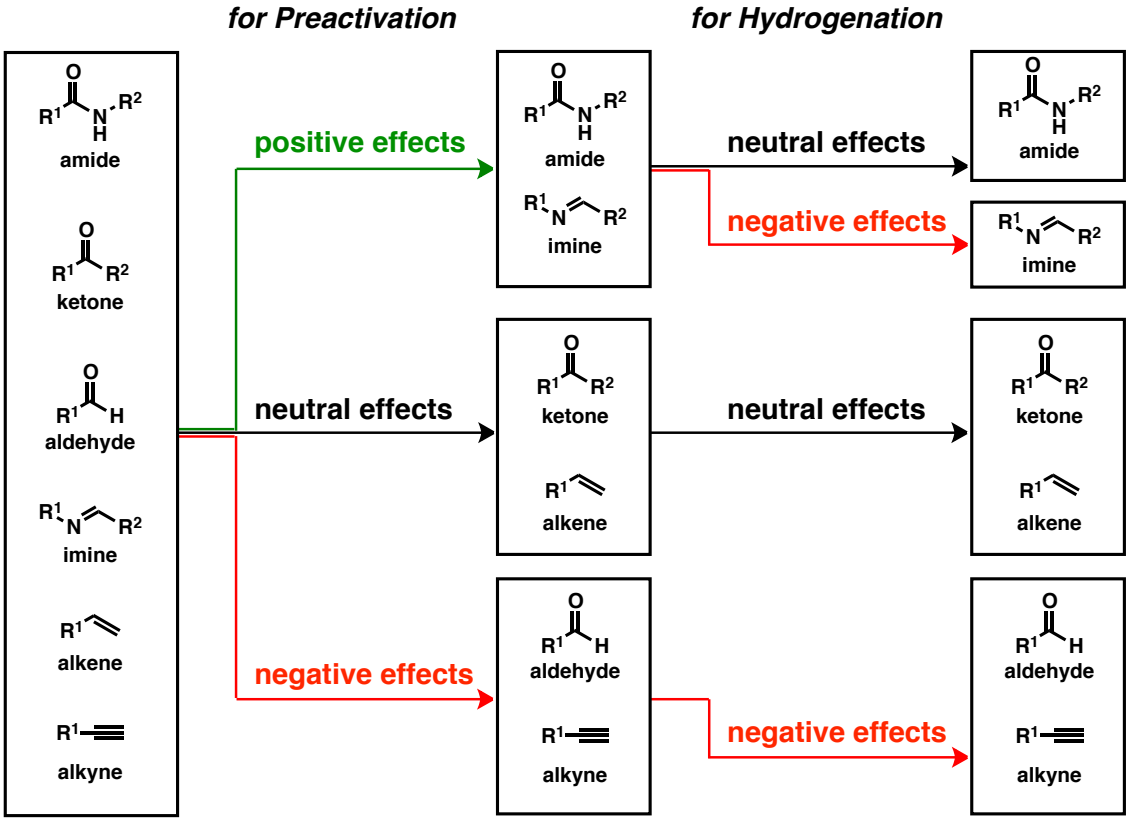

Figure 2. A plausible influence of substrates for the preactivation and hydrogenation steps under mild conditions (P_{H2} = 0.5 MPa, T = 100 °C).

3.4. Experimental section

3.4.1. General

All experiments were performed under an Ar atmosphere unless otherwise noted. ^{1}H NMR spectra were measured on JEOL ECA–600 (600 MHz), JEOL ECA–500 (500 MHz) at ambient temperature. Data were recorded as follows: chemical shift in ppm from internal tetramethylsilane on the δ scale, multiplicity (br = broad, s = singlet, d = doublet, t = triplet, q = quartet, quin = quintet m = multiplet), coupling constant (Hz), integration, and assignment. ^{13}C NMR spectra were measured on JEOL ECA–600 (150 MHz), JEOL ECA–500 (126 MHz) at ambient temperature. Chemical shifts were recorded in ppm from the solvent resonance employed as the internal standard (chloroform-*d* at 77.00 ppm or tetramethylsilane at 0 ppm). For thin–layer chromatography (TLC) analysis through this work, Merck precoated TLC plates (silica gel 60 GF254 0.25 mm) were used. The products were purified by preparative column chlomatography on silica gel 60 N (spherical, neutral) (40–100 μm; Kanto).

3.4.2. Materials

Diisopropylamine, HCl (2.0 M Et_2O solution), benzylamine, 4-*tert*-butylphenylacetylene (**6d**), nitrosobenzene (**6f**), diphenylacetylene (**6m**), 2,6-dimethylbenzaldehyde (**6l**) and benzaldehyde (**6a**) were purchased from Aldrich. $RuCl_2(PPh_3)_3$, chlorodicyclohexylphosphine, chlorodiisopropylphosphine, BH_3–THF complex (1.0 M in THF), *N*-benzylidenebenzylamine (**6e**), EtOAc and hexane were purchased from Wako Pure Chemical industries, Ltd. NaH (55% oil dispersion), mesitylene, hexane (anhydrous), toluene (anhydrous), dichloromethane, ^{n}BuLi (1.5 M in hexane), nitrobenzene (**6g**) and quinolone (**6j**), phenylisocyanate (**6h**) were purchased from Kanto Chemicals, Ltd. 2-methyl-2-adamantanol, dibenzylamine, acetophenone (**6b**), 4-*tert*-butylstyrene (**6c**), benzonitrile (**6i**), and indole (**6k**) were purchased from TCI, Ltd. $CDCl_3$ was purchased from Cambridge Isotope Laboratories, Inc. Hydrogen gas was purchased from Alpha System. These chemicals were used without further purification. 1-phenylethanol (**7a**),[6] benzyl alcohol (**7b**),[7] 4-ethyl-*tert*-butylbenzene (**7c**),[8] *N*-formyl aniline (**7h**),[9] 1,2,3,4-tetrahydroquinoline (**7j**),[10] 5,6,7,8-tetrahydroquinoline (**7j'**),[11] indoline (**7k**),[12] 2,6-dimethylphenylmethanol (**7l**),[13] 1,2-diphenylethane (**7m**)[14] and chalcone (**7ab**)[15] are all known compounds.

3.4.3. Experimental procedure.

Representative procedure for hydrogenation of unsaturated compounds: The reaction of benzaldehyde (6b).

Under a continuous Ar flow, RUPIP2 (**1a**) (2.94 mg, 0.005 mmol), sodium 2-methyl-2-adamantoxide (**2b**) (1.88 mg, 0.01 mmol), anhydrous toluene (1.5 mL), benzaldehyde (**6b**) (50.82 μL, 0.5 mmol) and a magnetic stirring bar were placed in a dried Teflon tube (21 mL capacity). The Teflon tube was quickly inserted into an autoclave, and the inside of the autoclave was purged 10 times with hydrogen gas (1 MPa). The autoclave was pressurized with a 2 MPa of hydrogen gas at 25 °C, and heated at 120 °C for 12 h under stirring (800 rpm). The autoclave was cooled to room temperature in an ice–water (0 °C) bath, and the reaction mixture was quenched with 2.0 M Et_2O solution of HCl (25 μL, 0.05 mmol). The organic phase was removed *in vacuo* (*ca.* 100 mmHg, 40 °C). The residue was diluted with $CDCl_3$, and analyzed by ^1H NMR. The yields of benzyl alcohol (**7b**) (>99%) was calculated based on the integral ratio among the signals of these compounds with respected to an internal standard (mesitylene).

Representative procedure for hydrogenation of unsaturated compounds with preactivated catalyst: The reaction of the mixture of acetophenone (6a) benzaldehyde (6b).

Under a continuous Ar flow, RUPIP2 (**1a**) (3.94 mg, 0.0067 mmol), sodium 2-methyl-2-adamantoxide (**2b**) (2.52 mg, 0.013 mmol), anhydrous toluene (2.0 mL) and a magnetic stirring bar were placed in a dried Teflon tube (21 mL capacity). The Teflon tube was quickly inserted into an autoclave, and the inside of the autoclave was purged 10 times with hydrogen gas (1 MPa). The autoclave was pressurized with a 1 MPa of hydrogen gas at 25 °C, and heated at 160 °C for 5 h under stirring (800 rpm). Then the autoclave was cooled to room temperature in an ice–water (0 °C) bath, and hydrogen was blown away under an Ar stream. Under the continuous Ar flow, to another autoclave, in which a dried Teflon tube charged with acetophenone (**6a**) (58.3 μL, 0.5 mmol) and benzaldehyde (**6b**) (50.8 μL, 0.5 mmol) had been in advance inserted, was transferred the reaction mixture (1.5 mL, 1 mol % Ru) using a gas-tight syringe (2.5 mL). The autoclave was purged (×10 with 1 MPa H_2 gas) and finally charged with 0.5 MPa of hydrogen gas, and the reaction mixture was heated at 100 °C for 12 h under

stirring (800 rpm). The autoclave was cooled to room temperature in an ice–water (0 °C) bath, and the reaction mixture was quenched with 2.0 M Et_2O solution of HCl (25 μL, 0.05 mmol). The organic phase was removed *in vacuo* (*ca.* 100 mmHg, 40 °C). The residue was diluted with $CDCl_3$, and analyzed by ^1H NMR. The yields of 1-phenylethanol (**7a**) (39%) and benzyl alcohol (**7b**) (>99%) were calculated based on the integral ratio among the signals of these compounds with respect to an internal standard (mesitylene).

3.5. Reference and notes

(1) Miura, T.; Held, I. E.; Oishi, S.; Naruto, M.; Saito, S. *Tetrahedron Lett.* **2013**, *54*, 2674–2678. (b) Saito, S.; Noyori, R.; Miura, T.; Naruto, M.; Iida, K.; Takada, Y.; Toda, K.; Nimura, S.; Agrawal, S.; Lee, S. JP patent, Appl. #2013–42385, Filed: Mar 4, 2013.

(2) *Handbook of Homogeneous Hydrogenation*; de Vries, J. G.; Elsevier, C. J., Eds.; Wiley-VCH: Weinheim, 2007.

(3) (a) Stoebenau, III, E. J.; Jordan, R. F. *J. Am. Chem. Soc.* **2003**, *125*, 3222–3223. (b) Candlin, J. P.; Oldham, A. R. *Discuss. Faraday Soc*. **1968**, *46*, 60–71. (c)

(4) (a) Marcazzan, P.; Patrick, B. O.; James, B. R. *Inorg. Chem.* **2004**, *43*, 6838–6841. (b) Vedejs, E.; Trapencieris, P.; Suna, E. *J. Org. Chem.* **1999**, *64,* 6724–6729. (c) Hansen, K. B.; Rosner, T.; Kubryk, M.; Dormer, P. G.; Armstrong, III, D. J. *Org. Lett.* **2005**, *7*, 4935-4938.

(5) (a) Li, C.; Villa-Marcos, B.; Xiao, J. *J. Am. Chem. Soc.* **2009**, *131*, 6967–6969. (b) Uematsu, N.; Fujii, A.; Hashiguchi, S.; Ikariya, T.; Noyori, R. *J. Am. Chem. Soc.* **1996**, *118*, 4916–4917. (c) Lukasiewicz, A. *Tetrahedron* **1963**, *19*, 1789–1799. (d) Borch, R. F.; Bernstein, M. D.; Durst, H. D. *J. Am. Chem. Soc.* **1971,** *93,* 2897–2904.

(6) Cao, L.; Ding, J.; Gao, M.; Wang, Z.; Li, Z.; Wu, A. *Org. Lett.* **2009**, *11*, 3810–3813.

(7) Cano, R.; Yus, M.; Ramón, D. J. *Tetrahedron* **2011**, *67*, 8079–8085.

(8) Imada, Y.; Iida, H.; Kitagawa, T.; Naota, T. *Chem. Eur. J.* **2011**, *17*, 5908–5920.

(9) Suchý, M.; Elmehriki, A. A. H.; Hudson, R. H. E. *Org. Lett.* **2011**, *13*, 3952–3955.

(10) Nador, F.; Moglie, Y.; Vitale, C.; Yus, M.; Alonso, F.; Radivoy, G. *Tetrahedron* **2010**, *66*, 4318–4325.

(11) Koltunov, K. Y.; Repinskaya, I. B. *Russ. J. Organ. Chem.* **2002**, *38*, 437–442.

(12) Guo, D.; Huang, H.; Zhou, Y.; Xu, J.; Jiang, H.; Chen, K.; Liu, H. *Green Chem.* **2010**, *12*, 276–281.

(13) Castro, L. C. M.; Bézier, D.; Sortais, J. B.; Darcela, C. *Adv. Synth. Catal.* **2011**, *353*, 1279–1284.

(14) Black, P. J.; Edwards, M. G.; Williams, J. M. J. *Eur. J. Org. Chem.* **2006,** 4367–4378.

(15) Schmink, J. R.; Holcomb, J. L.; Leadbeater, N. E. *Org. Lett.* **2009**, *11*, 365–368.

List of Publications

（副論文）

1. Catalytic Hydrogenation of Unactivated Amides Enabled by Hydrogenation of Catalyst Precursor
   Takashi Miura, Ingmar E. Held, Shunsuke Oishi, Masayuki Naruto, Susumu Saito
   Tetrahedron Lett. **2013**, *54*, 2674–2678.

2. Multifaceted Catalytic Hydrogenation of Amides via Diverse Activation of a "Molecular Surface" as Precatalyst
   Takashi Miura, Masayuki Naruto, Katsuaki Toda, Susumu Saito
   Nature Commun. in revision.

（参考論文）

1. Cu^{I}/H_2/NaOH-Catalyzed Cross-Coupling of Two Different Alcohols for Carbon–Carbon Bond Formation: "Borrowing Hydrogen"?
   Takashi Miura, Osamu Kose, Feng Li, Sun Kai, Susumu Saito
   Chem. Eur. J. **2011**, *17*, 11146–11151.

2. 分子性の触媒表面を用いる不活性アミドの触媒的水素化
   Takashi Miura, Ingmar E. Held, Shunsuke Oishi, Susumu Saito
   Catalysts & Catalysis **2012**, *54*, 455–459.

3. The Dual Role of Ruthenium and Alkali Base Catalysts in Enabling a Conceptually New Shortcut to *N*-Unsubstituted Pyrroles through Unmasked α-Amino Aldehydes
   Kazuki Iida, Takashi Miura, Junki Ando, Susumu Saito
   Org. Lett. **2013**, *15*, 1436–1439.